Contracted and Expanded Carbaporphyrinoids: Syntheses, Conformation and Coordination Chemistry

By

SANGYA CHITRANSHI

CHEM 11201504006

National Institute of Science Education and Research,

Bhubaneswar, Odisha

A thesis submitted to the
Board of Studies in Chemical Sciences
In partial fulfillment of requirements
for the Degree of

DOCTOR OF PHILOSOPHY

Of

HOMI BHABHA NATIONAL INSTITUTE

November, 2020

Homi Bhabha National Institute

Recommendations of the Viva Voce Committee

As members of the Viva Voce Committee, we certify that we have read the dissertation prepared by **Sangya Chitranshi** entitled **"Contracted and Expanded Carbaporphyrinoids: Syntheses, Conformation and Coordination Chemistry"** and recommend that it may be accepted as fulfilling the thesis requirement for the award of Degree of Doctor of Philosophy.

Chairman – Dr. Moloy Sarkar	Moloy Sarkar	Date: 10.11.2020
Guide / Convener – Prof. A. Srinivasan	Prof	Date: 10.11.2020
Examiner - Prof. V. G. Anand	V.G.	Date: 10/11/2020
Member 1- Dr. Nagendra K. Sharma	Nagendra	Date: 10.11.20
Member 2- Dr. V. Krishnan	V. Krishnan	Date: 10.11.2020
Member 3- Dr. Debasmita P. Alone	Debasmita Alone	Date: 10.11.2020

Final approval and acceptance of this thesis is contingent upon the candidate's submission of the final copies of the thesis to HBNI.

I/We hereby certify that I/we have read this thesis prepared under my/our direction and recommend that it may be accepted as fulfilling the thesis requirement.

Prof 10.11.2020

Date: 10.11.2020 **Signature**

Place: BHUBANESWAR **(Guide)**

STATEMENT BY AUTHOR

This dissertation has been submitted in partial fulfillment of requirements for an advanced degree at Homi Bhabha National Institute (HBNI) and is deposited in the Library to be made available to borrowers under rules of the HBNI.

Brief quotations from this dissertation are allowable without special permission, provided that accurate acknowledgement of source is made. Requests for permission for extended quotation from or reproduction of this manuscript in whole or in part may be granted by the Competent Authority of HBNI when in his or her judgment the proposed use of the material is in the interests of scholarship. In all other instances, however, permission must be obtained from the author.

Sangya Chitranshi

DECLARATION

I, hereby declare that the investigation presented in the thesis has been carried out by me. The work is original and has not been submitted earlier as a whole or in part for a degree / diploma at this or any other Institution / University.

Sangya Chitranshi

LIST OF PUBLICATIONS

Published

[#]1. **Sangya Chitranshi**[†], B. Adinarayana[†], Mainak Das, Won-Young Cha, Dongho Kim and A. Srinivasan[*], "Bis-4,4′ biphenyl Ring Embedded Octaphyrin with Three Distinct Conformational Structures", *Chem. Eur. J.* **2019**, *25*, 12911-12915. ([†]equally contributed)

[#]2. **Sangya Chitranshi**[†], Mainak Das[†], B. Adinarayana, Won-Young Cha, Dongho Kim and A. Srinivasan*, "Structurally Isomerized Bis-Biphenyl Moieties Embedded in Hexaphyrin(3.1.1.3.1.1) and Octaphyrin(1.1.1.0.1.1.1.0)", *Org. Lett.* **2020**, *22*, 1081-1085. ([†]equally contributed)

3. Mainak Das, **Sangya Chitranshi**, M. Murugavel, B. Adinarayana, C. H. Suresh, A. Srinivasan*, "Isosmaragdyrin(1.1.1.0.0) with a N_3C_2 Core: A Bimodular Ligand Stabilizing Rh(I) and Organo-Pt(II) Complexes", *Chem. Commun.* **2020**, *56*, 3551-3554.

Communicated

[#]1. **Sangya Chitranshi,** Mainak Das, B. Adinarayana and A. Srinivasan*, "Stablization of Rh(I) and Organo-Rh(III) Complexes by 6,11,16-Triarylbiphenylcorrole with an *adj*-CCNN Core", (Manuscript Communicated).

[#] pertaining to this thesis

Sangya Chitranshi

Conferences

1. "Expanded carbaporphyrinoids with biphenyl unit: Synthesis and Structural Diversity," **Sangya Chitranshi**, B. Adinarayana, Subhashree Nayak and A. Srinivasan* in International Symposium on Modern Trends in Inorganic Chemistry-XVII (MTIC-XVII), December 11-14th, 2017. Organized by Department of Chemistry, IISER Pune, NCL Pune, Savitribai Phule Pune University at Pune. (**Poster Presentation**).

2. "Synthesis and Characterization of Expanded Carbapyriporphyrin," **Sangya Chitranshi**, Mainak Das, Bidyadhara Sethy and A. Srinivasan* in ACS on campus symposium, July 23rd, 2018 Organized by NISER, Bhubaneswar. (**Poster Presentation**).

3. "Stabilization of Rh(I) and Organo-Rh(III) complexes by *adj*-dicarbacorrole with monoanionic core," **Sangya Chitranshi**, Mainak Das and A. Srinivasan* in National Bioorganic Chemistry Conference (NBCC-2018), December 22nd-24th, 2018 Organized by NISER, Bhubaneswar. (**Poster Presentation**).

Sangya Chitranshi

Dedicated to….

My Family

ACKNOWLEDGEMENTS

I am tremendously grateful to the **Almighty** for immense blessings. This journey would not have been possible without the grace of the **lord**.

I extend my deepest gratitude to my Supervisor, **Prof. A. Srinivasan**, NISER for his active support and giving me intellectual freedom in my work. His kind-heartedness, behavior and belief throughout the entire phase of my PhD will be remembered life-long.

I am thankful to, Director, **Prof. S. Panda**, NISER, **Prof. T. K. Chandrashekar**, founder-Director, NISER and also former-Director, **Prof. V. Chandrasekhar**, NISER, for providing the infrastructure and laboratory facilities.

I thank my Doctoral committee members, Chairman **Dr. M. Sarkar**, **Dr. V. Krishnan**, **Dr. N. K. Sharma**, **Dr. D. P. Alone** and all other faculties in SCS NISER, especially **Dr. S. Peruncheralathan**, **Dr. V. Krishnan**, **Dr. Arun Kumar** for their useful suggestions and support.

My sincere thanks to my collaborator, **Prof. Dongho Kim**, Yonsei University, Korea and his group member, **Dr. Won-Young Cha**, Kyoto University, Japan and Yonsei University, Korea for photophysical and theoretical studies described in the thesis.

I sincerely thank **Mr. Deepak**, **Mr. Sanjaya**, **Mr. Amit**, **Mr. Prakash**, **Dr. Mriganka** and **Mr. Raj Kumar**, NISER for performing characterization of my samples.

I would also like to express my gratitude to my seniors **Dr. B. Adinarayana**, **Dr. A. Ghosh** and **Dr. M. Murugavel**. I am extremely thankful to my colleagues and fellow research scholars **Subhashree**, **Syamasrit**, **Deepak**, **Mahaprasad**, **Dr. Narasingha Rao**, **Sourav**, **Rampal**, **Prakhar**, **Manas**, and most importantly my beloved junior and also a friend, **Prerna**.

Special thanks to my friends **Bratati** and **Pankaj** (NISER) for their help and support in various stages of my research work. I have great pleasure in acknowledging and thanking a very dear friend and senior **Dr. Mainak Das**, without whom it would have been impossible to accomplish the goal being away from family.

Nobody has been more important to me in the pursuit of this project than the members of my family. I would like to thank my **parents**; whose love and guidance are with me in whatever I pursue. Their unconditional love, sacrifices and blessings have strengthened me to face all the hurdles in my journey of life. Special thanks to my

husband, **Neeraj Srivastava**, for his continuous encouragement, support and understanding which helped me stay resilient throughout this tough period.

Finally, I am thankful to everyone who contributed for the accomplishment of my course and I express my apology for those whom I could not mention here.

Sangya Chitranshi

CONTENTS

SUMMARY

Porphyrins are tetra pyrrolic macrocycle containing 16 atoms in the inner core with 18π electrons in their conjugated pathway and follows Hückel aromatic character. By decreasing or increasing an atom in the inner core leads to contracted or expanded porphyrinoids. The contracted derivatives are utilized for stabilizing higher oxidation state metal ions, while the expanded analogues are exploited for aromatic-antiaromatic switching, conformational flexibility and stabilizing multi-metal ions in the macrocyclic core. By replacing one or more pyrrole units by polycyclic aromatic units such as arene unit led to carbaporphyrinoids and which are studied mainly for weak metal-arene interactions and stabilizing the organometallic complexes. With this background, this thesis is mainly focused on such analogs and highlights syntheses, conformation and coordination chemistry of contracted and expanded carbaporphyrinoids. The first chapter describes the literature survey of arene unit incorporated normal, contracted and expanded porphyrinoids. The second chapter deals with coordination chemistry of biphenyl-corrole with *adj*-CCNN core; especially Rh(I) and organo-Rh(III) metal ions. The third chapter outlines the synthesis of bis-biphenyl moiety (*o-p* and *m-p*) embedded expanded porphyrin such as hexaphyrin (*o-p*) and its structural isomer octaphyrin (*m-p*), where one isomer can be switched to another by interchanging the bond connectivity of the bis-biphenyl moiety. The fourth chapter reports the synthesis, spectral, structural and coordination chemistry of bis-biphenyl moiety (*p-p*) based octaphyrin analogue with three distinct conformational structures triggered by protonation and bis Rh metal ion insertion.

List of Tables

List of Schemes

List of Figures

Thesis Highlight

Name of the Student: SANGYA CHITRANSHI

Name of the CI/OCC: NISER **Enrolment No.: CHEM11201504006**

Thesis Title: Contracted and Expanded Carbaporphyrinoids: Syntheses, Conformation, and Coordination Chemistry

Discipline: Chemical Science **Sub-Area of Discipline: Inorganic Chemistry**

Date of viva voce: 10.11.2020.

Porphyrins are highly conjugated 22 π electronic systems in the comprehensive conjugation pathway, while the shortest conjugation pathway contains 18 π electrons. Henceforth, the macrocycle obeys [4n+2]π Hückel rule and appears as aromatic molecule. The general molecular formula of porphyrin is $C_{20}H_{14}N_4$ and the inner core of the macrocyclic framework contains 16 (C/N) atoms. The name “porphyrin” stem from the Greek word "***porphyra***" which means purple color.

The intrinsic properties of porphyrin induced to explore different porphyrinoids with distinct type of modifications in the core as well as periphery for numerous applications. Such porphyrinoids are, (a) Core modified porphyrinoids; (b) N-confused/ Isomeric porphyrinoids; (c) Contracted porphyrinoids and (d) Expanded porphyrinoids. By decreasing or augmenting an atom in the inner core leads to contracted or expanded porphyrinoids, whereas, by replacing one or more pyrrole units by polycyclic aromatic units such as arene unit led to carbaporphyrinoids and such analogues can act as an astute probe to study metal-arene interactions by developing organo-metallic complexes. This thesis is predominantly engrossed on such analogs. The initial part of the thesis is mainly focused on the contracted porphyrinoids like; coordination chemistry of biphenylcorrole and in the second part, *o-p* biphenyl incorporated expanded porphyrin such as Hexaphyrin is highlighted, where by tuning the bond connectivity of the biphenyl unit from *o-p* to *m-p* its structural isomer Octaphyrin is obtained.

In the last part of the thesis, synthesis, spectral and structural chemistry of expanded carbaporphyrinoids such as *p-p* biphenyl ring incorporated Octaphyrin is discussed. Also, its judicial exploitation of core by Rhodium metal ion incorporation is highlighted. The octaphyrin is exploited for its structural diversity after protonation and metal ion incorporation (Figure 1).

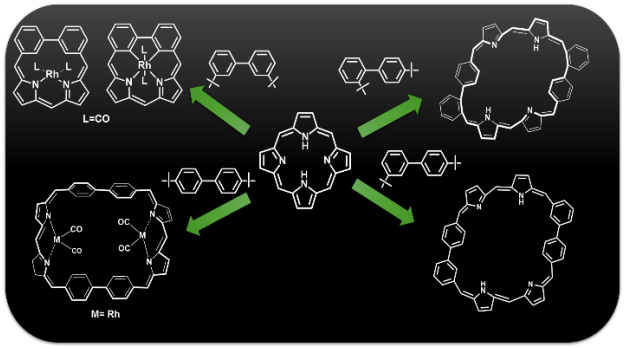

Figure 1. Representative examples of contracted and expanded porphyrin analogues highlighted in the thesis.

Overall, the thesis describes the synthesis of several contracted and expanded porphyrinoids and their coordination complexes, which are well-characterized by various spectral techniques.

CHAPTER 1

Evolution of Porphyrins and its derivatives

1.1 Porphyrins

Porphyrins represent one of the extensively studied of all investigated macrocyclic ring systems.[1] These are naturally existing tetrapyrolic macrocycles[2] and play diverse role in both biological and chemical processes such as; i) oygen transport in hemoglobin and myoglobin; ii) electron transfer in cytochroms and iii) harvesting the light energy for photosynthesis.[3-5] These are therefore backbone of various important natural pigments, including heme, vitamin B_{12}, chlorophyll and bacteriochlorophyll and are aptly known as "pigments of life."[1] In addition, it has also proven to be efficient sensitizers for photodynamic therapeutic (PDT) applications,[6,7] non-linear optical properties,[8,9] and found applications in many scientific fields ranging from biology, material sciences, electronics, catalysis and medicine.[2]

The name "porphyrin" is derived from the Geek word "porphyra" denoting purple color. The general molecular formula is $C_{20}H_{14}N_4$. Porphyrins are highly conjugated 22 π electronic systems and the shortest conjugation pathway comprises of 18 π electrons.[2] Thus the macrocycle obeys $[4n+2]\pi$ Hückel rule and is aromatic. The macrocycle contains two imine and two amine nitrogens in the core and is a dianionic tetradentate square planar ligand. The carbon atoms which connect two pyrrole units in a porphyrin skeleton are known as *meso* carbons. A salient feature of porphyrin **1** is the presence of sp^2 hybridized *meso* carbon atoms which leads to full conjugation throughout the macrocyclic frame, a trait that bestows to their stability and special aromatic nature.[10] The ubiquty of function into nature led resarchers towards focusing there atention on their macrocyclic analogues.[11,12]

Porphyrins and their derivatives are intense in color and show strong absorption bands in the UV-visible region. The electronic absorption spectrum of a classic aromatic porphyrin consists of a sharp intense band around 400 nm, which is a result of transition from ground to second excited state (S0 – S2) and termed as Soret. Another occurs to the excited state (S0 - S1) that gives the Q bands ranging from 450-700 nm (Figure 1.1).

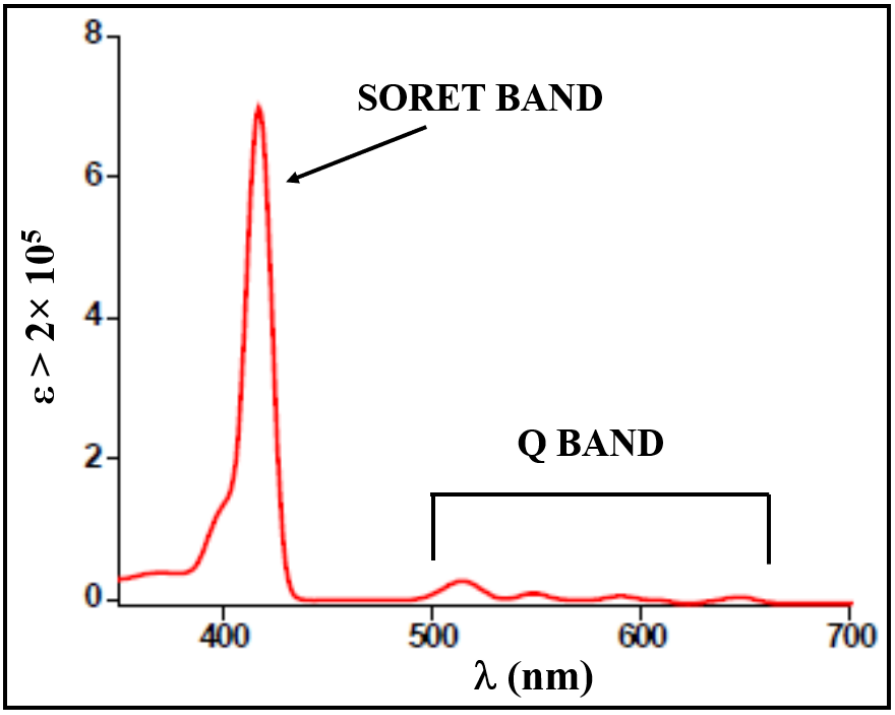

Figure 1.1: Typical electronic absorption spectrum of porphyrins

The electronic absorption spectral pattern of porphyrin is based on Gouterman four orbital model (Figure 1.2). The model suggests that there are two sets of orbitals that are degenerate, HOMO and another is the LUMO. The HOMO is labeled as a_{2u} and a_{1u} and the LUMO is e_{gx} and e_{gy} respectively. Electronic transitions between $a_{2u} \rightarrow e_{gx}$ and $a_{1u} \rightarrow e_{gy}$ are optically allowed, which gives the intense Soret band with high molar extinction coefficient, whereas, the cross transitions between $a_{2u} \rightarrow e_{gy}$ and $a_{1u} \rightarrow e_{gx}$ are optically forbidden and produces weak Q-bands.[13]

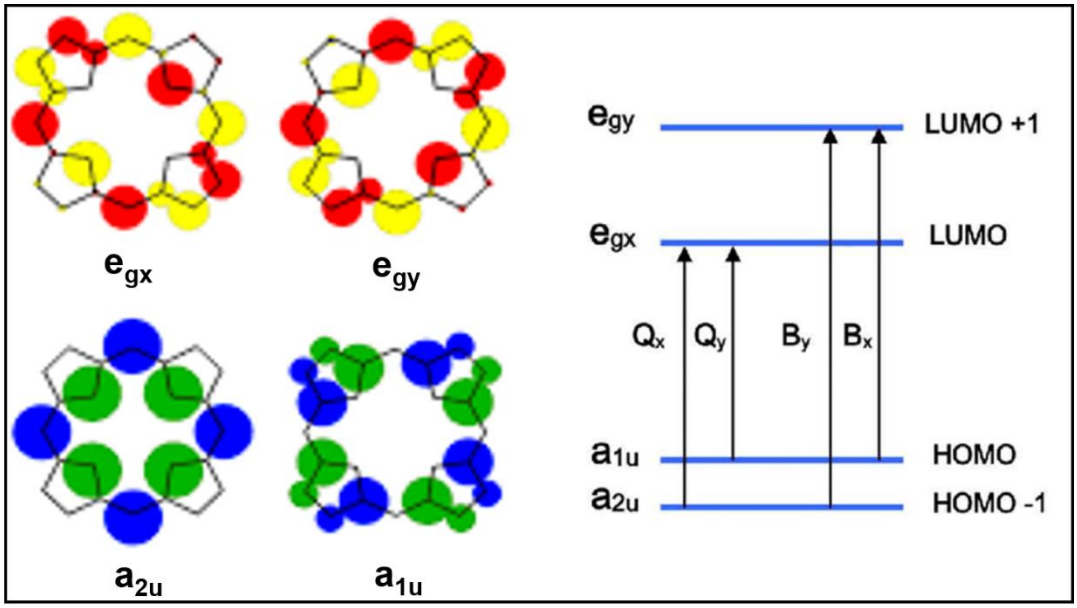

Figure 1.2: Frontier molecular orbital of porphyrin molecule

1.2 Synthesis

Porphyrin **1** (Scheme 1.1a) was first synthesized by Rothemund in 1935,[14] by condensation of pyrrole and aldehydes in methanol at different temperatures. Subsequently, various advanced synthetic methodologies have been established; i) condensing pyrole and benzaldehyd by using propionic acid in air condition under reflux condition (Scheme 1.1b)[15] which was reported by Adler and Longo and ii) Lindsey and co-workers used protic or condensation of pyrrole and aryl aldehydes oxidised with chloranil or 2,3-dichloro-5,6-dicyano-*p*-benzoquinone(DDQ) to synthesize porphyrins in good yield (Scheme 1.1c).[16]

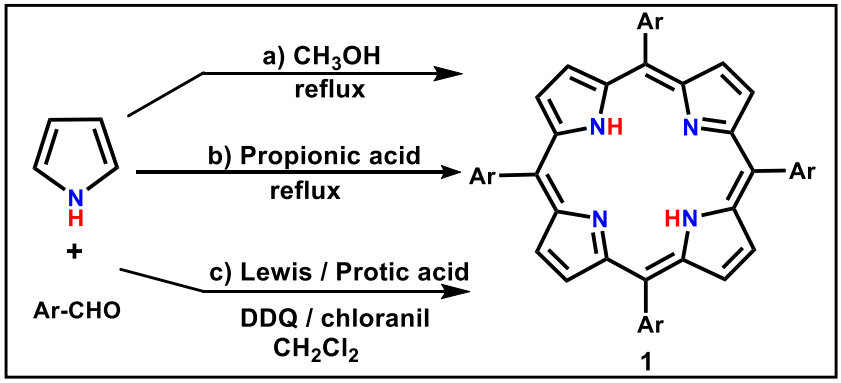

Scheme 1.1: Synthesis of porphyrin **(1)**.

1.3 Nomenclature:

The nomenclature of porphyrins is contingent on the numbering of five-membered heterocycles (pyrrole, furan and thiophene etc). According to the convention, the 2- and 5-positions are denoted as the alpha (α) positions, whereas the 3- and 4-positions are commonly referred as the beta (β) positions. The same nomenclature is followed when these heterocycles are incorporated into the porphyrin skeleton. Thus, the 1-, 4-, 6-, 9-, 11-, 14-, 16-, 19-positions of a porphyrin system are mentioned as α positions while 2-, 3-, 7-, 8-, 12-, 13-, 17- and 18- are termed as β positions. The bridging atoms connecting the heterocyclic units are called as "*meso*" and therefore, the 5-, 10-, 15- and 20-positions of a porphyrin ring are termed as *meso*-positions (Figure 1.3).

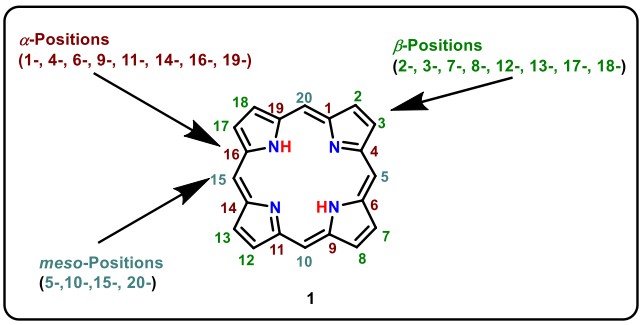

Figure 1.3: Nomenclature of porphyrin molecule

Advancement in porphyrin chemistry led to several complexities in the IUPAC nomenclature of the porphyrin molecule. Thus, trivial names were assigned to porphyrin and its derivatives by their discoverers on the basis of the colour or other characteristics of the macrocycle, followed by the sufix "rin" taken from parent porphyrin macrocycle. Woodward and co-workers initiated such nomenclature by assigning the term "sapphyrin" to a pentapyrrolic macrocycle, as the molecule crystallizes as dark blue solid.[17] Later on, many molecules were named accordingly, e.g rubyrin (red-coloured). Franck and Nonn, in order to avoid trivial name, further suggested the nomenclature depending on three essential parts: (i) the number of π electrons in the shortest pathway in brackets; (ii) a core name indicating the no. of pyroles or other heterocyclic units in the complete systems [e.g., pentaphyrin (five pyrroles), hexaphyrin (six pyrroles), etc.] and (iii) the no. of *meso* carbon atoms present between each pyrrole / heterocyclic ring are represented in numbers in round brackets segregated by dots that is followed by the main name. The numbers in bracket commences with largest *meso* carbon bridge.[42] For eg., pophyrin **1** will be called as [18]tetraphyrin(1.1.1.1) according to the nomenclature.

1.4 Modifications of porphyrins

The unique properties of porphyrin motivated the researchers to develop novel porphyrinoids with several types of modifications in the porphyrin core as well as the periphery. Such porphyrinoids are listed in (Figure 1.4); (a) *Peripheral modification*: Substitution at the peripheral *β*-carbon atom and / or *meso*-carbon bridges;[18-20] (b) *Contracted porphyrinoids*: decreasing the number of pyrole and / or *meso*-carbon in the porphyrin skeleton;[21-23] (c) *N-confused porphyrinoids*: instead of the α, α'-linkage, one or more pyrrole rings are linked by α, β'-linkages;[24-25] (d) *Core-modified porphyrinoids*:

swapping one or more pyrrole nitrogen atoms by chalcogen atoms;[26-27] (e) *porphyrinoids*: replacing one or more pyrrole nitrogen atoms by chalcogen atoms;[26-27] (e) *Expanded porphyrinoids*: increasing one or more pyrrolic / heterocyclic rings and/or number of *meso* carbon units leads to formation of expanded porphyrinoids.[28-29]

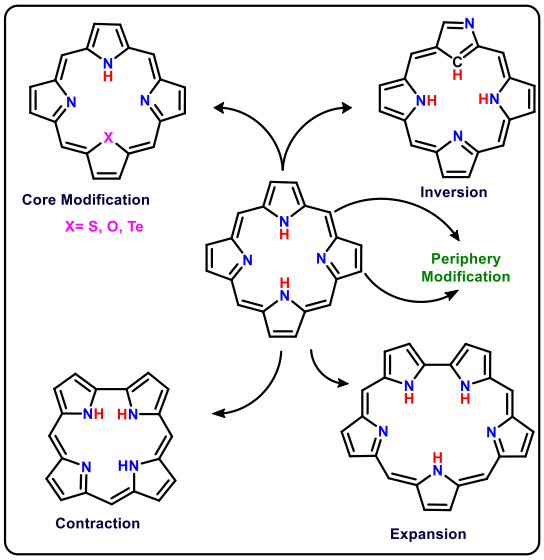

Figure 1.4: Types of modifications in Porphyrinoids.

1.5 Carbaporphyrinoids

Carbaporphyrinoids (**2-9**) are porphyrin analogues in which more pyrrole nitrogens the porphyrin core is altered by carbon. The incorporation of carbocyclic rings in porphyrin skeleton lead to distinct physical and chemical properties. These analogues (Figure 1.5) provide a unique platform to study aromaticity, organometallic chemistry and weak metal C-H bond interactions in the macrocyclic environment. Thus, researchers have used efficient synthetic methodologies to develop novel carbaporphyrinoids and explored their novel properties.

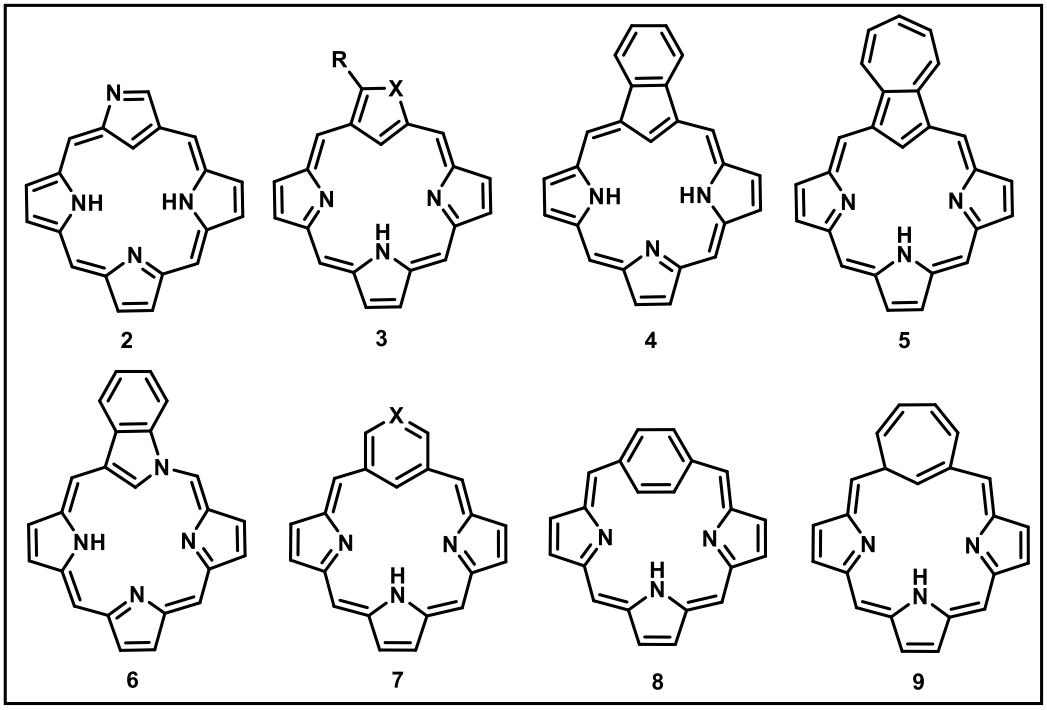

Figure 1.5: Structures of carbaporphyrinoids.

1.5.1 Synthetic methodologies

The principle synthetic pathway for the synthesis of carbaporphyrinoids is the [3+1] MacDonald condensation.[30] In this method, the tripyrrane derivatives with aromatic dialdehydes were condensed by acid-catalyst followed by oxidation furnished corresponding carbaporphyrinoid (Scheme 1.2). This method has been proven to be effective for the synthesis of novel carbaporphyrin analogues. The second synthetic approach is one-pot synthesis where the pyrrole, aromatic dicarbinol and aryl aldehyde were condensed in acid-catalyst and by oxidation with DDQ (Scheme 1.3).[31,32]

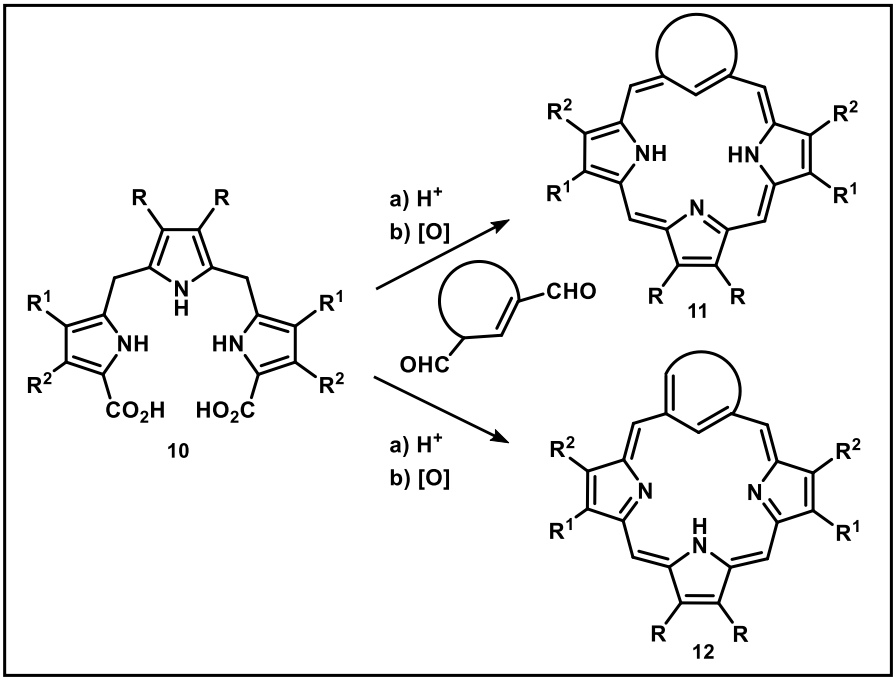

Scheme 1.2: [3+1] MacDonald condensation reaction.

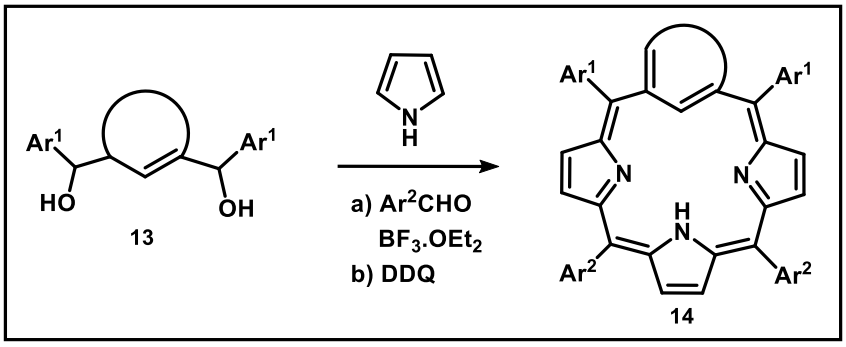

Scheme 1.3: One-pot syntheses of carbaporphyrinoids.

This thesis is mainly engrossed in the syntheses, spectral, structural characterization and coordination chemistry of arene unit incorporated contracted as well as expanded porphyrinoids. The brief introduction about particular carbaporphyrinoids are highlighted in the respective chapters. Hence, this chapter describes the brief literature survey on contracted and expanded carbaporphyrinoids.

1.5.2 Arene ring embedded carba derivatives

Incorporation of six-membered rings such as arenes into the porphyrins tunes the macrocyclic environment and leads to distinguishable physical and chemical properties. Till date, a series of six-membered rings embedded porphyrins are reported which include benziporphyrins, naphthiporphyrins[38] and anthriporphyrins.[39] Among these, benziporphyrin is widely studied carbaporphyrinoid.

i) Benziporphyrin

Benziporphyrins are analogues porphyrin where one among other pyrole ring has been converted by benzene units. These analogues are further classified according to the bonding modes of benzene unit in the macrocycle. These are i) 1,3-linkage referred as *meta*-benziporphyrins and ii) 1,4-linkage called as *para*-benziporphyrins.[33]

a) *meta*-Benziporphyrin:

Berlin and Breitmaier in 1994 reported *m*-benziporphyrin **15**.[34] The β-alkyl substituted derivative (**15**) was synthesized by acid-catalyzed [3+2] MacDonald type condensation employing isophthaladehyde (**15a**) with a tripyrrane dicarboxylic acid (**15b**) followed by oxidation. (Scheme 1.4) Later Grażyński and co-workers gave an improved synthetic pathway for *meso*-aryl substituted *m*-benziporphyrin **16** by the Lewis acid-catalyzed condenstion of pyrrole, C_6H_5CHO, and 1,3- bis(phenylhydroxymethyl)benzene (**16a**) followed by DDQ oxidation (Scheme 1.5).[35] The *m*-phenylene moiety in **16** interrupts the π-electron conjugation of the macrocycle, thus adopting nonaromatic behavior. The presence of C-H inside the core is further exploited for coordination chemistry and weak metal C-H bond interactions in the macrocyclic environment, thus, series of

organometallic complexes with Pd(II), Pt(II), Ni(II) and Rh(III) and weak metal-arene interaction with Zn(II), Cd(II), Hg(II), Ni(II) and Fe(III).[32]

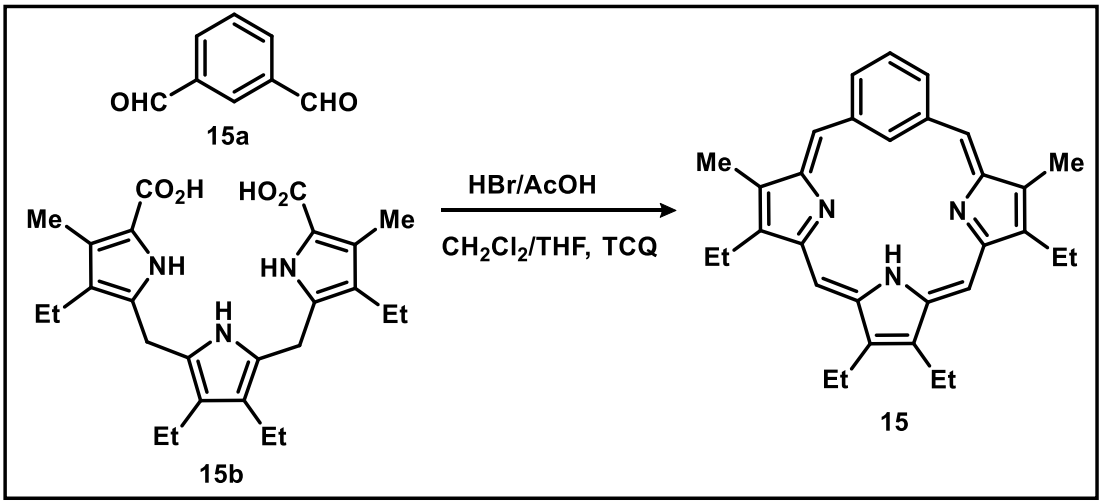

Scheme 1.4: Synthesis of *meta*-benziporphyrin.

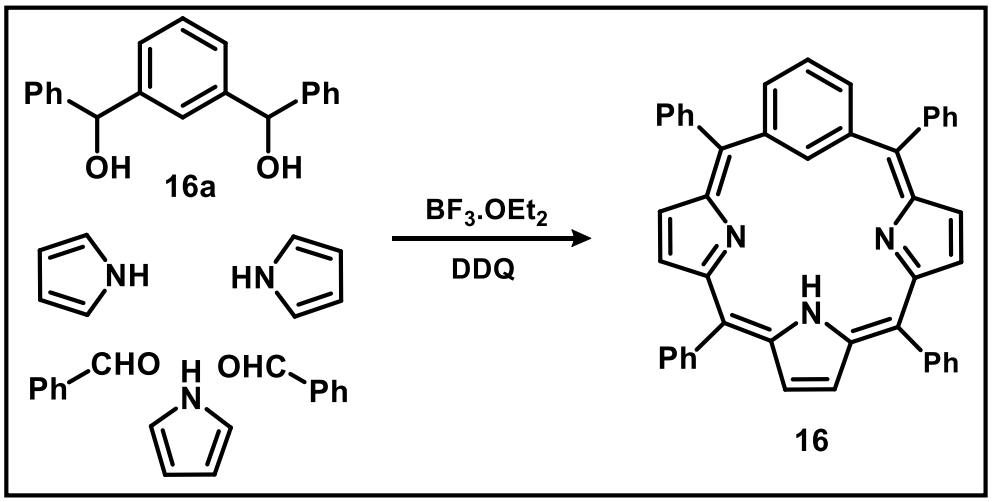

Scheme 1.5: Synthesis of tetraphenyl-*m*-benziporphyrin.

b) *para*-Benziporphyrin:

p-benziporphyrin **17** is a structural isomer of *m*-benziporphyrin where the binding mode is altered from *m*-phenylene to *p*-phenylene. *Meso*-substituted *p*-benziporphyrin is obtained by a slight modification in the synthetic protocol described for the *m*-

benziporphyrin, in which the precursor 1,3-substituted dicarbinol (**16a**) is replaced by 1,4-substited dicarbinol (**17a**) (Scheme 1.6).[36] The structural and spectral features suggest porphyrin like aromaticity thus confirm 18π electrons in the framework. As exploited in **16**, the *p*-benziporphyrins are also an astute platform to study the weak metal arene interaction as well as coordination.[37]

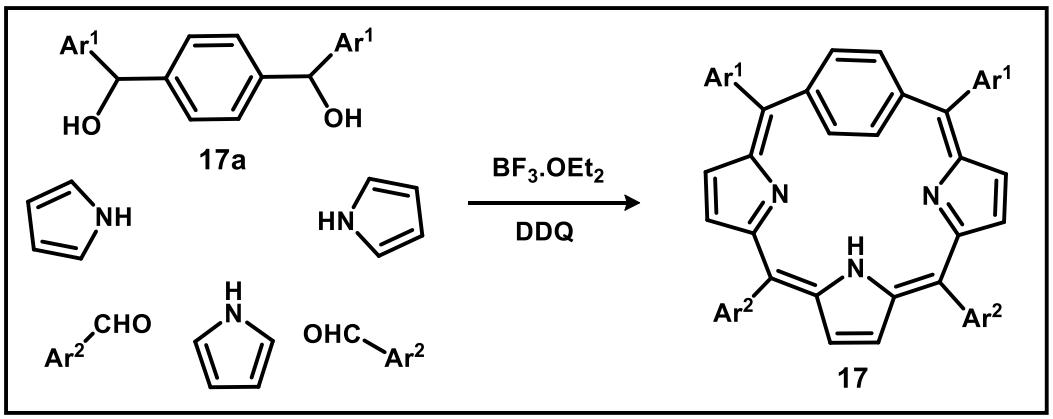

Scheme 1.6: Synthesis of tetraaryl-*p*-benziporphyrin.

Recently biphenyl unit with *ortho-meta* connectivity was introduced in place of arene ring by our group.[40] A Grignard reaction of biphenyl-2,3'-dicarbaldehyde **18** as the precursor followed by Lewis acid-catalyzd condensatn. reaction with pyrole under refluxing temp. to form the required precursor **20**. The final step is the trifluoroacetic (TFA) acd-catalyzed condenstion reactin with pentafluorobenzaldhyde folowed by oxidizing DDQ afforded **21**. The π-electron conjugation in the macrocyclic frame is extended up to *o*-phenylene unit, however it was curbed in the *m*-phenylene unit and thus adopted nonaromatc character. Its core was further efectively utilization to stabilized B(III) complexes.

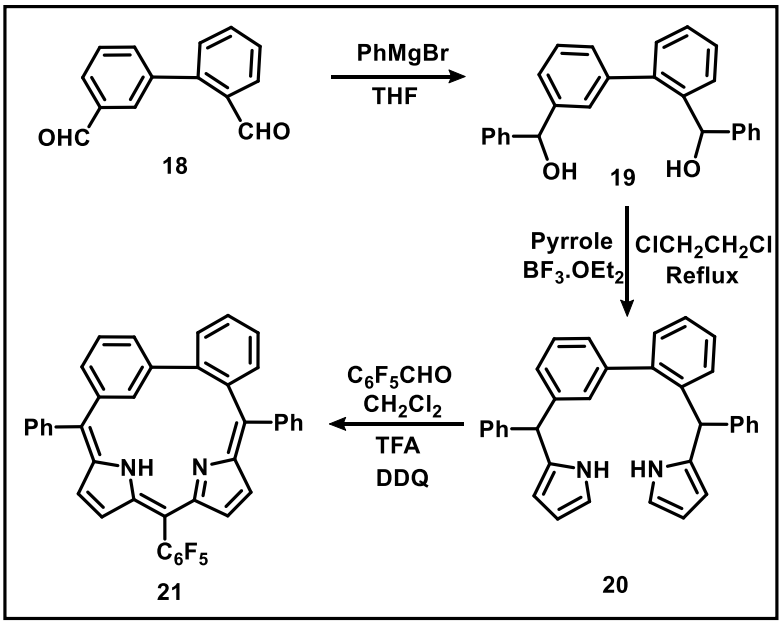

Scheme 1.7: Synthesis of **21**.

1.6 Contracted porphyrins

Contracted porphyrin has one *meso*-carbon / pyrrole rings less in their macrocyclic core, due to which the internal cavity of corresponding macrocycle becomes smaller. Several contracted porphyrinoids have been synthesized till date. Among them, corroles **(22)** is well known and discussed further (Figure 1.6).

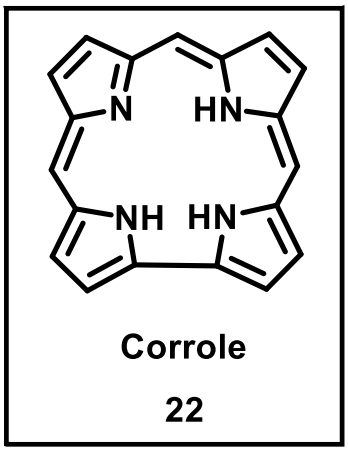

Figure 1.6: Contracted porphyrinoid.

1.6.1 Corroles

Vitamin B_{12} is a naturally occurring tetrapyrrolic porphyrin macrocycle, with one *meso* carbon unit less in its corrin ring. After successful elucidation of Vitamin B_{12}, the research on contracted porphyrins was initiated to develop efficient synthetic methodologies for such molecule.[21,41] Subsequently, Johnson & Price, in 1960, developed a series of metallic derivatives of pentadehydrocorrins and coined the term corroles to such derivatives.[22] Later, the same group synthesized corrole in its freebase form, which proved that corrole is an oxidized form of corrin system and can act as an intermediate between porphyrins and corrins.[43] Thus corrole is structurally distinct from porphyrin as it has one *meso*-carbon less with direct pyrrole-pyrrole linkage between two pyrrole rings.

1.6.1.1 Characteristic properties of corrole

Corroles are aromatic and contain 18π electrons in the shortest conjugation pathway like porphyrin. Their electronic absorption spectra resemble the B and Q-type bands of porphyrins. It exhibits band at aroud 400 nm and not so intense spectral peak in the span of 500-600 nm.[43] These are fluorescent molecule and the luminescence is observed span of 600-700 nm with a fluorescence lifetime in nanosecond range.[44] Corroles are more acidic in nature than porphyrins. Freebase corrole liberates a proton gradually to produce mono-, di- and trianinoic species in presence of dilute bases.[43] While, with dilute acids, it forms monoprotonated species.[43,45] The aromatic characteristics of corroles are reflected from ^{1}H NMR analyses. Pyrrolic *β*-CH protons and the *meso*-protons appear in the strongly deshielded region, whereas, inner imino protons resonate in the shielded region between -2.00 and -3.00 ppm, as a broad singlet pointing out the presence of diatropic ring current. The broadness of peak has been attributed for the

tautomerism and acidic nature of corrole.[46] The first X-ray characterization of corrole revealed that macrocycle is slightly deviated from the planarity in order to curtail the steric pressure inside the macrocyclic core resulting from the direct C–C bond of the two pyrrole units.[47] Low temperature X-ray analysis reveals that one of the inner core protons are in the mean corrole plane while the other two are above and below the plane respectively, due to the saddling of the pyrrole rings.

1.6.1.2 Synthetic Protocols

Corrole was first synthesized by Johnson and Kay in the year 1965.[43] Since then, several improved synthetic methodologies have been reported to increase the yields of corrole. The research on corrole chemistry gained momentum only after introducing the proficient synthetic methods by different groups, such as Gross *et al*., Paolesse *et al*., and Gryko *et al*.[23,48,49] Gross *et al*. used one pot synthetic methodology (Scheme 1.8), where pyrrole and aryl aldehyde are condensed to obtain freebase corrole **23**.[23]

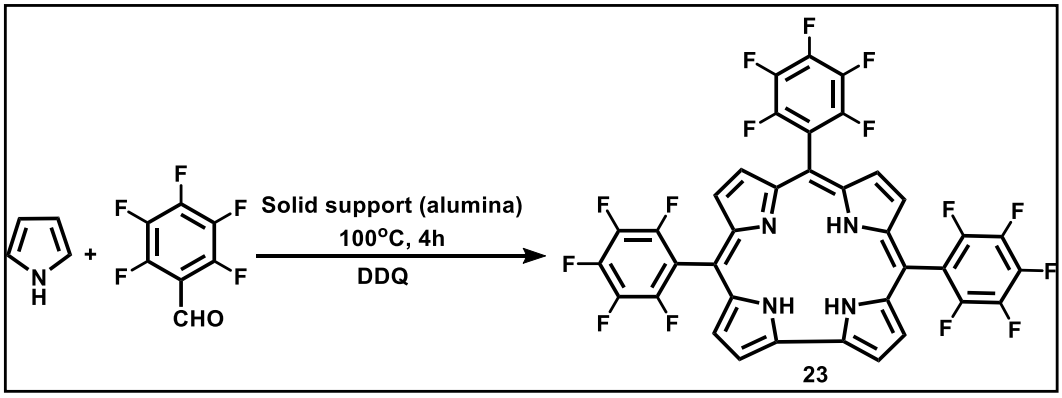

Scheme 1.8: Synthesis of *meso*aryl corrole **(23)**.

1.6.1.3 Metallocorroles

Corroles are excellent ligands to stabilize plethora of metal ions due to its trianionic core. Fundamentally, two synthetic methodologies have been adopted for stabilization

of metal ions in the core: a) as a metal template for macrocyclization and b) usual metal ion inclusion into the corrole cavity. In both the cases, however, choice of the metal ion plays a remarkable role. A variety of elements ranging from alkali metals and transition metals to lanthanides and actinides have been utilized for the respective purpose (Figure 1.7).

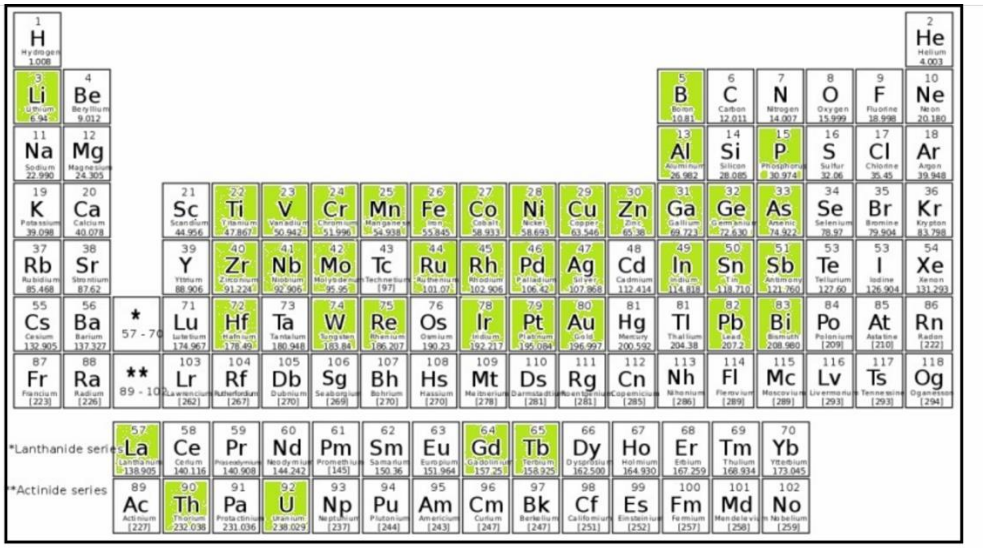

Figure 1.7: Periodic table indicates the elements stabilized by corrole ligand.

1.6.1.3.1 Coordination Modes in Metallocorroles

Four different kind of binding modes are known for metallocorrole (Scheme 1.9). The most common is the squar-pyramid configuration of the sitting metal ion.[50] The dome shaped configuration acquired by pentacoordination is due to the axial deracination of the central metal atom from the N4 plane. Such geometry is observed in case of complexes with Cr, Mo, Mn, Fe, Co, Rh, Ge, Sn or P having neutral as well as anionic axial ligands such as triphenylphosphine, pyridine or halides (F^-, Cl^-, Br^- and I^-), phenyl, methyl and also exist as oxo, nitride and nitrosyl complexes.[51,52]

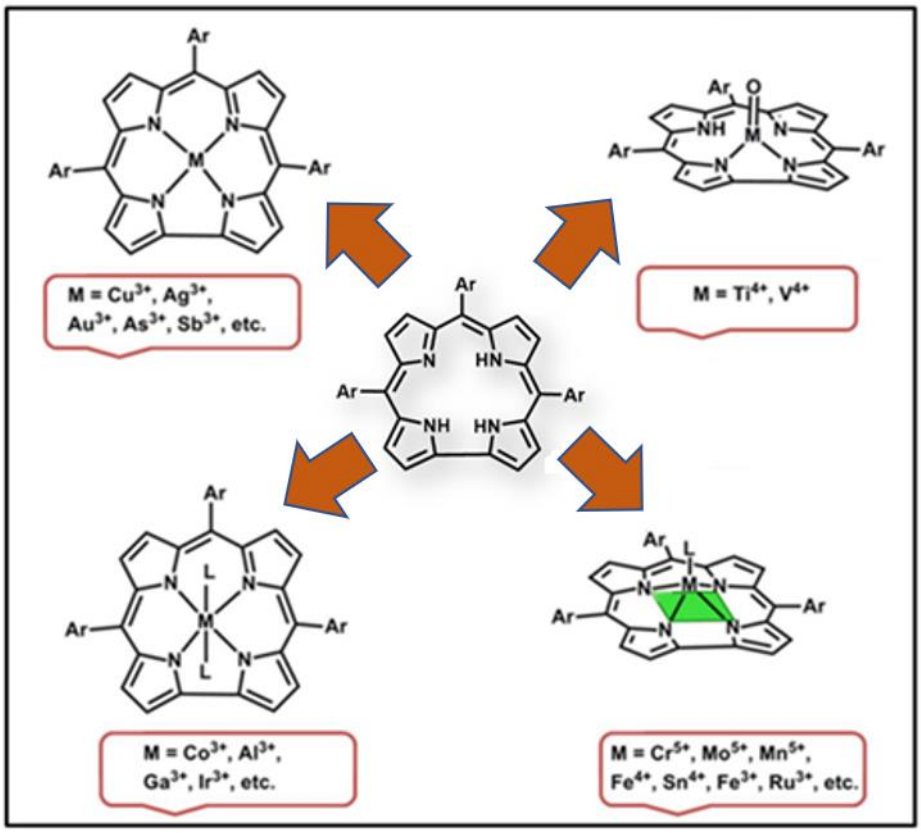

Scheme 1.9: Coordination modes in metallocorroles.

Another common coordination mode is the one observed in hexa-coordinated complexes (Scheme 1.9). The octahedral geometry is observed in the axially coordinated pyridine complexes of Co(III), Al(III), Ga(III) and Ir(III) complexes.[53-56] Few transition metals and main group metals such as Cu(III), Ag(III), Au(III), In(III), As(III), Sb(III) and Bi(III) form four-coordinated complexes and thus attain square planar geometry.[57-60] The same geometry is also adopted by corrole complexes of Co(III), Mn(III) and Ru(III) in the absence of any coordinating solvents.[43,61,62]

Although, in most cases corroles behave as trianionic and tetradentate ligands, in some cases, they act as tridentate and dianionic ligands, such as in oxo-V(IV) and oxo-Ti(IV) complexes of corroles (Scheme 1.9).[63]

1.7 Expanded porphyrins

Expanded porphyrins are analogues of porphyrin that are obtained by augmenting the no.of heterocyclic rings or *meso*-carbon atoms or both in a way that inward pathway accomodate minmum of 17 atom in the core.[29] There are more than 18π electrons in their shortest conjugation pathway. These macrocycles received much attention mainly due to; i) the large core size can harbor more one metal ions to fabricate multi-metallic complexes; ii) bind with anionic and neutral substrates and iii) study the nature of aromaticity and aromaticity switching.

The first expanded porphyrins, sapphyrin (**24**) was serendipitously discoverd by Wodward and co-workers.[17] In sapphyrin, the five pyrole units are conected via 4 *meso* linkages and one direct pyrrole-pyrrole linkage. In early stages (1966–1990), sapphyrins were mainly investigated by Johnsun and co-workers. After many years a series of octaphyrin derivatives were discvred by Vogal and co-workers.[64] Simultaneously, the chemistry of core-modified expanded porphyrins was also explored by many groups.[65-67] However, considerable efforts have been devoted by Sessler and Osuka towards efficient synthetic methodologies of expanded porphyrins and demonstrating them as potential candidates in several spectrums encompassing anion recogniton, functonal dyes, aromaticity, (MRI), and photodinamic therapies (PDT).[29] This contributed to the renaissance of these porphyrins which includes sapphyrins **24**,[17] homoporphyrin **25**, smaragdyrins,[45] pentaphyrins,[68] amethyrins **26**,[70] rubyrins **27**,[74] hexaphyrins **28**,[69] heptaphyrins **29**,[71] octaphyrins **30**,[64] nonaphyrins **31**,[73] turcasarins **32**,[75] dodecaphyrins, hexadecaphyrins, icosapphyrins, tetracosapphyrin and the expanded derivative with 96π electron in the macrocyclic framework. Few exampls are depicted in Figure 1.8.

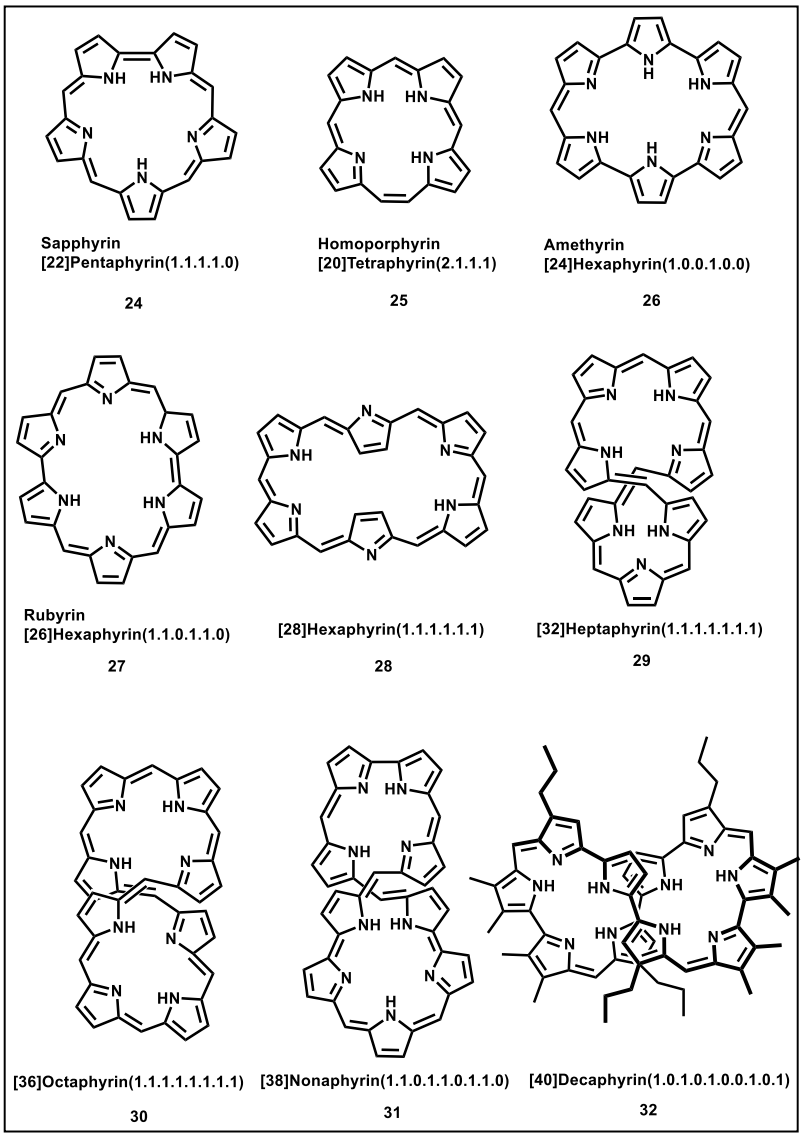

Figure 1.8: Structurs of expanded porphyrinoids.

1.7.1 Expanded carbaporphyrinoids

The first expanded carbaporphyrin with carbocyclic unit **35** was reported by T. D. Lash.[76] Benzocarbasapphyrin **35** was prepared from indene dialdehyde **33** and tetrapyrrole dicarboxylic acid **34** in the TFA environment folowed by oxidizing agent DDQ (Scheme 1.10). However, much increased yields were obtained by using aqueous ferric chloride as oxidizing agent. The compound **35** in freebase form was unstable and thus isolated as stable hydrochloride salt. The respective monocationic species (**35.H**$^{+}$)

was found to be aromatic. Till date various carbocyclic unit embedded expanded porphyrinoids are known in literature such as cyclopentadiene, azulene, benzene, phenanthrene and neo-confused pyrrole rings.[72]

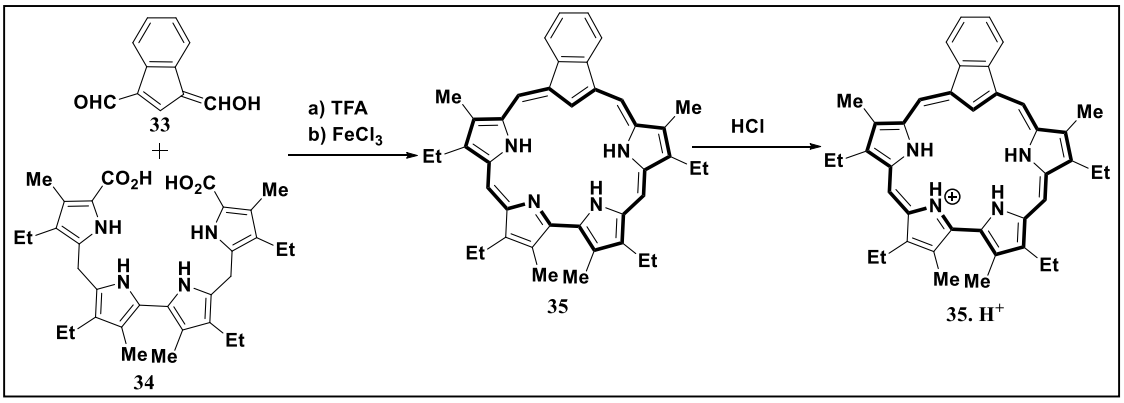

Scheme 1.10: Synthesis of benzocarbasapphyrin (**35**).

1.7.1.1 Expanded benziporphyrins

Expanded benziporphyrins were obtained by incorporating arene moiety in macrocyclic core. Herein, the synthesis of first expanded *m*-benzi and *p*-benziporphyrinoid are described below. Further, the other expanded *m*- and *p*-benzi analogues which are known the literature till date are included as Figures.

1.7.1.1.1 Expanded *m*-benziporphyrinoids

The first example of an expanded *m*-benziporphyrin, dibenzihexaphyrin (1.0.0.1.0.0) (**37**) was reported by Corriu and co-workers.[77] The *cis*- and *trans*-isomers were synthesized by reaction between *m*-dipyrrolylbenzene (**36**) and benzaldehyde in refluxing acetic acid (Scheme 1.11). Dibenziamethyrin (**37**) was obtained by oxidation with DDQ in toluene.[77-78] The *m*-arene in macrocyclic core restricts the macrocyclic conjugation, thus revealed nonaromatic characteristics. Till date, the reported expanded *m*-benziporphyrinoids (**38**-**43**) are shown in Figure 1.9.

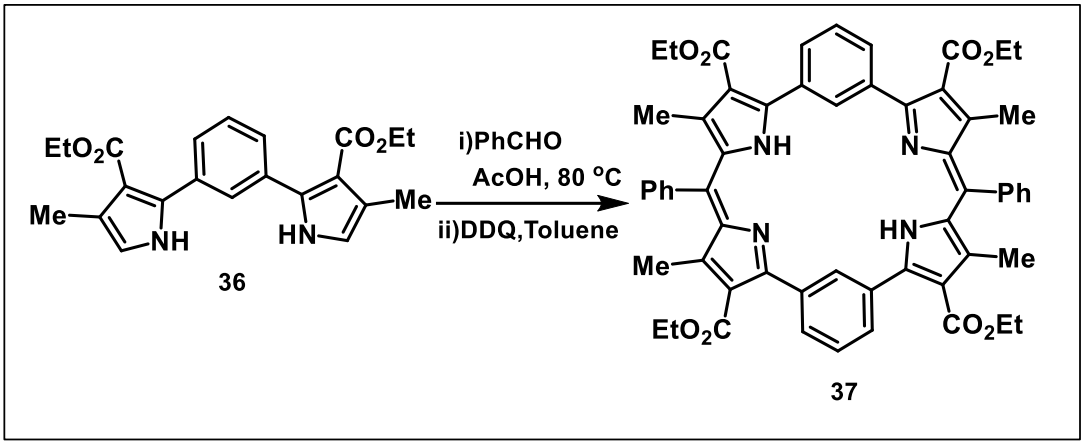

Scheme 1.11: Synthesis of *m*-dibenziamethyrin (**37**).

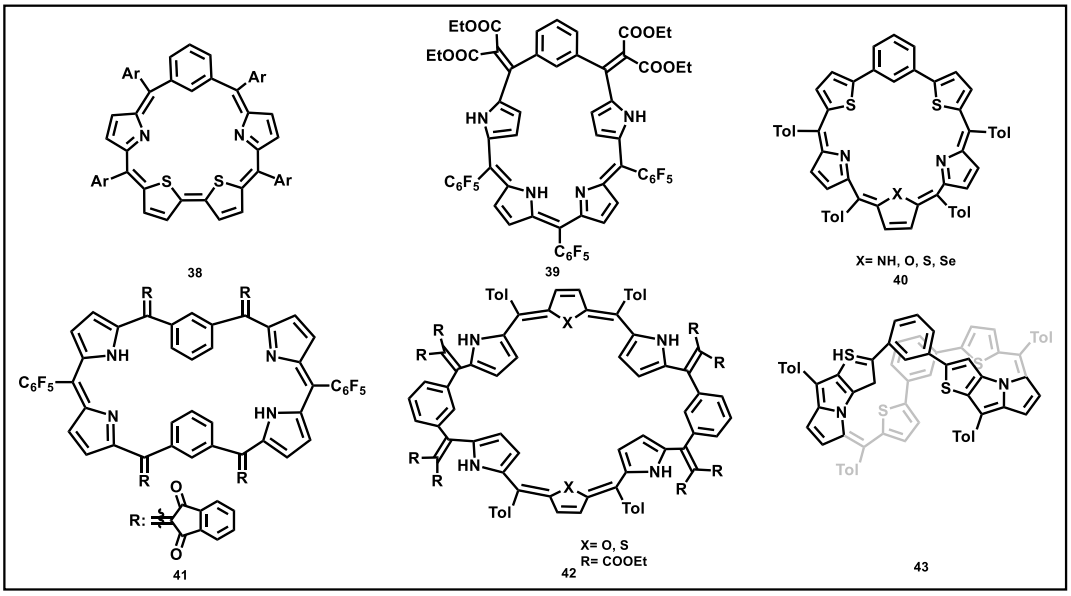

Figure 1.9: Structures of expanded *m*-benziporphyrinoids.

1.7.1.1.2 Expanded *p*-benziporphyrinoids

By varying the substitution mode of the phenylene moiety expanded *p*-benziporphyrinoid can be generated. The first *p*-arene ring based expanded porphyrin, A,D-*p*-di-benzihexaphyrin (**45**) was synthesized by Grażyński and co-workers.[79] Dicarbinol **44** was reacting with pyrole and benzaldhyde in the environment of Lewis acid and oxidising agent DDQ to give dibenzhexaphyrin **45**. The crystal conformation for **45** revel figure-eght Möbius geomtry that can ease aromatic 28π elctron

delocalization. Studies in solution manifested of two conformations were there, a planar antiaromtic Hückel form and a Möbius aromtic confrmation.

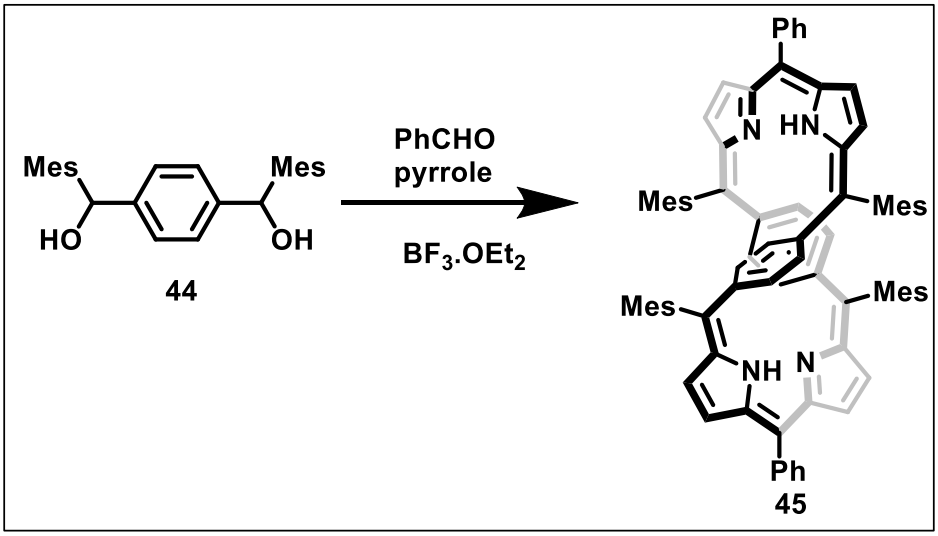

Scheme 1.12: Synthesis of *p*-di-benzihexaphyrin (**45**).

Like *p*-benziporphyrinoids, the presence of *p*-phenylene units in the expanded *p*-benziporphyrinoids allowed effective π-electron delocalization within the macrocycle, thus, received much attention as compared to respective *m*-analogues. Some of the reported expanded *p*-benziporphyrinoids (**46**-**51**) till shown in Figure 1.10.

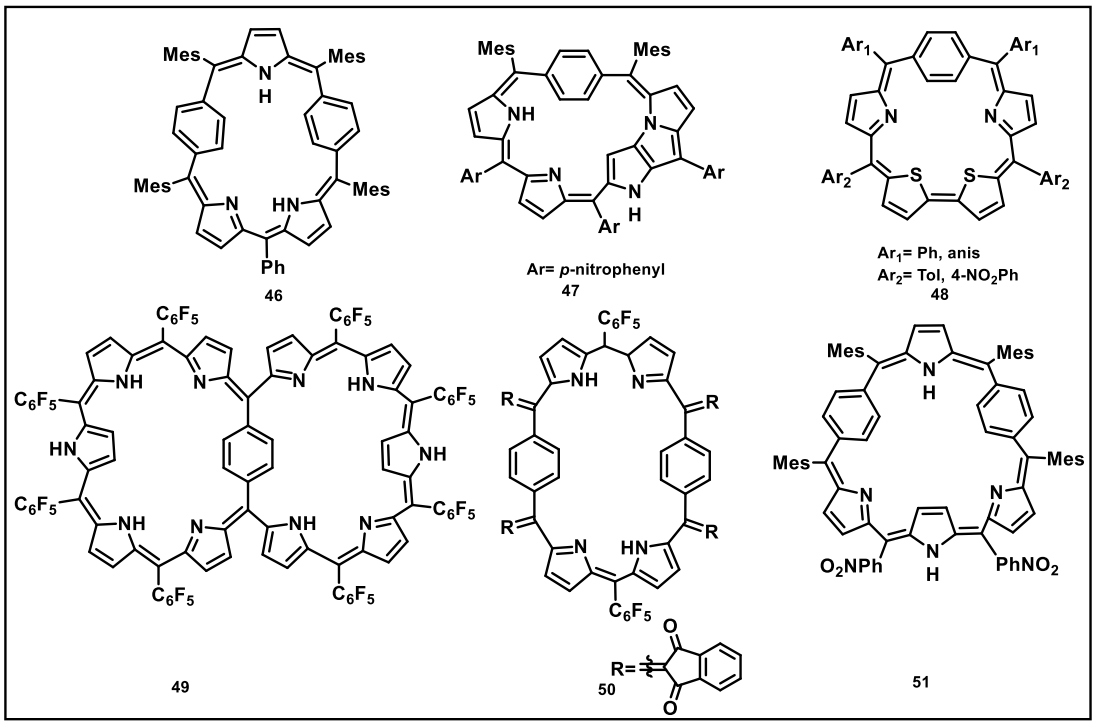

Figure 1.10: Structures of expanded *p*-benziporphyrinoids.

Recently from our group, terphenyl moiety was introduced in the porphyrin macrocycle with *p*-*o*-*p* (**52**),[80] *m*-*o*-*m* (**54**)[80] and *m*-*m*-*m* (**56**)[81] type of bonding mode to obtain homoporphyrin (**52** & **54**) and octaphyrin (**56**). The spectral and structural analyses revealed the nonaromatic characteristics of these macrocycles. Further the core was utilized for stabilization of mono and bis-RhI(I) ions (**53**, **55** & **57**) (Figure 1.11).

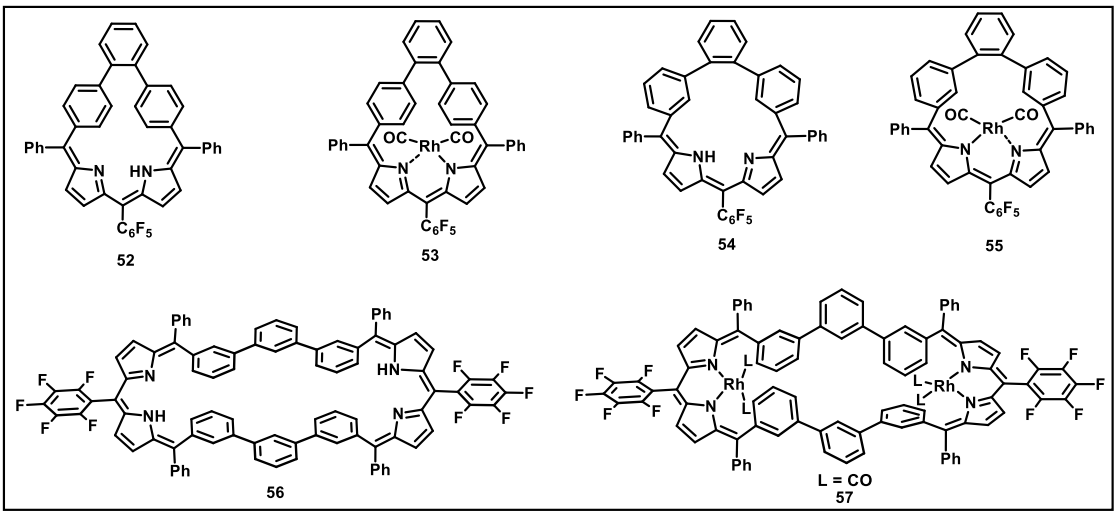

Figure 1.11: Structures of homoporphyrin (**52** & **54**), decaphyrin (**56**) and their Rh(I) complexes (**53**, **55** & **57**).

1.8 Conclusion

From the brief introduction, the chemistry of carbocyclic embedded macrocycles has emerged as an interesting area of research in recent years. So far, the research is mainly focused on mono-carba porphyrinoids. However, the dicarba porphyrinoids are scarcely reported in the literature. Hence, the development of such derivatives provides an ideal platform to explore diverse applications. It is also pertinent to point out that the synthetic methodologies involved to obtain the contracted and expanded derivatives with arene unit as a part of the macrocyclic framework is relatively less explored. The main objective of the present thesis is to develop new synthetic methodologies for the contracted and expanded porphyrinoids by introducing the polycyclic arene units in the macrocyclic framework. In addition, the reactivity, structural diversity and coordination chemistry of these macrocycles are discussed in the respective chapters.

1.9 References

1. A. R. Battersby, C. J. R. Fookes, G. W. J. Matcham, E. McDonald, *Nature* **1980**, *285*, 17-21.
2. K. M. Kadish, K. M. Smith, R. Guilard, The Porphyrin Handbook, Volume 1: Synthesis and Organic Chemistry. Academic Press–San Diego, CA and London, UK: **2000**.
3. J. M. Vanderkooi, M. Erecinska, *Eur. J. Biochem*. **1975**, *60*, 199-207.
4. J. L. R. Anderson, C. T Armstrong, G. Kodali, B. R. Lichtenstein, D. W. Watkins, J. A. Mancini, A. L. Boyle, T. A. Farid, M. P. Crump, C. C. Moser, P. L. Dutton, *Chem. Sci*. **2014**, *5*, 507-514.
5. S. J. Lippard, J. M. Berg, *Principles of bioinorganic chemistry*. University Science Books: **1994**.
6. T. J. Dougherty, S. L. Marcus, *Eur. J. Cancer* **1992**, *28*, 1734-1742.
7. J. Moan, K. Berg, *Photochem. Photobiol*. **1992**, *55*, 931-948.
8. T. K. Chandrashekar, S. Venkatraman, *Acc. Chem. Res*. **2003**, *36*, 676-691.
9. J.-Y. Shin, K. S. Kim, M.-C. Yoon, J. M. Lim, Z. S. Yoon, A. Osuka, D. Kim, *Chem. Soc. Rev*. **2010**, *39*, 2751-2767.
10. S. K. Pushpan, T. K. Chandrashekar, *Pure Appl. Chem.*, **2002**, *74*, 2045-2055.
11. J. L. Sessler, S. J. Weghorn, Expanded, contracted & isomeric porphyrins. Elsevier: **1997**; Vol. 15.
12. A. Jasat, D. Dolphin, *Chem. Rev*. **1997**, *97*, 2267-2340.
13. M. Gouterman, G. H. Wagniére, L. C. Snyder, *J. Mol. Spectrosc.* **1963**, *11*, 108-127.
14. P. Rothemund, *J. Am. Chem. Soc*. **1935**, *57*, 2010-2011.

15. A. D. Adler, F. R. Longo, J. D. Finarelli, J. Goldmacher, J. Assour, L. Korsakoff, *J. Org. Chem*. **1967**, *32*, 476.
16. J. S. Lindsey, I. C. Schreiman, H. C. Hsu, P. C. Kearney, A. M. Marguerettaz, *J. Org. Chem*. **1987**, *52*, 827-836.
17. V. J. Bauer, D. L. J. Clive, D. Dolphin, J. B. Paine, F. L. Harris, M. M. King, J. Loder, S. W. C. Wang, R. B. Woodward, *J. Am. Chem. Soc*. **1983**, *105*, 6429-6436.
18. X.-D. Xu, J. Zhang, L.-J. Chen, R. Guo, D.-X. Wang, H.-B. Yang, *Chem. Commun*. **2012**, *48*, 11223-11225.
19. H. Yorimitsu, A. Osuka, *Asian J. Org. Chem*. **2013**, *2*, 356-373.
20. K. A. D. de Freitas Castro, F. Wypych, A. Antonangelo, K. M. Mantovani, A. Bail, G. M. Ucoski, K. J. Ciuffi, T. E. Cintra, S. Nakagaki, *J. Colloid Interf. Sci*. **2016**, *478*, 374-383.
21. A. W. Johnson, A. Todd, *Vitamins & Hormones* **1957**, *15*, 1-30.
22. A. W. Johnson, R. Price, *J. Chem. Soc*. **1960**, 1649-1653.
23. Z. Gross, N. Galili, I. Saltsman, *Angew. Chem. Int. Ed*. **1999**, *38*, 1427-1429.
24. H. Furuta, T. Asano, T. Ogawa, *J. Am. Chem. Soc*. **1994**, *116*, 767-768.
25. P. J. Chmielewski, L. Latos-Grażyński, K. Rachlewicz, T. Głowiak, *Angew. Chem. Int. Ed. Engl*. **1994**, *33*, 779-781.
26. R. Kumar, R. Misra, T. K. Chandrashekar, *Org. Lett*. **2006**, *8*, 4847-4850.
27. E. Pacholska-Dudziak, M. Szczepaniak, A. Książek, L. Latos-Grażyński, *Angew. Chem. Int. Ed*. **2013**, *52*, 8898-8903.
28. J. L. Sessler, D. Seidel, *Angew. Chem. Int. Ed*. **2003**, *42*, 5134-5175.
29. S. Saito, A. Osuka, *Angew. Chem. Int. Ed*. **2011**, *50*, 4342-4373.
30. T. D. Lash, *Chem. Eur. J*. **1996**, *2*, 1197-1200.

31. T. D. Lash, *Eur. J. Org. Chem*. **2007**, 5461-5481.

32. T. D. Lash, *Chem. Asian J.* **2014**, *9*, 682-705.

33. M. Stępień, L. Latos-Grażyński, *Acc. Chem. Res*. **2005**, *38*, 88-98.

34. K. Berlin, E. Breitmaier, *Angew. Chem., Int. Ed. Engl*. **1994**, *33*, 1246-1247.

35. M. Stępień, L. Latos-Grażyński, *Chem. Eur. J*. **2001**, *7*, 5113-5117.

36. M. Stępień, L. Latos-Grażyński, *J. Am. Chem. Soc*. **2002**, *124*, 3838-3839.

37. M. Stępień, L. Latos-Grażyński, L. Szterenberg, J. Panek, Z. Latajka, *J. Am. Chem. Soc*. **2004**, *126*, 4566-4580.

38. T. D. Lash, A. M. Young, J. M. Rasmussen, G. M. Ferrence, *J. Org. Chem.* **2011**, *76*, 5636-5651.

39. B. Szyszko, L. Latos-Grażyński, L. Szterenberg, *Chem. Commun.* **2012**, *48*, 5004-5006.

40. B. Adinarayana, A. P. Thomas, P. Yadav, V. Mukundam, A. Srinivasan, *Chem. Eur. J*. **2017**, *23*, 2993-2997.

41. D. C. Hodgkin, J. Kamper, J. Lindsey, M. MacKay, J. Pickworth, J. Robertson, C. B. Shoemaker, J. White, R. Prosen, K. Trueblood, In the Structure of Vitamin B12. An Outline of the Crystallographic Investigation of Vitamin B12, Proceedings of the Royal Society of London A: Mathematical, Physical and Engineering Sciences, The Royal Society: **1957**; pp 228-263.

42. B. Franck, A. Nonn, *Angew. Chem. Int. Ed.* **1995**, *34*, 1795-1811.

43. A. Johnson, I. Kay, *J. Chem. Soc*. **1965**, 1620-1629.

44. R. Paolesse, F. Sagone, A. Macagnano, T. Boschi, L. Prodi, M. Montalti, N. Zaccheroni, F. Bolletta, K. M. Smith, *J. Porphyrins Phthalocyanines*, **1999**, 3, 364-370.

45. M. J. Broadhurst, R. Grigg, G. Shelton, A. W. Johnson, *J. Chem. Soc., Perkin Trans. 1*, **1972**, 143-151.

46. Y. S. Balazs, I. Saltsman, A. Mahammed, E. Tkachenko, G. Golubkov, J. Levine, Z. Gross, *Magn. Reson. Chem*. **2004**, *42*, 624-635.

47. H. R. Harrison, O. J. R. Hodder, D. C. Hodgkin, *J. Chem. Soc. B* **1971**, 640.

48. R. Paolesse, S. Mini, F. Sagone, T. Boschi, L. Jaquinod, D. J. Nurco, K. M. Smith, *Chem. Commun*. **1999**, 1307-1308.

49. D. T. Gryko, K. Jadach, *J. Org. chem*. **2001**, *66*, 4267-4275.

50. I. Aviv-Harel, Z. Gross, *Chem. Eur. J.* **2009**, *15*, 8382-8394.

51. Z. Gross, *J. Biol. Inorg. Chem*. **2001**, *6*, 733-738.

52. L. Simkhovich, A. Mahammed, I. Goldberg, Z. Gross, *Chem. Eur. J*. **2001**, *7*, 1041-1055.

53. J. H. Palmer, M. W. Day, A. D. Wilson, L. M. Henling, Z. Gross, H. B. Gray, *J. Am. Chem. Soc.* **2008**, *130*, 7786-7787.

54. A. Mahammed, I. Giladi, I. Goldberg, Z. Gross, *Chem. Eur. J*. **2001**, *7*, 4259-4265.

55. J. Bendix, I. J. Dmochowski, H. B. Gray, A. Mahammed, L. Simkhovich, Z. Gross, *Angew. Chem. Int. Ed.* **2000**, *39*, 4048-4051.

56. A. Mahammed, Z. Gross, *J. Inorg. Biochem*. **2002**, *88*, 305-309.

57. S. Will, J. Lex, E. Vogel, H. Schmickler, J. -P. Gisselbrecht, C. Haubtmann, M. Bernard, M. Gorss, *Angew. Chem. Int. Ed. Engl*. **1997**, *36*, 357-361.

58. K. M. Kadish, C. Erben, Z. Ou, V. A. Adamian, S. Will, E. Vogel, *Inorg. Chem.* **2000**, *39*, 3312-3319.

59. K. E. Thomas, A. B. Alemayehu, J. Conradie, C. Beavers, A. Ghosh, *Inorg. Chem*. **2011**, *50*, 12844-12851.

60. C. Brückner, C. A. Barta, R. P. Brinas, J. A. K. Bauer, *Inorg. Chem*. **2003**, *42*, 1673-1680.

61. Z. Ou, C. Erben, M. Autret, S. Will, D. Rosen, J. Lex, E. Vogel, K. M. Kadish, *J. Porphyrins Phthalocyanine*s, **2005**, *9*, 398-412.

62. F. Jérôme, B. Billier, J. M. Barbe, E. Espinosa, S. Dahaoui, C. Lecomte, R. Guilard, *Angew. Chem. Int. Ed*. **2000**, *39*, 4051-4053.

63. S. Licoccia, R. Paolesse, E. Tassoni, F. Polizio, T. Boschi, *Dalton Trans*. **1995**, 3617-3621.

64. E. Vogel, M. Bröring, J. Fink, D. Rosen, H. Schmickler, J. Lex, K. W. K. Chan, Y.-D. Wu, D. A. Plattner, M. Nendel, K. N. Houk, *Angew. Chem. Int. Ed. Engl*. **1995**, *34*, 2511-2514.

65. R. Misra, T. K. Chandrashekar, *Acc. Chem. Res*. **2008**, *41*, 265-279.

66. N. Sprutta, L. Latos-Grażyński, *Chem. Eur. J*. **2001**, *7*, 5099-5112.

67. S.-D. Jeong, J. L. Sessler, V. Lynch, C.-H. Lee, *J. Am. Chem. Soc*. **2008**, *130*, 390-391.

68. H. Rexhausen, A. Gossauer, *J. Chem. Soc., Chem. Commun*. **1983**, 275.

69. A. Gossauer, *Bull. Soc. Chim. Belg*. **1983**, *92*, 793-795.

70. J. L. Sessler, S. J. Weghorn, Y. Hiseada, V. Lynch, *Chem. Eur. J*. **1995**, *1*, 56-67.

71. J. L. Sessler, D. Seidel, V. Lynch, *J. Am. Chem. Soc*. **1999**, *121*, 11257-11258.

72. Y. Rao, W. Zhou, L. Xu, M. Zhou, B. Yin, T. Tanaka, A. Osuka, J. Song, *J. Am. Chem. Soc.* **2019**, *141*, 18836-18844.

73. Y. Kamimura, S. Shimizu, A. Osuka, *Chem. Eur. J*. **2007**, *13*, 1620-1628.

74. J. L. Sessler, T. Morishima, V. Lynch, *Angew. Chem. Int. Ed. Engl*. **1991**, *30*, 977-980.

75. J. L. Sessler, S. J. Weghorn, V. Lynch, M. R. Johnson, *Angew. Chem. Int. Ed. Engl*. **1994**, *33*, 1509-1512.

76. T. D. Lash, D. T. Richter, *J. Am. Chem. Soc*. **1998**, *120*, 9965- 9966.

77. R. J. P. Corriu, G. Bolin, J. J. E. Moreau, C. Vernhet, *J. Chem. Soc., Chem. Commun.* **1991**, 211-213.

78. B. Szyszko, N. Sprutta, P. Chwalisz, M. Stępień, L. Latos-Grażyński, *Chem. Eur. J*. **2014**, *20*, 1985-1997.

79. M. Stępień, L. Latos-Grazyński, N. Sprutta, P. Chwalisz, L. Szterenberg, *Angew. Chem. Int. Ed*. **2007**, *46*, 7869–7873.

80. B. Adinarayana, M. Das, C. H. Suresh, A. Srinivasan, *Chem. Eur. J*. **2019**, *25*, 4683 – 4687.

81. M. Das, B. Adinarayana, M. Murugavel, S. Nayak, A. Srinivasan, *Org. Lett.* **2019**, *21*, 2867−2871.

CHAPTER 2

Stabilization of Rh(I) and Organo-Rh(III) Complexes by 6,11,16-Triarylbiphenylcorrole with an adj-CCNN Core

2.1 Introduction

2.1.1 Corrole analogues

Porphyrin macrocycles contain four pyrrole units connected by four *meso*-carbon atoms, however eliminating 1 of them *meso*-carbone in a porphyrn skeleton leads to porphyrinoids such as corrole (NNNN).[1,2,3,6] The term "corrole" was coined by Johnson and Price due to its structural resemblance with the naturally occuring corrin ring, found in vitamin B_{12}.[4,5] Corrole is also an 18 π-electronic aromatic macrocycle which acts as a trianionic ligand and stabilize the unusually high oxidation state transition metal ions. It has wide application ranging from catalysis to sensors and most importantly dye-sensitized solar cells.[6] Structural modification alters the electronc structure of parent corrole, thus leads to optical, photophyical and cordination properties.[7] In order to achieve such properties, several core-modified corroles have been synthesized. The modified corrole analogues are *iso*-carbacorrole,[8] N-confused derivative,[9] norrole,[10] benzonorrole,[11] oxacorrole,[12] dioxacorrole,[13] and thiacorrole.[14]

2.1.2 Carbacorroles

Among corrole analouges, carbacorroles with CNNN in the inner core are less known in the literature. Few reported carbacorroles include isocarbacorrole,[8] N-confused corroles,[9] norrole and benzonorrole (Figure 2.1).[11] The nonaromatic N-confused corrols attach affectively through anions[9] while isocarbacorrole stabilize Orgaeno-Cu(3) and Ag(3) complexes.[8] Norroles also show versatile coordination chemistry and anion binding ability.[9] Benzonorrole forms organometallic Ir(III) complexes which exhibits near-infrared phosphoresence at room temperature.[36]

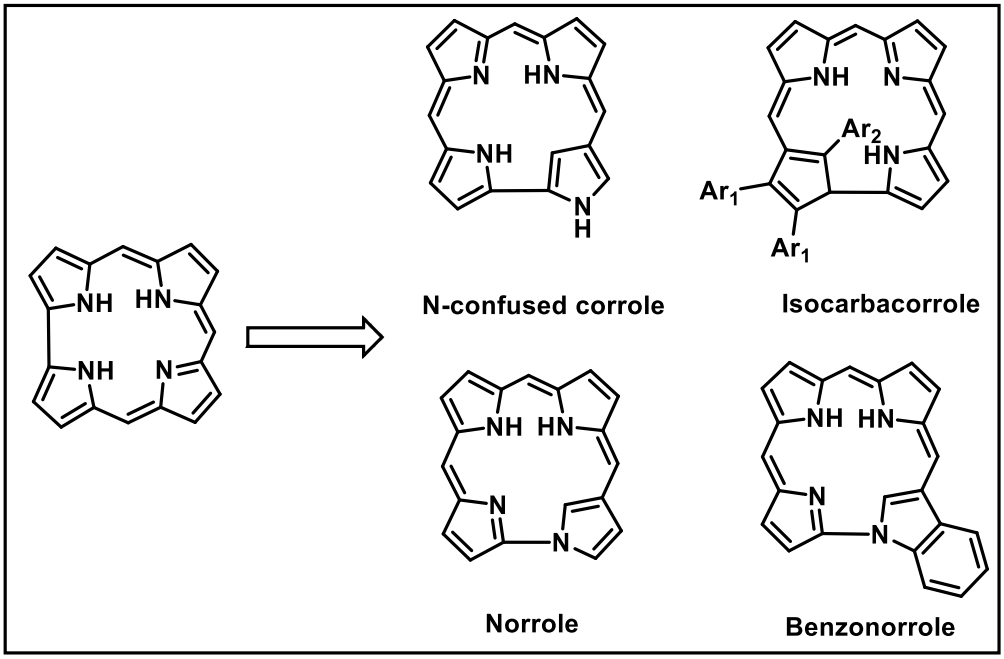

Figure 2.1: Structures of carbacorrole analogues.

By replacing one more N-atoms by C-atom in the carbacorrole leads to the formation of dicarbacorrole **1**. Such macrocycle was reported by our group. The macrocycle was acheved by bipyrole moiety in the corrole framework with a biphenyl unit. Analyses charaterization reveled that the macrocycle was found nonaromatic in nature. The core was effectively utilized to stabilize organo-Cu(III) complex **2**.[15] (Figure 2.2) The stabilization of higher oxidation state in such a core could be an ideal platform to coordinate various other metal in different oxidation states.

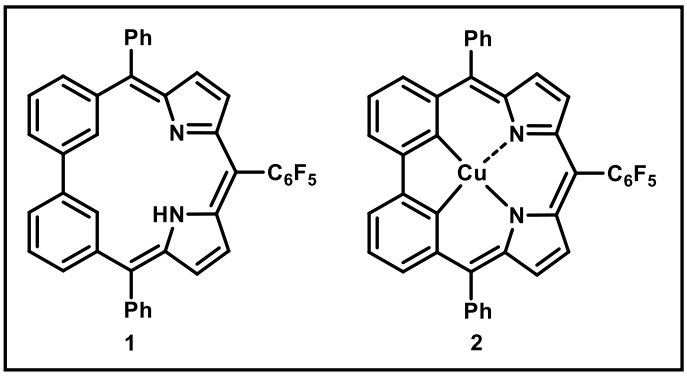

Figure 2.2: Structures of dicarbacorrole (**1**) and Cu(III) complex (**2**).

Later, Sessler and co-workers reported bis-dicarbacorrole[16] **3**. It was synthesised by incoporating a dibenzo[g,p]chrysene moiety in macrocyclic structure. The two trianionic core in the freebase were stabilized by two Cu(III) ions (**4**) and a Cu & a Pd (**5**) ions. The hetro bis-metal complex (**5**) exhibits organic π-radical charactr (Figure 2.3).

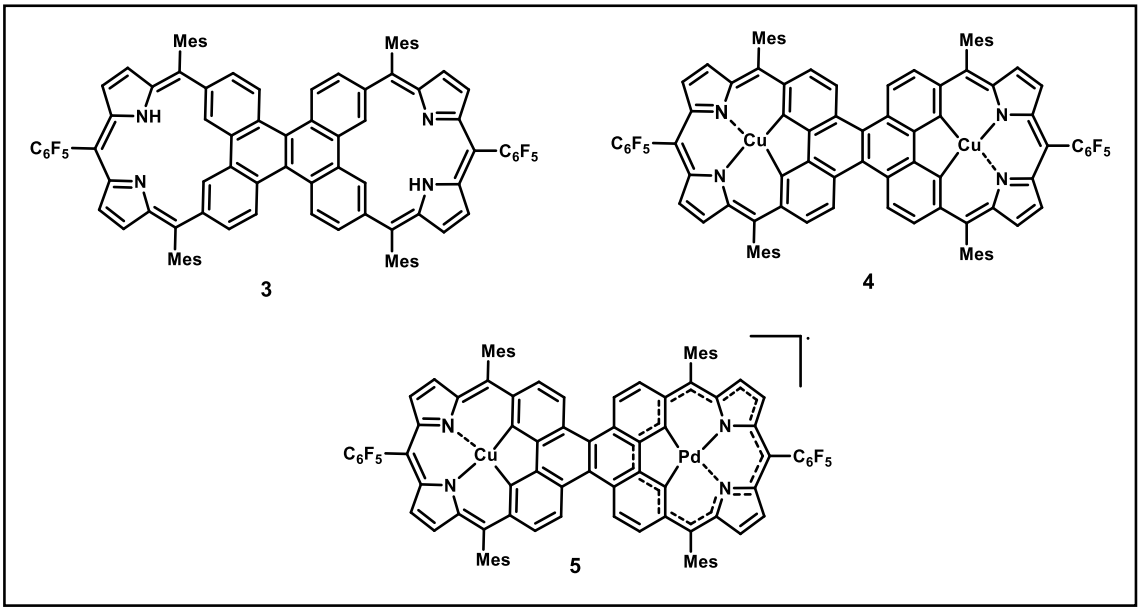

Figure 2.3: Structures of dicarbacorrole (**3**), Cu(III) complex (**4**) and Cu(III).Pd(II) complex (**5**).

Recently, azulene incorporated corrole has been introduced by Ghosh and co-workers.[17] The azulicorrole **6** was synthesized by condensation of pyrole, 4-trifluoromethylbenzaldehyde and azulene followed by (DDQ) oxidation. The coordination chemistry was further performed with Cu(II) and Au(III) salts and afforded Cu in +3 oxidation state **7** and Au in +3 oxidation state **8** complexes (Scheme 2.1)

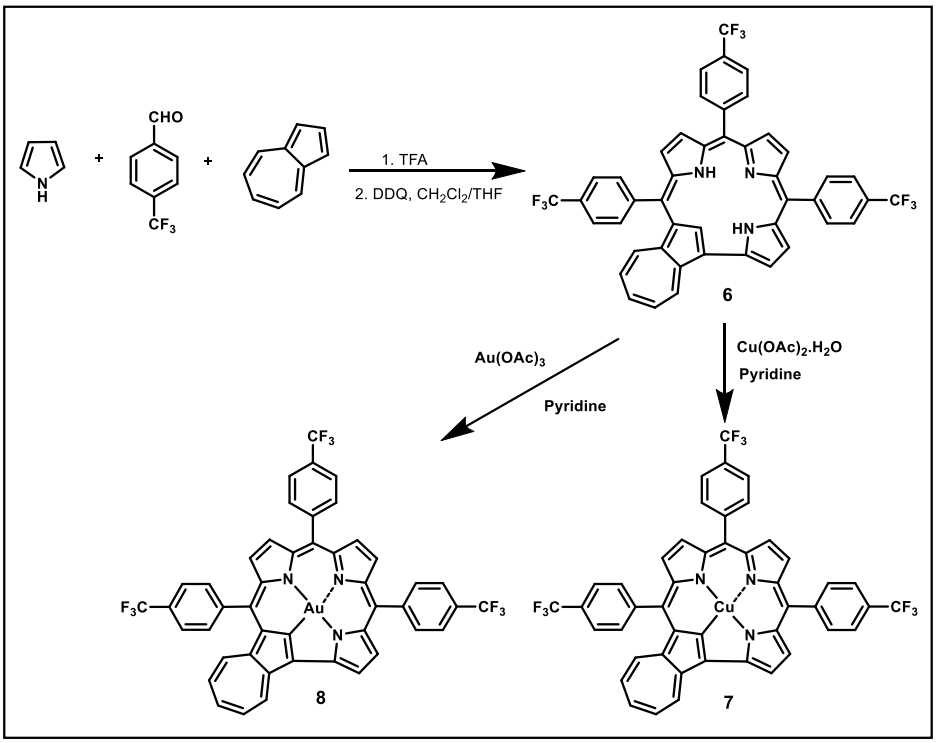

Scheme 2.1: Synthesis of **6**, **7** and **8**.

2.2 Objective of our work

The chemistry of Rh ion inserted corrole complexes are now well documented in the literature.[18-24] But Rh metal ion stabilization with higher oxidation state using carba porphyrinoids are quite sparse.[25,26,31] Functionalization of hydrocarbons by selective CHA by transiton-metal complees is a significant area of resarch in organometalic chemistry.[27-29] There are plethora of examples, where Rh(III) porphyrins have demonstrated for proficient and selective carbon-hydrogen activation. The Rh(I) and Rh(III) complexes were reported by Zeev Gross and co-workers. The Rh(I) complexes (**10a**–**c**) were obtained by refluxing dichloromethane soluton of **9** with $[Rh(CO)_2Cl]_2$. One of the Rh(I) intermediate (**10c**) was further oxidized in presnce of exces $P(C_6H_{11})_3$ and afforded Rh(III) complex (**10d**) (Schem 2.2).[30]

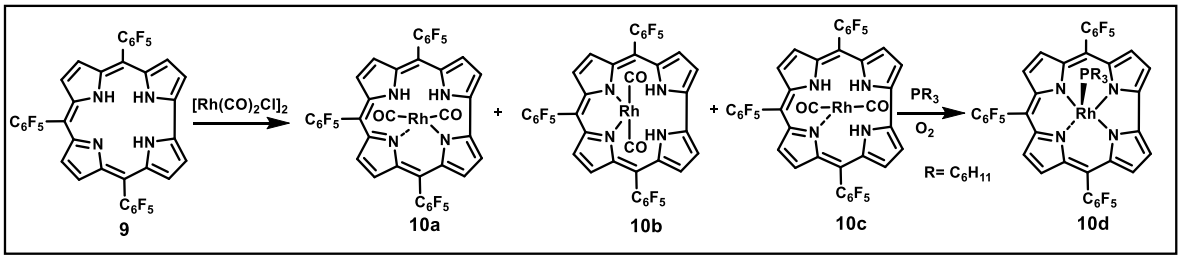

Schem 2.2: Synthes of Rh(III) corrole complxes (**10**).

The Rh(III) complex was further reported by the same group under different reaction condition.[30] Zeev Gross and coworkers synthesized Rh(I) and Rh(III) corroles which were utilized as carbene transfer catalysts.[21] Both the complexes were obtained by using tris(pentafluorophenyl)corrole **9**. Its reaction with phosgene afforded the chiral derivative **12**. The insertion of Rh into **12** arise the rhodium(I) complex **13a** and **13b**. The bis(pyridine) rhodium (III) corrole **14** was obtained through metal insertion in the freebase corrole **9** with pyridine. The Rh(III) corrole **15** with the cordinated non-racemic **16**, was synthesized from **9** where the coordination was performed in benzene and 500 mol% of **16**. (Scheme 2.3) Hence, it is noteworthy to mention that higher oxidation state of rhodium metal complexes can act as prudent catalyst for several type of reactions.

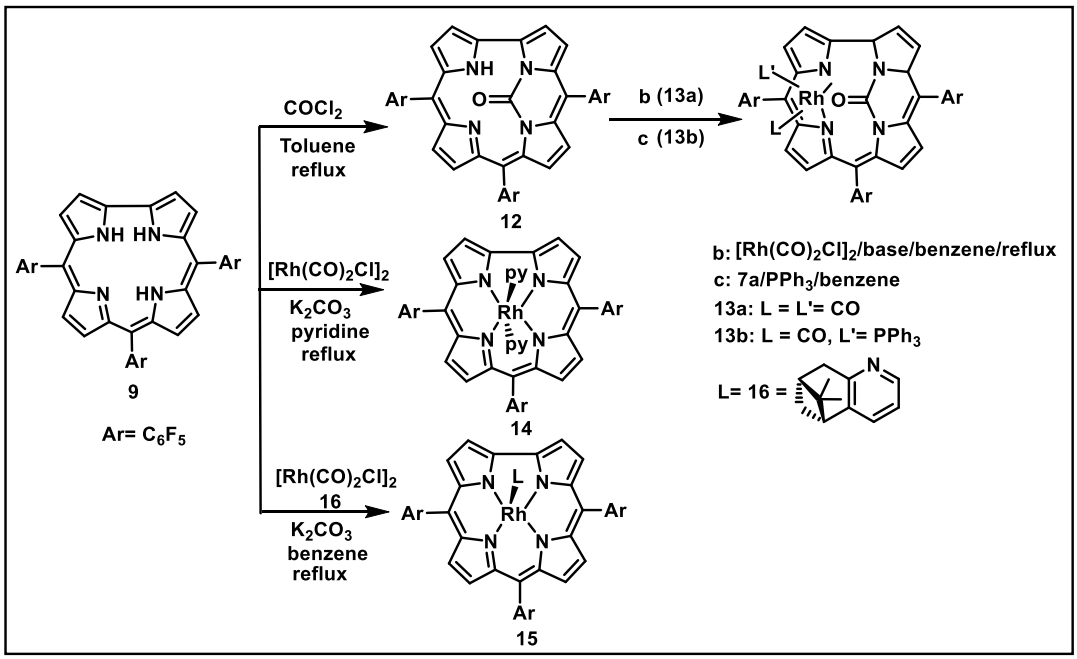

Scheme 2.3: Synthesis of Rh(I) (**13 a** and **b**) and Rh(III) corrole complexes (**14** and **15**).

As compared to Rh(I) and Rh(III) corrole complexes, the respective metal ion inserted carba analogues are less known in literature. Here, we desire to report the synthesis, structures properties of Rh(I) **17** and Rh(III) **18** *adj*-dicarbacorrole complexes (Figure 2.4), where the monoanoinic and trianionic core of **1** is successfully stabilized by Rh metal ion for the first time.

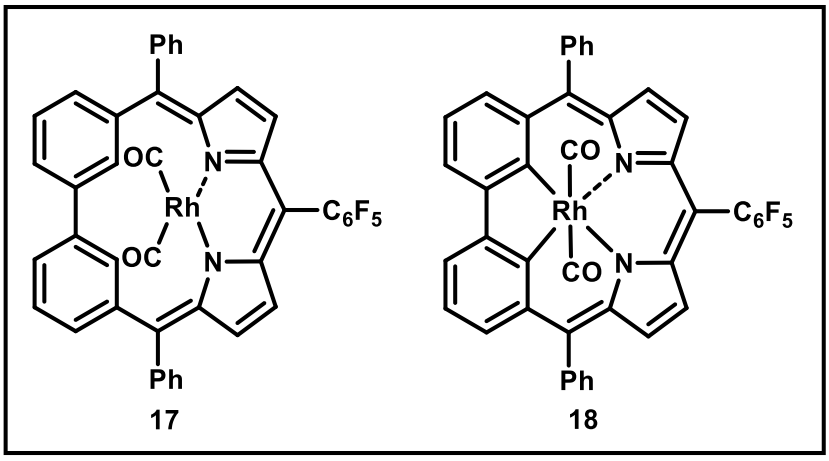

Figure 2.4: Structures of Rh(I) (**17**) and Rh(III) (**18**) dicarbacorrole complexes.

2.3 Results and discusions

2.3.1 Synthesis

The cordination chemistry of **1** was performd by (i) trating a DCM solutn of **1** with $[Rh(CO)_2Cl]_2$ in mthanol and aforded **17** in 30% yield and (ii) the insrtion of Rh(III) was achievd by reflxing an acetonitrile soluton of **1** with same rhodium salt for 8 hours (Scheme 2.4) and obtained organometallic complex **18** in 11% yield.

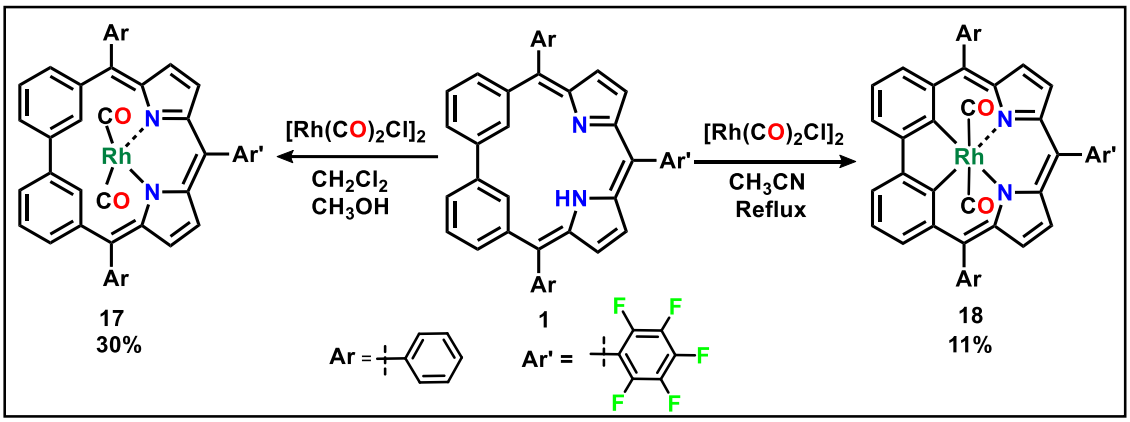

Scheme 2.4: Synthesis of **17** and **18**.

2.3.2 Spectral Characterization

2.3.2.1 Mass spectrometric analysis

The molecular composition of **17** and **18** was confrmed by mass spctrometric anlysis. Rh(I) complex (**17**) showed moleculr signal at *m/z*: 797.0741 [M +1] corresponding to the chmical fomula $C_{43}H_{22}F_5N_2O_2Rh$ (Figure 2.5) whereas Rh(III) complex (**18**) was identified with the mass peak at 766.0554 [M-CO] ($C_{42}H_{20}F_5N_2ORh$; Figure 2.6). It can be envisaged from the mass patern that compond **18** might have an octahdral geometry with two axialy cordinated carbonyl liands.

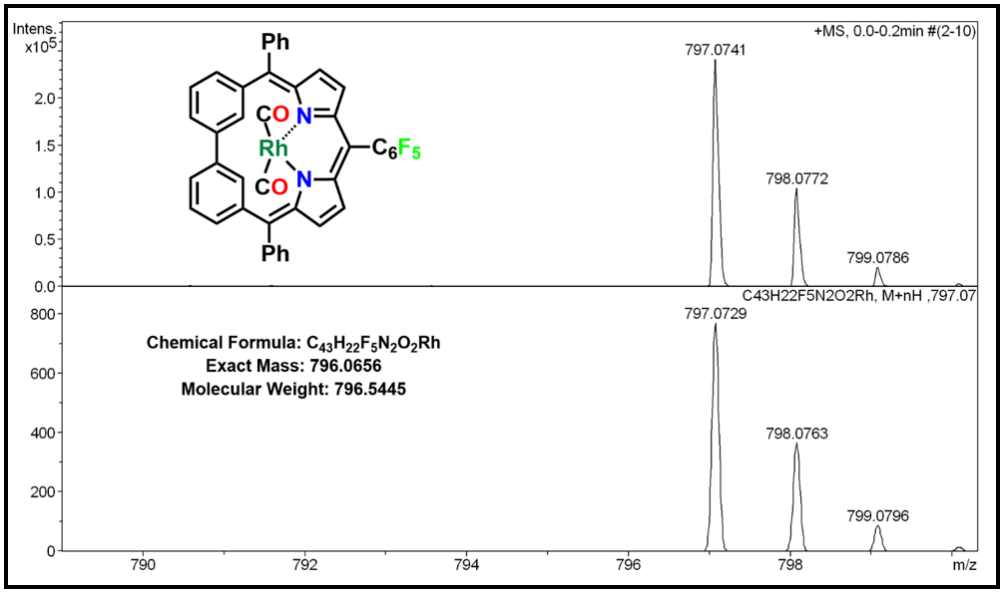

Figure 2.5: ESI-MS spectrum of **17**.

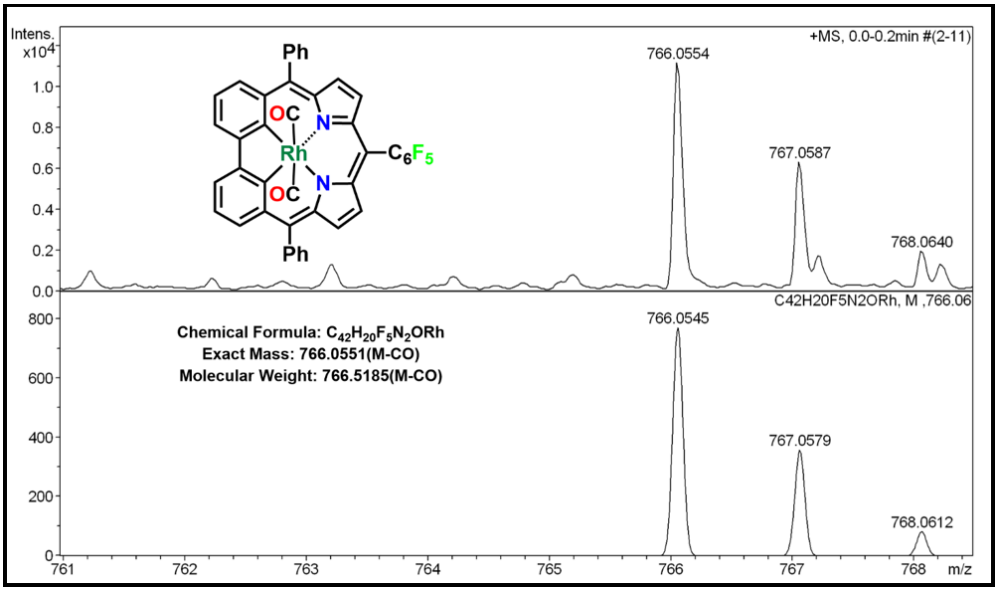

Figure 2.6: ESI-MS spectrum of **18**.

2.3.2.2 NMR analysis

The ^{1}H NMR spectral analyses of **17** and **18** in CD_2Cl_2 at room temperature are shown in Figure 2.7. Both the complexes are highly symmetric and exhibit only half of the signals. In complex **17** (Figure 2.7a), there are four doublets in the region between 6.48 and 8.11 ppm, where the inital 2 doublts at 6.48 [H(21,33)] and 6.93 ppm

[H(22,32)] are pyrrolic β-CH protons. The other 2 doublts at 7.11 [H(2,10)] and 8.11 ppm [H(4,8)] correspond to the peripheral CH protons of biphenyl moiety, where the remaining outer biphenyl CH [H(3,9)] protons were peak on 7.53 ppms. Disappearance NH signal and present of 2 inner *m*-phnylene CH protns [(6,12)] at 8.86 ppms confirms that there cordination occus only in the dipyrromethane moity.

Whereas, the disappearance of both NH and inner *m*-phenylene CH protons [H(6,12)] suggest the formation of organo-Rh(III) complex (**18**) (Figure 2.7b) and reveal the different mode of binding as compared to **17**. The biphenyl protons in **18** are resonated as doublet at 8.03 [H(4,8)] & 7.64 ppm [H(2,10)] and as a multiple at 7.60 ppm [H(3,9)]. The prrolic β-CHs protos apear as pair doublts at 7.18 [H(22,32)] and 7.01 ppm [H(21,33)]. Overall, the spectra in **17** and **18** bear analogy with typical non-aromtic characterstics, obsrved in *m*-benziporphyrnoids.[15]

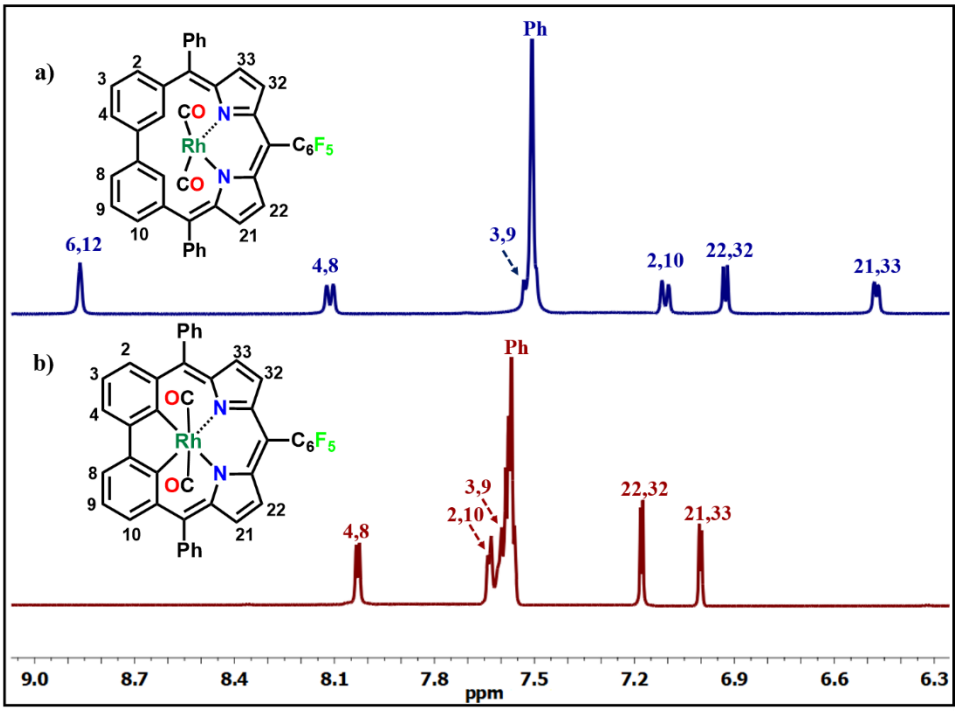

Figure 2.7: ^{1}H-NMR spectra of **17** (a) and **18** (b) in CD_2Cl_2 at 298 K.

2.3.2.3 Crystal structure and analys of 17 and 18.MeOH

The molecular structure of **17** and **18** were unambigously verified by crystal analyses and show in Figure 2.8. The crystal data is presented in Table 2.2. The crystls of **17** were grwn by slow evaporationa DCM soluton in hexane and crystallized in monoclnic crystal latice with $P2_1/n$ space grop (Figure 2.8a-d). As envisioned from the spectral analyses, the dipyrromethene unit is coordinated with $Rh(CO)_2$ unit, where the bond lenghs of Rh1-N1 and Rh1-N2 are 2.09(2) and 2.090(1) Å respectively (Figure 2.10) and mentioned values are comparable with Rh(I) complex of *m*-benziporphyrinoids.[32] The Rh(I) ion is projected above the mean macrocyclic plane containing 15 inner atoms with a distance of 1.50 Å and the geometry of the complex is square planar. The biphenyl moiety and pyrrole ring [N2] are slightly deviated from the mean plane with the dihedral angle of 14.92(4)º and 11.25(6)º, whereas pyrrole ring [N1] is tilted by 24.60(5)º. These results are further reflected from the saddling dihedral angle values as shown in Table 2.1. The crystal analyses reveal that one of the inner CH (C6-H6) protons of the biphenylne units develop weak anagostic interactions with Rh(I) ion. The bond length & angle of C6-H6···Rh1 is 2.679(3) Å & 110.76(1)º respectively (Figure 2.8a).[33] Also compound **17** generates four different types of self-asembled dimers by H-bonding and Ph(π)-Ph(π) interactions as shown in Figure 2.9.

On the other hand, crystals of **18.MeOH** were obtained in a CH_2Cl_2/MeOH solvent mixture of **18** and shown in Figure 2.8 c-d. The complex was crystallized in triclnic crystal latice with *C*2/c space grp. In the molecular structure of **18.MeOH**, Rh(III) ion is present exctly at the centr of the ligad and located 0.08 Å above the mean plane. The geomtry surround the metalion is octahdral wth a basel plan contaning N1-Rh1-N2, C12-Rh1-N1, C12-Rh1-C6 and C6-Rh1-N2 angles of 90.18(1)º, 92.81(2)º, 84.13(2)º and 92.63(2)º and the Rh1-C6, Rh1-C12, Rh1-N2, Rh1-N1 bond lengths are

2.006(5) Å, 2.027(5) Å, 2.064(4) Å and 2.045(4) Å, respectively (Figure 2.11). The bond length values of Rh1-N1 and Rh1-N2 are slighty longer thn that of the reportd Rh(III) corroles[34] but akin to Rh(III) benzocarbaporphyrin.[25] One of the axial position is occupied by carbonyl ligand with the bond distance of Rh1-C43 is 1.819(5) Å, whereas an additional axial coordination site is occupied by MeOH and the coordination is observed between Rh1 and O1 with bond distance of 2.159(4)Å. In contrast to **17**, the biphenyl moiety and pyrrole rings in **18.MeOH** are not that deviatio from a meen planin with maxima deviaton of the biphenyl moiety by 3.10(7)° which reveals that the complex is almost planar. These results are further confirmed by the saddling dihedral angle values (Table 2.1). The saddling dihedral angles of **17** (χ1–χ4) (Figure 2.12) are between 11.55(3) and 75.50(4)º (Table 2.1) which are comparable with reported rhodium(I) corrole[22] and moderately higher than rhodium(I) complex of carbachlorin[37] whereas, the saddling dihedral angles of **18.MeOH** (χ1–χ4) (Figure 2.12) are from 0.22(1) to 2.76(1)° (Table 2.1), which are far less than **17** and akin to rhodium(III) complex of carbachlorin[37] but reasonably lower than rhodium(III) corrole.[34]

Furthermore, the crystal analyses of **17** and **18.MeOH** reveal that (i) the bond lengths of the dipyrromethene units take alternatively an sp^2-sp^2 single (1.462(8) Å) and double (1.336(8) Å) bond character; (ii) the phenylene unit is connected with another phenylene unit and the dipyrromethene units with sp^2-sp^2 single bond character (1.484(3) Å); and (iii) the bond lenths with the phenylen unts of the biphenyl moieties exhibit the sp^2-sp^2 double bond character (1.366(9)-1.430(8) Å). Overall, the π-conjugation of the biphenl unit is maintained by its indivdual aromatic character and did not participate overall macrocyclic aromaticity, thus both **17** and **18.MeOH** displayed nonaromatic character as reflected from the NMR spectral analyses.

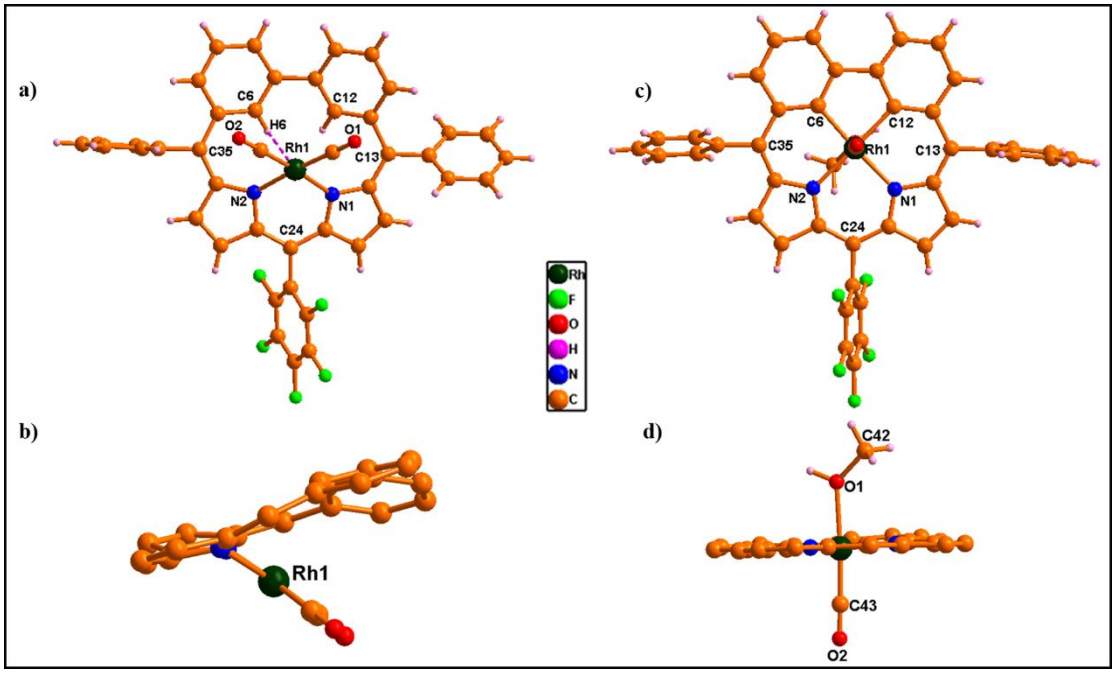

Figure 2.8: Crystal X-ray structures of **17** and **18.MeOH**. a) & c) Top and b) & d) side views.

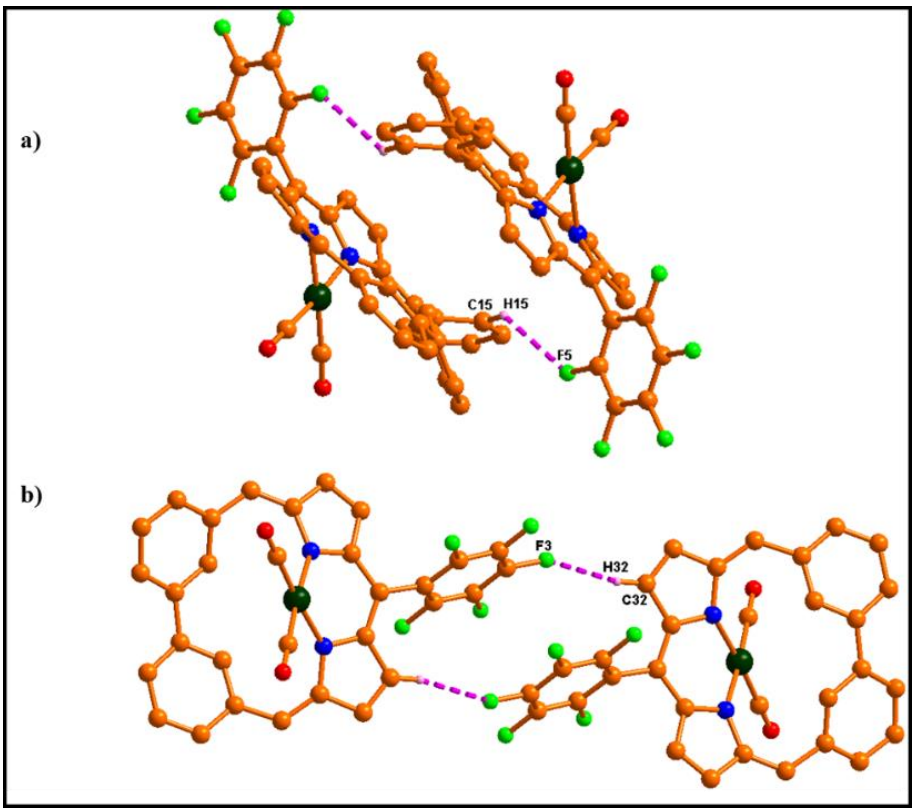

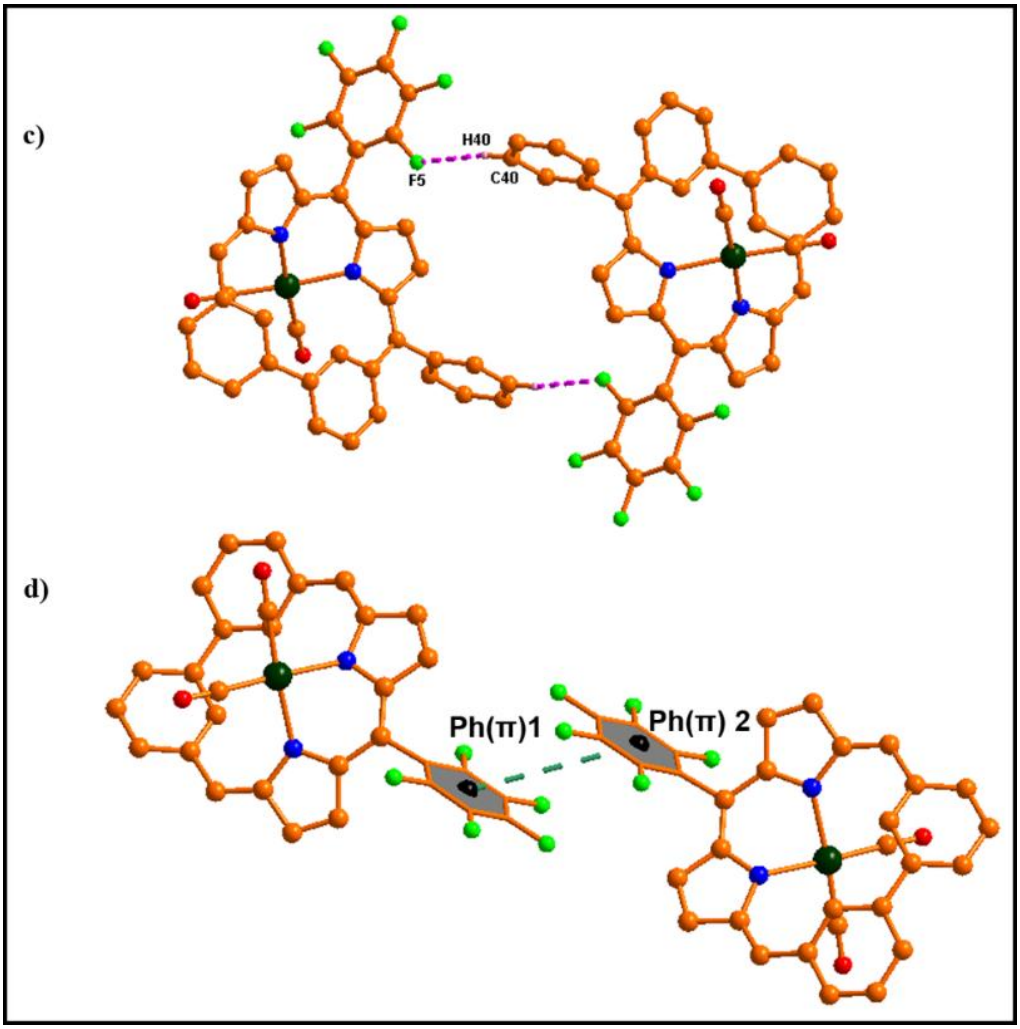

Figurre 2.9: Crystal analysis of **17**. a), b), c), d) are Self-asembled dimers. The bond dstances and angls are: a) C15-H15…F5: 2.706(1) Å & 130.03(1)°; b) C32-H32…F3: 2.821(1) Å & 157.84(1)°; c) C40-H40…F5: 2.591(1) Å & 167.04(2)°; d) Ph(π)1 - Ph(π)2: 4.856(2) Å respectively.

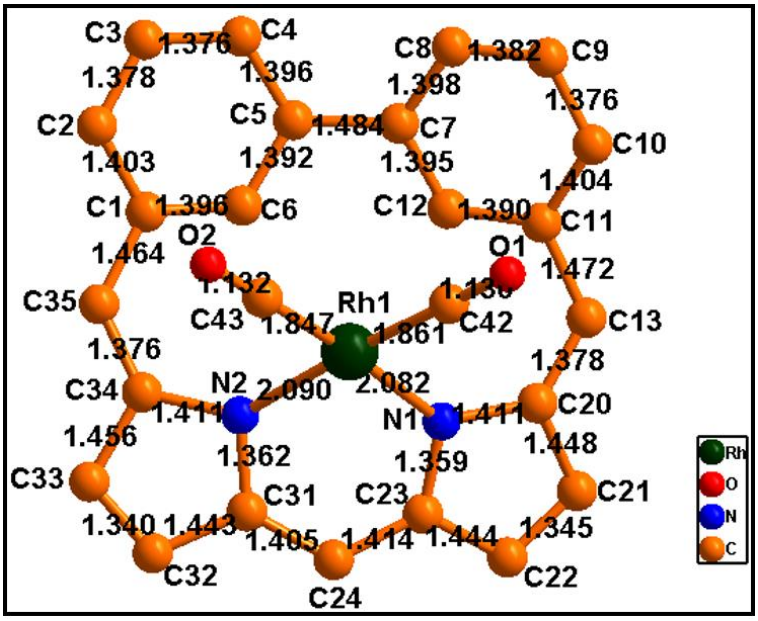

Figure 2.10: Bond lengths of **17** in (Å).

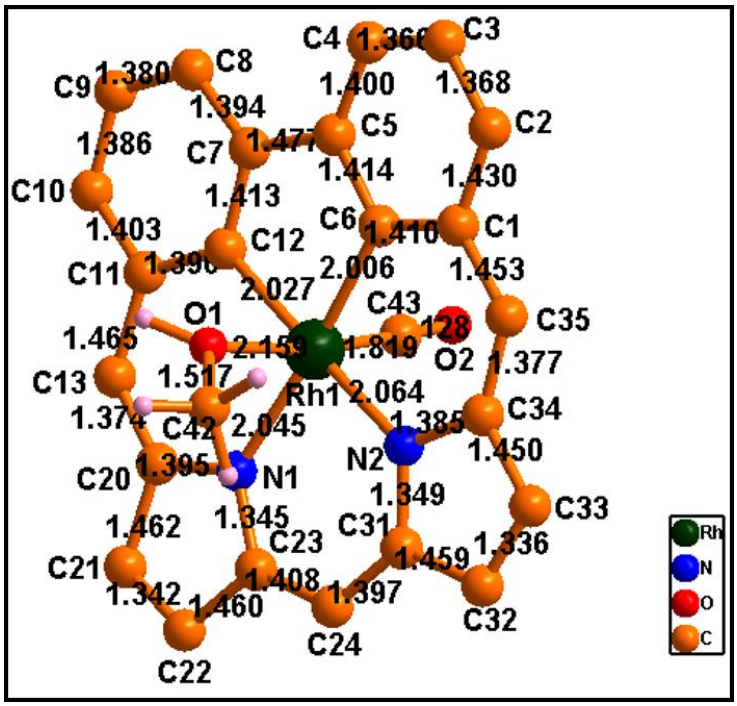

Figure 2.11: Bond lengths of **18.MeOH** in (Å).

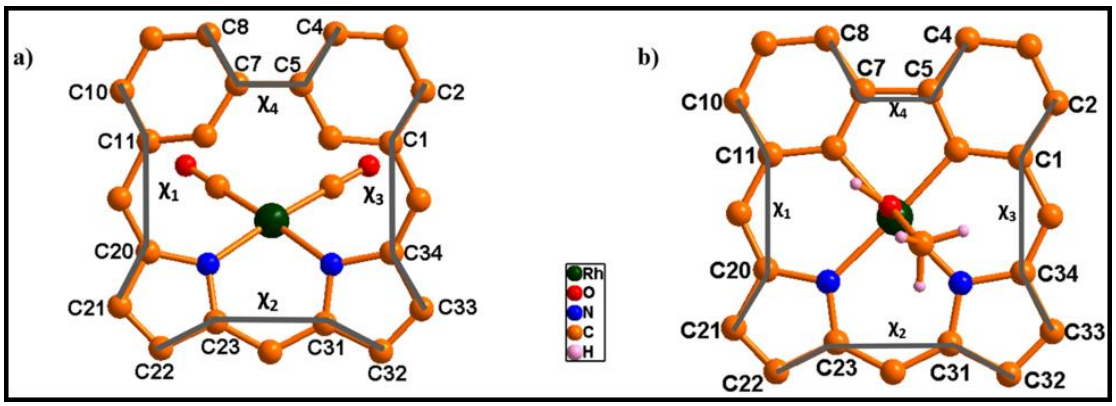

Figure 2.12: Saddling dihedral angles of **17** and **18.MeOH**.

Table 2.1. Saddling dihedral angle (°) in **17** and **18.MeOH**.

χ	**Saddling dihedral angle**	**17(°)**	**18.MeOH (°)**
χ_1	C8-C7-C5-C4	11.55(3)	2.49(9)
χ_2	C10-C11-C20-C21	75.50(4)	0.22(1)
χ_4	C22-C23-C31-C32	12.55(6)	0.83(1)
χ_5	C2-C1-C34-C33	47.02(5)	2.76(1)

Table 2.2: Crystal data for **17** and **18.MeOH**:

Crystal parameters	**17**	**18.MeOH**
Formula	$C_{43}H_{22}F_5N_2O_2Rh$	$C_{43}H_{24}F_5N_2O_2Rh$
M/g mol^{-1}	796.53	798.55
T/K	296.15 K	293K
Crystal dimensions/mm^3	0.15 × 0.08 × 0.07	0.25 × 0.18 × 0.11
Crystal system	monoclinic	monoclinic
Space group	$P2_1/n$	$C2/c$
a/Å	13.1238(5)	19.7163(5)
b/Å	18.9177(7)	11.2311(3)
c/Å	14.5904(5)	35.7344(9)
α/°	90	90
β/°	105.390(2)	91.062(2)
γ/°	90	90
V/Å^3	3492.5(2)	7911.5(4)
Z	4	1
ρ_{calcd}/g m^{-3}	1.515	1.341
μ/mm^{-1}	0.557	4.007
F(000)	1600.0	3216.0
Reflns. collected	58685	31592
Indep.reflns.[R(int)]	9807 [0.0575]	7063 [0.0759]
Max/min transmission	0.962 and 0.948	0.644 and 0.442
Data/restraints/parameters	9807/0/478	7063/2/481
GOF on F^2	1.045	1.062
Final R indices[$I > 2\sigma(I)$]	R_1 = 0.0355, wR_2 = 0.0873	R_1 = 0.0748, wR_2 = 0.1753
R indices (all data)	R_1 = 0.0594, wR_2 = 0.1017	R_1 = 0.0824, wR_2 = 0.1788
Largest diff peak and hole [e Å^{-3}]	0.50 and -0.68	1.53 and -1.06

2.3.2.4 Electronic absorption and emission spectral analysis:

The UV spectrum of **17** and **18** was recorded in dichloromthane and showed in Figure 2.13. Their molar extinctin coeficients are given in Table 2.3 and the values in **17** are approximately twelve times lower as compared to **18**. In **17** three bands were observed at 364, 390 and 742 nm. In contrst, **18** exhibis cut high intense bands at 375 and 389 nm and promient bands 597 and 648 nm along with shoulder band at 769 nm.

The spectrum pattern is compared with and bathochromicaly shifting with respct to the 2 bands of Rh(3) corole.[35]

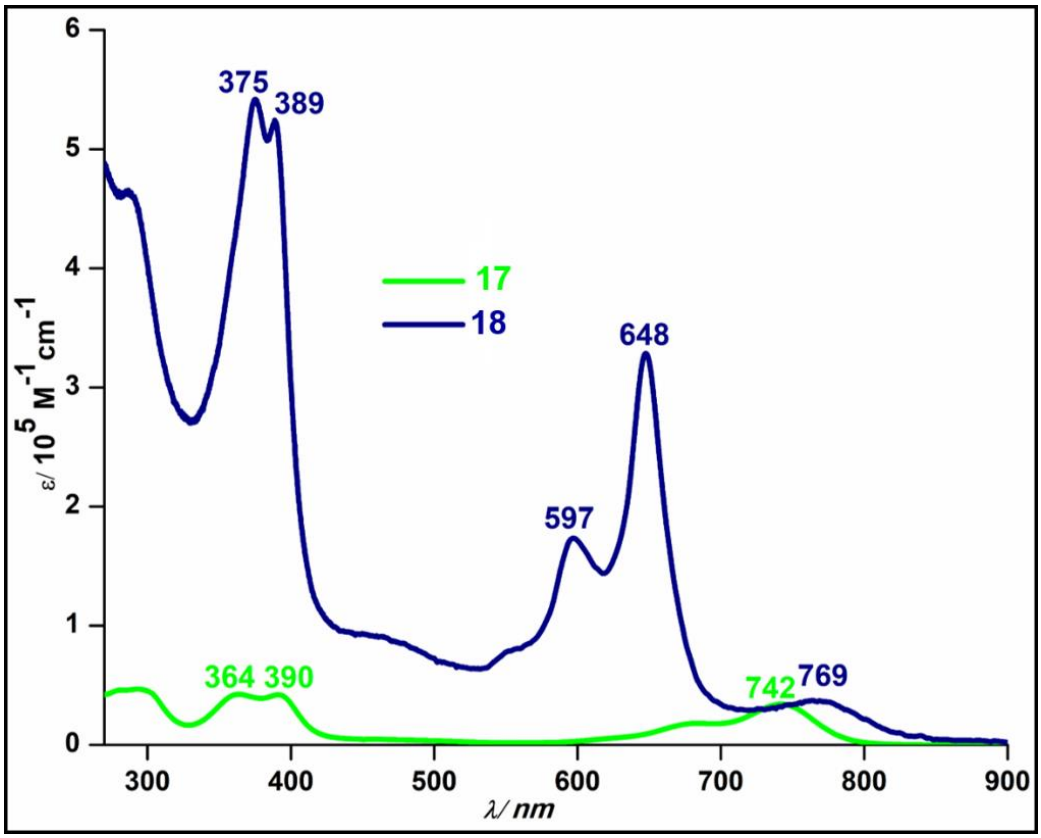

Figure 2.13: UV absorption of **17** and **18** in CH_2Cl_2.

Table 2.3. UV absorption spectrum data of **17** and **18** (concentration ≈ 10^{-6} M)

Compounds	λ_{max}/nm (ε[$M^{-1}cm^{-1}$]x10^5)
17	364 (0.42), 390 (0.41), 742 (0.34)
18	375 (5.41), 389 (5.23), 597 (1.73), 648 (3.26), 769 (0.03)

2.3.2.5 Electrochemical analyse:

The electrochemical properties of **1**, **17** and **18** have investgated by cyclic voltammetry and diferential pulse voltametry in a dichlormethane solutin having 0.1 M tetrabutylamonium hexafluorophoshate ($TBAPF_6$) as the suporting electrolyte and shown in Figure 2.15 (Table 2.5). Compound **1** exhibits three distinct oxidation potentials with a reversible peak at 0.17 V, two irreversible peaks at 0.48 and 0.85 V and one quasi-reversible reductin potential at -1.63 V. The oxidation potentals of **1** are remniscent to the oxidatin potentials of fre-base dicarbacorrole (**3**).[16] The Rh(I) complex **17** possess a quasi-revesible and an irreversible oxidation potential at 0.06 and 0.75 V and a quasi- reduction peak at -1.71 V. On the other hand, the Rh(III) complex **18** exhibits an irreversible oxidation and reduction peaks at -0.19 and -1.82 V. Interestingly we observed that the redox potential peak is metal centric. The eletrochemical HOMO−LUMO of **1**, **17** and **18** were calcuated and found to be 1.80, 1.77 and 1.63 V, respectively. (Table 2.5)

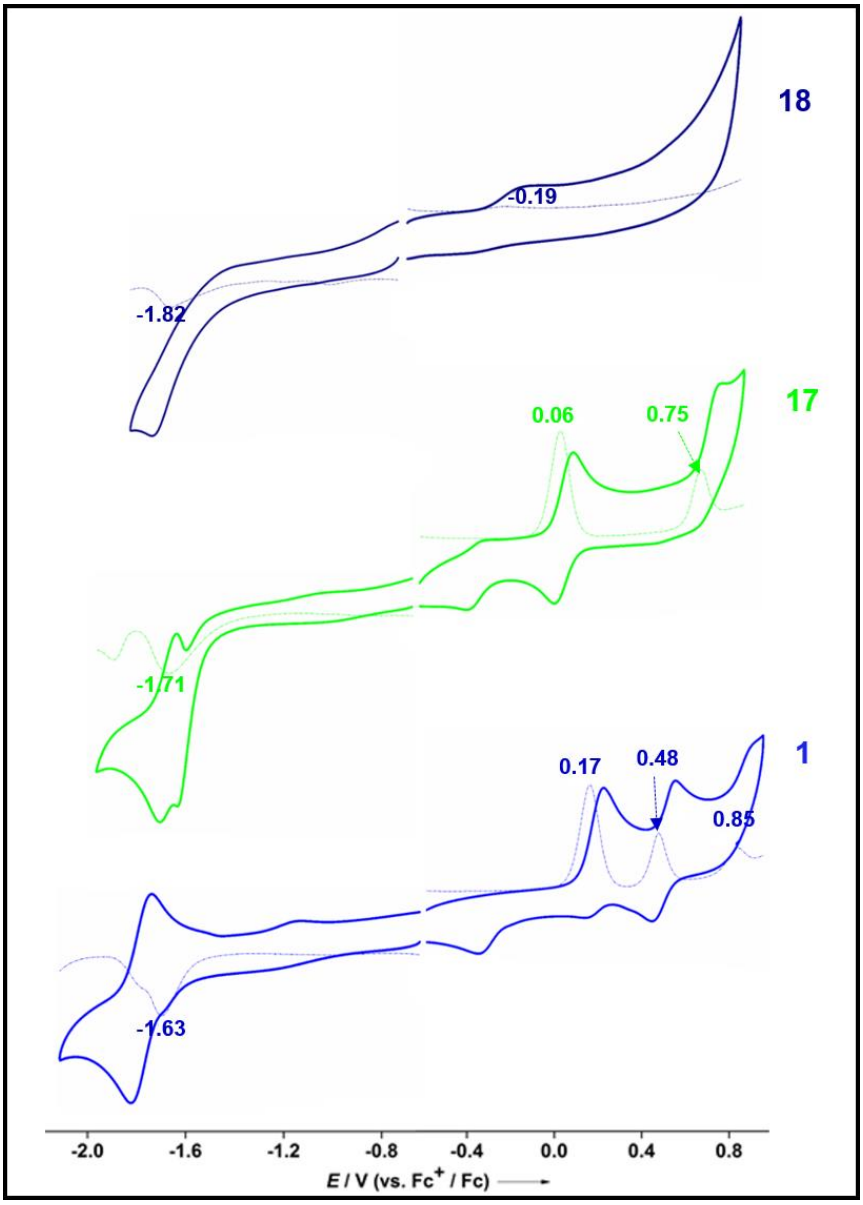

Figure 2.14. Cyclic (_) and differential pulse (....) voltammograms of **1**, **17** and **18**.

Table 2.4. Electrochemical data of **1**, **17** and **18**.

Compound	E_{ox3}	E_{ox2}	E_{ox1}	E_{Red1}	ΔE_{HL}(V)
1	0.85	0.48	0.17	-1.63	1.80
17	---	0.75	0.06	-1.71	1.77
18	---	---	-0.19	-1.82	1.63

2.4 Conclusion

Overall, we have sucessfully presented the coordination versatility of 6,11,16-triarylbiphenylcorrole by using $[Rh(CO)_2Cl]_2$ salt. The *adj*-CCNN core of dicarba corrole was effectively utilized to stabilize Rh ion in two different oxidation states. The dipyrromethene unit bound with Rh(I) ion in square planar geometry, whereas, Rh(III) ion is coordinated in the inner core to form organo-Rh(III) complex in octahedral geometry. The spectra and structure analys revealed that both complexs adopted nonaromatc characteristics.

2.5 Experiment Section

2.5.1 General Information

The regents for the synthsis was applied from Sigmaa Aldrch chemcal supliers. All solvent and dry by clean process before use. NMR solvens were as receved and spectrum was shown in Bruker 700 and 400 MHz spectromeer with Tetramethylsilane as standard. Mass spectrum were obtained in Bruker, micro-TOF-QII mass spectrometer. The electronic absorption spectra were recorded in Jasco V-730 UV-Visible spectrophotometer. Electrochemical studies of **17** and **18** were carried out on a CHI1120A instrument in DCM with 0.1 M *n*-Bu_4NPF_6 as suporting electrolyte. Potentials were determined vs ferrocene/ferrocenium ion by cyclic and differential pulse voltammograms using a 3 electrodes tier, which consist of a platinm disc as the workig electrode, a pt wires as there countr electrode, and Ag/AgCl as the refeence electrodes. Crystal X- ray difraction data of **17** was colected in a Bruker KAPPA APEX-II and **18** was collected in Rigaku Oxford diffractometer.

2.5.2 Synthetic procedure and spectral characterization

2.5.2.1 Synthesis of 17: Compound **1** (0.01 g, 0.015 mmol) was dissolved in 20 mL CH_2Cl_2 and 10 mL methanol. 21 μL of triethylamine was poured into the reaction mixture under N_2 atmosphere. After 5 min, $[Rh(CO)_2Cl]_2$ (17 mg, 0.04 mmol) was aded and stired for 12 hours at room temp. The crude reacn mixture was passed through neutral alumina. Green colour part was elute with 5% CH_2Cl_2/*n*-hexane and identified as **17**. Compound further recrystalized from CH_2Cl_2/*n*-hexane to afford green crystalline solid **17** in 30% (4 mg, 0.004 mmol) yield.

^{1}H NMR (400 MHz, CD_2Cl_2, 298K): δ = 8.86 (s, 2H), 8.11 (d, *J* = 7.7 Hz, 2H), 7.53 (m, 2H), 7.51-7.49 (m, 10H), 7.11 (d, *J* = 7.8 Hz, 2H), 6.93 (d, *J* = 5.1 Hz, 2H), 6.48 (d, *J* = 5.0 Hz, 2H).

^{13}C NMR (101 MHz, CD_2Cl_2): δ = 183.81, 183.05, 162.07, 157.17, 141.52, 139.12, 137.82, 137.13, 135.33, 131.39, 129.86, 128.97, 128.36, 127.92, 126.58, 123.28.

ESI-MS: *m/z* calculated for $C_{43}H_{22}F_5N_2O_2Rh$ = 796.0656; found = 797.0741 [M+1].

UV-Vis (CH_2Cl_2): λ_{max}/nm (ε/$M^{-1}cm^{-1}$): 364 (0.42×10^5), 390 (0.41×10^5), 742 (0.34×10^5).

2.5.2.2 Synthesis of 18: Compund **1** (0.01 g, 0.015 mmol) was disolved in 6 mL CH_3CN. $[Rh(CO)_2Cl]_2$ (24 mg, 0.06 mmol) was then aded to the soln. within N_2 environment. The rean was allowed refluxing for 8 h. Crude part mixture was passed through neutral alumina column and the blue fraction was obtained with 30% CH_2Cl_2/*n*-hexane. A Blue crystalline solid was obtained in CH_2Cl_2/*n*-hexane and identified as **18** in 11% (1 mg, 0.001 mmol).

^{1}H NMR (700 MHz, CD_2Cl_2, 298K): δ = 8.03 (d, *J* = 7.4 Hz, 2H), 7.64 (d, *J* = 7.2 Hz, 2H), 7.60 (m, 2H), 7.59 – 7.57 (m, 10H), 7.18 (d, *J* = 4.9 Hz, 2H), 7.01 (d, *J* = 4.9 Hz, 2H).

^{13}C NMR (176 MHz, CD_2Cl_2): δ = 153.76, 152.72, 146.79, 141.09, 138.59, 137.20, 135.86, 131.86, 131.70, 131.01, 128.31, 127.78, 127.62, 127.52, 125.36, 119.65.

ESI-MS: *m/z* calculated for $C_{42}H_{20}F_5N_2ORh$ = 766.0551 (M-CO); found = 766.0554 [M-CO].

UV-Visible (deuterated dcm): λ_{max}/nm (ε/$M^{-1}cm^{-1}$): 375 (5.41×10^5), 389 (5.23×10^5), 597 (1.73×10^5), 648 (3.26×10^5), 769 (0.03×10^5).

2.6 References

1. Z. Gross, N. Galili, I. Saltsman, *Angew. Chem. Int. Ed*. **1999**, *38*, 1427-1429.
2. I. A. -Harel, Z. Gross, *Chem. Eur. J.* **2009**, *15*, 8382-8394.
3. R. Orłowski, D. Gryko, D. T. Gryko, *Chem. Rev.* **2017**, *117*, 3102−3137.
4. A. Johnson, R. Price, *J. Chem. Soc.* **1960**, 1649-1653.
5. A. Johnson, A. Todd, *Vitamins & Hormones*. **1957**, *15*, 1-30.
6. L. Flamigni, D. T. Gryko, *Chem. Soc. Rev.* **2009**, *38*, 1635-1646.
7. H. L. Buckley, J. Arnold, *Dalton Trans.* **2015**, *44*, 30-36.
8. J. Skonieczny, L. Latos-Grażyński, L. Szterenberg, *Chem. Eur. J.* **2008**, *14*, 4861-4874.
9. K. Fujino, Y. Hirata, Y. Kawabe, T. Morimoto, A. Srinivasan, M. Toganoh, Y. Miseki, A. Kudo, H. Furuta, *Angew. Chem. Int. Ed.* **2011**, *50*, 6855-6859.
10. M. Toganoh, Y. Kawabe, H. Furuta, *J. Org. Chem.* **2011**, *76*, 7618-7622.
11. M. Toganoh, Y. Kawabe, H. Uno, H. Furuta, *Angew. Chem. Int. Ed.* **2012**, *51*, 8753-8756.
12. C. H. Lee, W. S. Jo, J. W. Ga, H. J. Kim, P. H. Lee, *Bull. Korean Chem. Soc.* **2000**, *21*, 429-433.
13. M. Pawlicki, L. Latos-Grażyński, L. Szterenberg, *J. Org. Chem.* **2002**, *67*, 5644-5653.

14. V. S. Shetti, U. R. Prabhu, M. Ravikanth, *J. Org. Chem.* **2010**, *75*, 4172-4182.
15. B. Adinarayana, A. P. Thomas, C. H. Suresh, A. Srinivasan, *Angew. Chem. Int. Ed.* **2015**, *54*, 10478-10482.
16. X. -S. Ke, Y. Hong, P. Tu, Q. He, V. M. Lynch, D. Kim, J. L. Sessler, *J. Am. Chem. Soc.* **2017**, *139*, 15232-15238.
17. S. Larsen, L. J. M. -McPherson, S. J. Teat, A. Ghosh, *ACS Omega* **2019**, *4*, 6737-6745.
18. R. Grigg, J. T. -Grimshaw, V. Viswanatha, *Tetrahedron Lett.* **1976**, *17*, 289-292.
19. A. M. Abeysekera, R. Grigg, J. T. -Grimshaw, V. Viswanatha, *J. Chem. Soc., Perkin Trans. 1* **1977**, 36-44.
20. S. J. Thompson, M. R. Brennan, S. Y. Lee, G. Dong, *Chem. Soc. Rev.* **2018**, *47*, 929-981.
21. I. Saltsman, L. Simkhovich, Y. Balazs, I. Goldberg, Z. Gross, *Inorg. Chim. Acta*. **2004**, *357*, 3038-3046.
22. I. Saltsman, Y. Balazs, I. Goldberg, Z. Gross, *J. Mol. Catal. A: Chem*. **2006**, *251*, 263-269.
23. A. Srinivasan, M. Toganoh, T. Niino, A. Osuka, H. Furuta, *Inorg. Chem*. **2008**, *47*, 11305-11313.
24. T. Boschi, S. Licoccia, R. Paolesse, P. Tagliatesta, *Inorg. Chim. Acta* **1988**, *141*, 169-171.
25. V. A. K. Adiraju, G. M. Ferrence, T. D. Lash, *Dalton Trans*. **2016**, *45*, 13691-13694.
26. L. M. Stateman, G. M. Ferrence, T. D. Lash, *Organometallics* **2015**, *34*, 3842-3848.

27. X. Zhou, R. -J. Wang, F. Xue, T. C. W. Mak, K. S. Chan, *J. Organomet. Chem.* **1999**, *580*, 22-25.

28. Y. W. Chan, K. S. Chan, *Organometallics* **2008**, *27*, 4625-4635.

29. K. S. Chan, P. F. Chiu, K. S. Choi, *Organometallics*, **2007**, *26*, 1117-1119.

30. L. Simkhovich, A. Mahammed, I. Goldberg, Z. Gross, *Chem. Eur. J*. **2001**, *7*, 1041-1055.

31. K. Hurej, M. Pawlicki, L. Szterenberg, L. Latos-Grażyński, *Angew. Chem. Int. Ed.* **2016**, *55*, 1427-1431.

32. M. Das, B. Adinarayana, M. Murugavel, S. Nayak, A. Srinivasan, *Org. Lett.* **2019**, *21*, 2867-2871.

33. F. F. Awwadi, H. A. Hodali, *J. Mol. Struct.* **2018**, *1154*, 373-381.

34. J. P. Collman, H. J. H. Wang, R. A. Decreau, T. A. Eberspacher, C. J. Sunderland, *Chem. Commun*. **2005**, *19*, 2497-2499.

35. J. H. Palmer, A. Mahammed, K. M. Lancaster, Z. Gross, H. B. Gray, *Inorg. Chem.* **2009**, *48*, 9308-9315.

36. Y. K. Maurya, T. Ishikawa, Y. Kawabe, M. Ishida, M. Toganoh, S. Mori, Y. Yasutake, S. Fukatsu, H. Furuta, *Inorg. Chem.* **2016**, *55*, 6223-6230.

37. T. D. Lash, W. T. Darrow, A. N. Latham, N. Sahota, G. M. Ferrence, *Inorg. Chem.* **2019**, *58*, 7511−7526.

CHAPTER 3

Structurally Isomerized Bis-Biphenyl Moieties Embedded in Hexaphyrin(3.1.1.3.1.1) and Octaphyrin(1.1.1.0.1.1.1.0)

3.1 Introduction

Porphyrins are widely studied macrocycles and its unique properties have attracted much attention for the researchers to explore in various field.[1] This motivates to develop the novel porphyrinoids with several distinct types of modifications in the porphyrin core. One of the most important modifications is the porphyrin isomers.[2]

Isomeric porphyrins are porphyrin analogues with same molecular formula and can be obtained by rearranging pyrrole and *meso*-carbons in porphyrin structure. These are classified on the basis of "nitrogen in" and "nitrogen out" isomers. The “nitrogen in” category includes i) porphycene (2.0.2.0) (**1**)[3] ii) corrphycene (2.1.0.1) (**2**)[4] iii) hemiporphycene (2.1.1.0) (**3**)[5] and iv) isoporphycene (3.0.1.0) (**4**)[6] while under the "nitrogen out" category is the N-confused porphyrin (NCP) (**5**)[7,8] (Figure 3.1). These are structural isomers of porphyrin. With the advancement of porphyrin chemistry, the porphyrin skeletal mutated further and by N-Cα connected bonding confusion approach, unprecedented N-linked isomers, trivially known as Neo-confused porphyrinoids had emerged.[9] In this special type of isomers, the nitrogen atom is not part of “in” or “out” arrangement, instead fused with rest of the macrocyclic core. This specific class of isomer comprises Neo-confused porphyrin (**6**) (Figure 3.1).

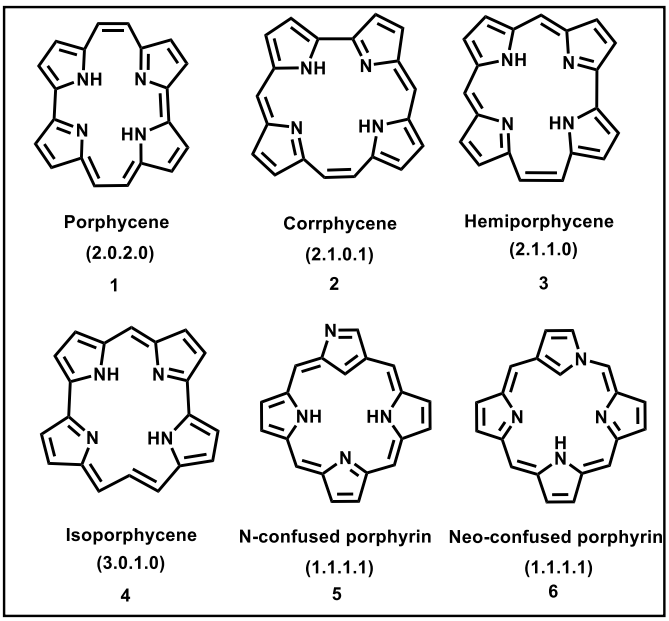

Figure 3.1: Structures of porphyrin isomers.

3.1.1 Expanded porphyrins and their structural isomers:

Expanded porphyrins an intriguing class of functional molecules in view of their striking optical, electrohemical, and cordination properties.[10-14] Varying the bonding mode in macrocyclic framework of expanded porphyrins tends to the formation of its structural isomers thus leading to changes in its properties. These expanded derivatives and their isomers have been frequently reported in the literature, which includes (i) sapphyrin **7**[15] and its N-confused analogues **8**[16] (ii) smaragdyrins **9**[17] and its doubly neo-fused analogues **10**[18] (iii) hexaphryins **11**[19] and their doubly **14**[20] and triply N-confused derivatives **15**[21] (iv) figure-eight octaphyrins **16**[22] and their neo-confused derivative **17**[23] and (v) *p*-*o*-*p*-terphenyl moiety-embedded homoporphyrin **18** and its *m*-*o*-*m* analogue **19**[24] (Figure 3.2). In this chapter we will mainly focus on the hexaphyrins and octaphyrins. Hence, the synthesis of respective macrocycles and its structural analogues are highlighted along with their spectral properties.

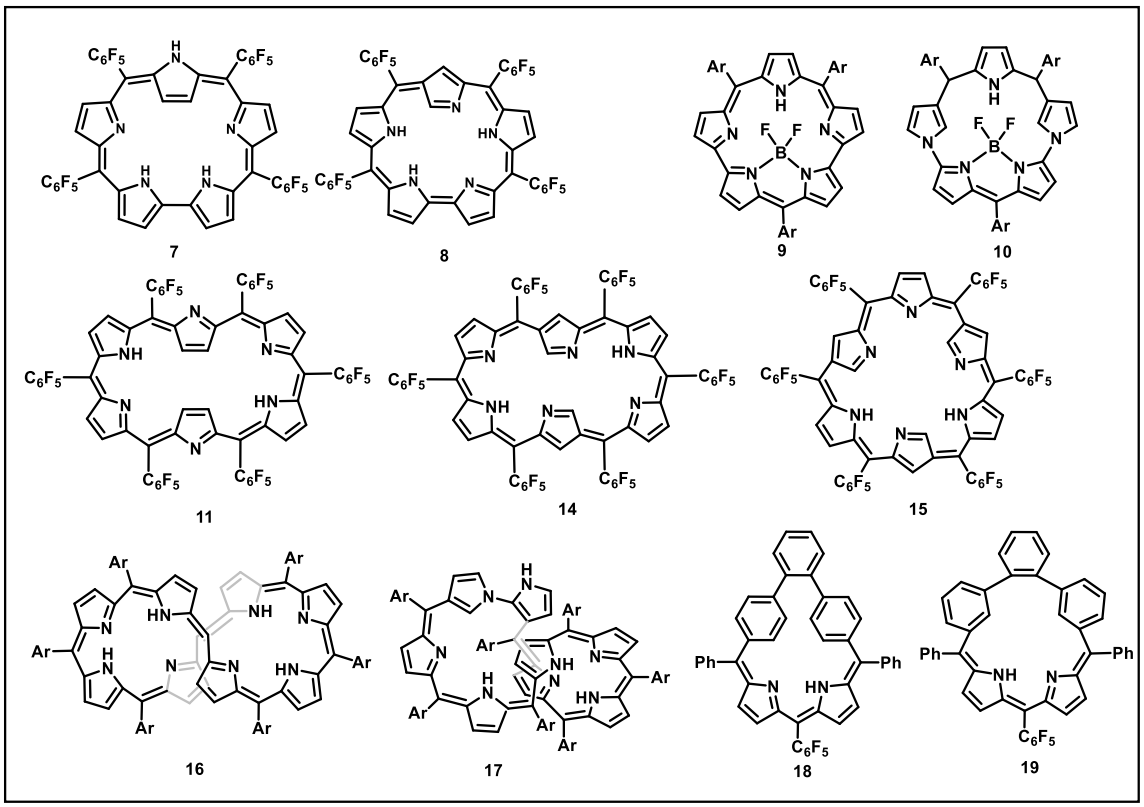

Figure 3.2: Structures of expanded porphyrins and their structural isomers

3.1.1.1 Hexaphyrin and their structural isomers:

Expanded porphyrins connected by *meso*-carbon atoms are called hexaphyrins. The number of *meso*-carbons can be increased or decresed in the hexaphyrin core.[25]

Cavaleiro and co-workers synthesized *meso*-hexa(pentafluorophenyl) hexaphyrins **11** and **12** in 15% and 1% yield respectively.[19] Addition of pentafluorobenzaldehyde to a refluxing mixture of 17(N) acetic acid and nitro benzene, followed by dropwise addition of pyrrole and refluxed further for 45 min led to formation of two different *meso*-hexa(pentafluorophenyl) hexaphyrins as violet (**11**) and bluish (**12**) colored compound (Scheme 3.1). Both the compounds (**11** and **12**) are interconverted by hydrogenation and dehydrogenation process. By reacting **12** with DDQ, compound **11** is obtained and reduction of the **11** with $TsNHNH_2$ gives

compound **12**. The ^{1}H NMR spectral analysis proved that the compound **11** is aromatic, whereas the compound **12** is non/antiaromatic.

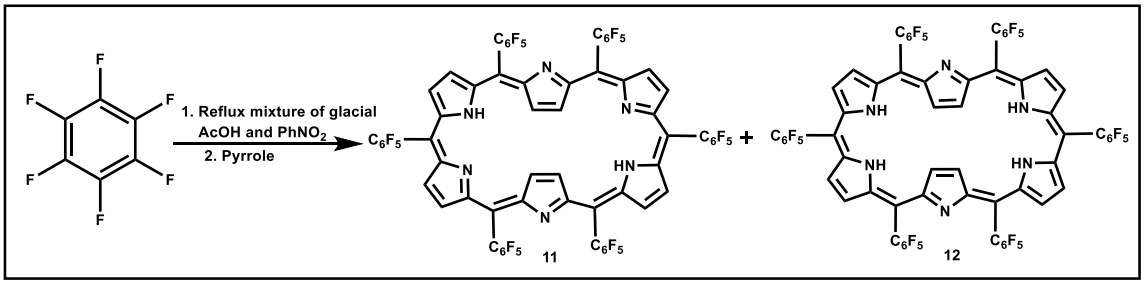

Scheme 3.1: Synthesis of **11** and **12**.

To introduc two confused pyrrol units in normal hexaphyrin framework a doubly N-confused hexaphyrin was introduced by Furuta and co-workers.[20] The doubly N-confused *meso* hexaarylhexaphyrin (**13** and **14**) was synthesized (Scheme 3.2). By treating N-confused tripyrrane **20** with pentafluorbenzaldehyde in the presence of *p*-TSA, followed oxidation with *p*-chloranil to afford **13** and **14** in 7 and 3% yields, respectively. The ^{1}H NMR spectrum of **13** was proved as nonaromatic, whereas **14** was aromatic. The aromatic character of **14** was reflected from the electronic spectral analysis with a strong band at 591 nm and four bands from 650 to 1100 nm.[8] However, **14** was oxidized into its amide form at room temperature.

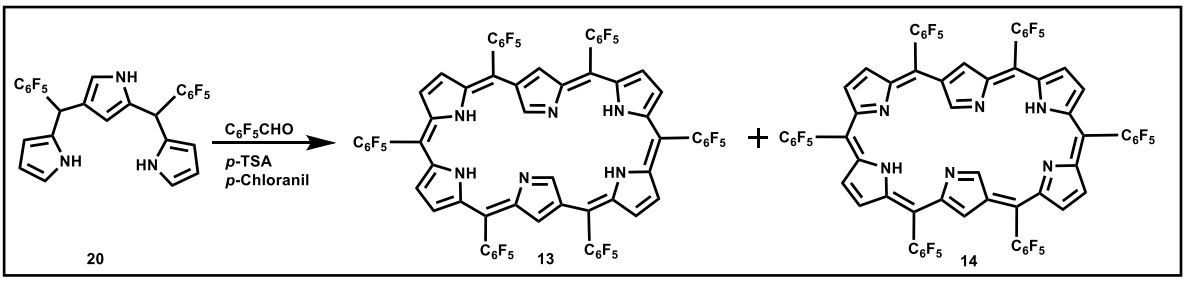

Scheme 3.2: Synthesis of **13** and **14**.

Following the synthesis of C_2 symmetric rectangular shaped doubly N-confused hexaphyrin (**13** and **14**), by introducing three N-confusion in the hexaphyrin skeleton, the same group synthesized triply N-confused meso-pentafluorophenylhexaphyrin **15** in 2009.[21] It was synthesized by an acid-catalyzed [2+2+2] self-condensation of N confused dipyrromethane carbinol **21** followed by oxidation with *p*-chloranil (Scheme 3.3). The spectral analysis revealed that the macrocycle was aromatic. Nevertheless, in terms of stability, it is steadily oxidized to its tri-amide derivative in solution.

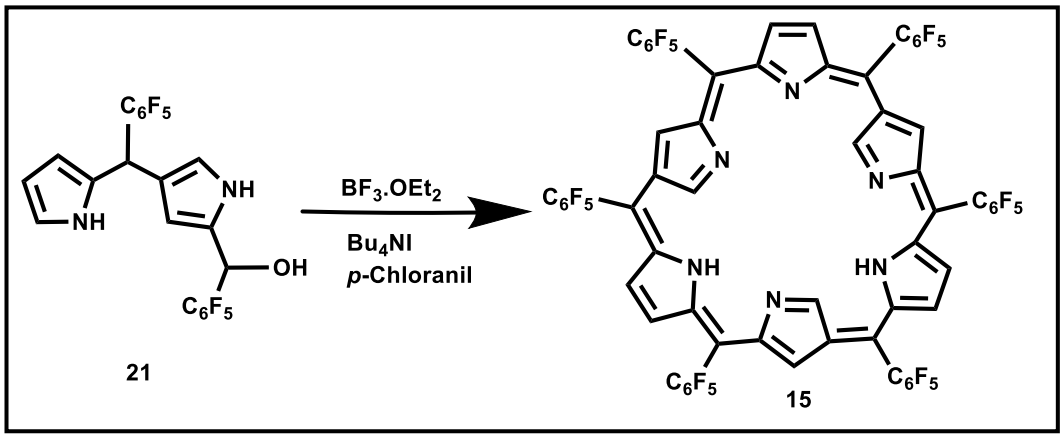

Scheme 3.3: Synthesis of **15**.

3.1.1.2 Octaphyrin and their structural isomers:

The expanded macrocycles with eight pyrrolic/heterocyclic units in the core are linked with eight *meso*-carbon atoms are called octaphyrins. The number of *meso*-carbons can be varied in the core.[25]

The first *meso*-aryl-substituted octaphyrin **16** was synthesized by Osuka and co-workers via condensation of C_6F_5CHO and pyrrole followed by oxidation with DDQ to form **16** (Scheme 3.4).[22] The ^1H NMR spectrum of **16** exhibited four doublets of the β-Hs from 7.67 to 6.11 ppm and two broad signals NHs at 13.25 and 8.59 ppm which suggested that the molecule possess a C_2 symmetric signal pattern with nonaromatic

characteristics. Further, the crystal analyses revealed that the compound **16** adopts "figure-eight" C_2 symmetry. The electronic absorption spectra of **16** shows broad band at 638 nm, which is substantially bathochromically shifted compared with the B-like band of its hexaphyrin analogue. It is pertinent to point out that after DDQ oxidation of **16**, an intense sharp band well as Q- like small band appeared at 1264 nm which resembled with a 34π electronic aromatic system.

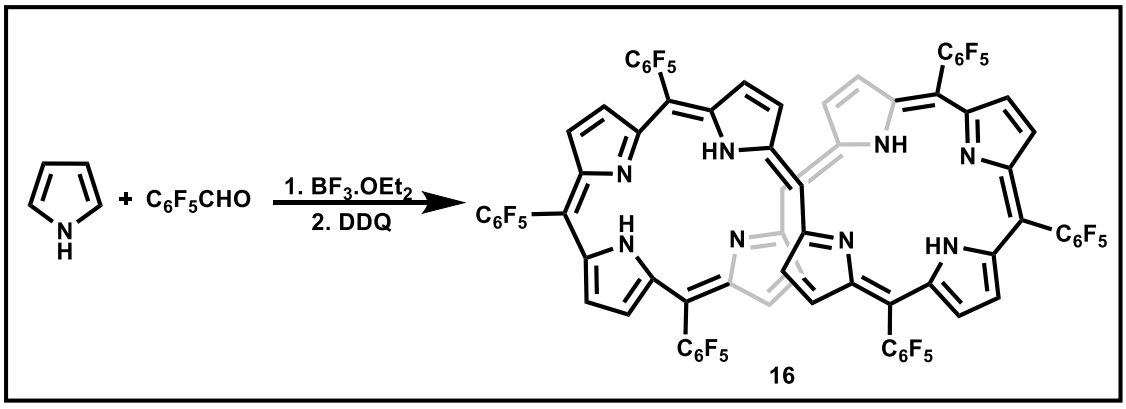

Scheme 3.4: Synthesis of **16**.

Neo-confused octaphyrin **17**[23] (Figure 3.3), the structural isomer of **16**, was obtained by Furuta, Xie and co-workers. The ring closure of the octapyrrane with terminal β-linked pyrroles produces unprecedented neo-confused octaphyrin embedded with a unique N−Cα bond. The detailed synthetic procedure of **17** is described in the forthcoming chapter. The ^{1}H NMR spectral analyses of **17** revealed the absence of diatropic ring current with figure eight configuration which led to generate nonaromaticity.

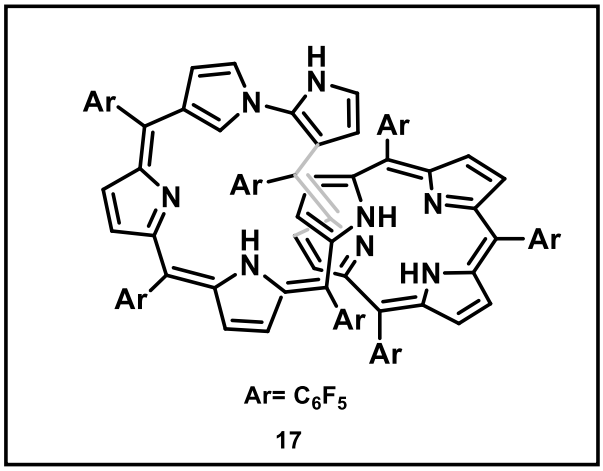

Figure 3.3: Neo-confused octaphyrin (**17**).

3.2 Objective of our work

Each expanded porphyrin and the number of respective structural isomers are less as compared to porphyrins and its structural isomers. In addition, all these isomers are similar class of an expanded family, however, different classes of expanded analogues are hitherto unknown in the literature.

Herein, we report the synthesis of the hexaphyrin(3.1.1.3.1.1) analogue in which a macrocyclic framework is embedded with a bis-*o*-*p*- biphenyl unit (**25**) and its structural isomer, octaphyrin(1.1.1.0.1.1.1.0) with a bis-*m*-*p*-biphenyl unit (**29**) (Figure 3.4)[26] and octaphyrin(1.1.1.0.1.1.1.0) isomer with bis-*p*-*p*-biphenyl moiety. The structural isomers were achieved by reorganizing the connectivity of the *o*-, *m*- and *p*-arene units and attached to the *p*-phenyl ring. The synthesis, photophysical properties and structural characterization of **25** and **29** are discussed in this chapter, whereas, bis-*p*,*p*-biphenyl moieties embedded octaphyrin(1.1.1.0.1.1.1.0) is discussed in Chapter 4

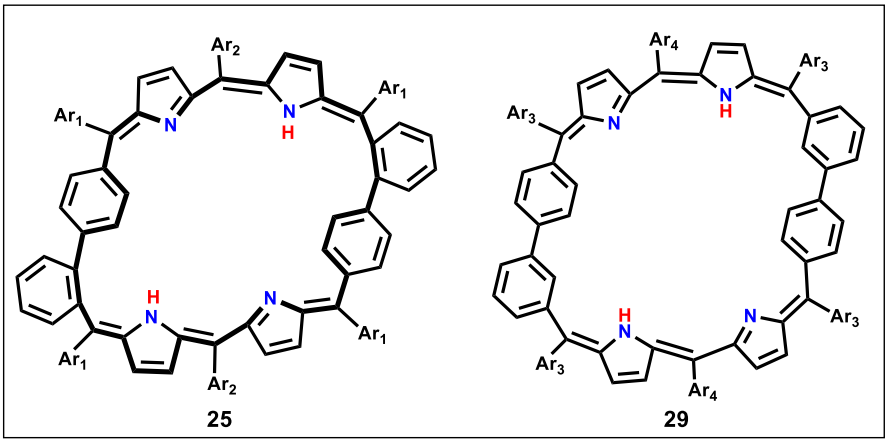

Figure 3.4: Hexaphyrin (**25**) and its octaphyrin analogue (**29**).

3.3 Results and discussion

3.3.1 Synthesis

The synthesis of hexaphyrin (**25**) and its structural isomer, octaphyrin (**29**) are shown in Scheme 3.5. The starting materials such as 1,1′-biphenyl based 2,4′- and 3,4′-dicarbaldehyde (**22** and **26**, respectively) were synthesized as per the literature procedure.[27] The Grignard reaction of **22** and **26** with arylmagnesium bromide in dry THF afforded respective aryldiols **23** and **27** in 97% and 79% yields, respectively. Compounds **23** and **27** were further treated with pyrrole in the presence of $BF_3.OEt_2$ to form the final precursors, 2,2'-([1,1'-biphenyl]-2,4'-diylbis(mesitylmethylene)] bis(1H-pyrrole) (**24**) and 2,2'-([1,1'-biphenyl]-3,4'-diylbis(phenylmethylene)] bis(1H-pyrrole) (**28**) in 35% yield, respectively. The [3+3] acid catalyzed condensation of **24** with 4-nitrobenzaldehyde in the presence of *p*-toluenesulfonic acid (*p*-TSA) was followed by 2,3-dichloro-5,6-dicyano-*p*-benzoquinone (DDQ) oxidation to form **25** in 10% yield. A [4+4] acid-catalyzed condensation of **28** with 2,3,4,5,6-pentafluoro benzaldehyde in the presence of trifluoroacetic (TFA) acid followed by oxidation with DDQ to afforded **29**

in 6% yield. Both the compounds (**25** and **29**) were purified by silica gel column by using CH_2Cl_2/*n*-hexane solvent mixture and obtained as blue color compound.

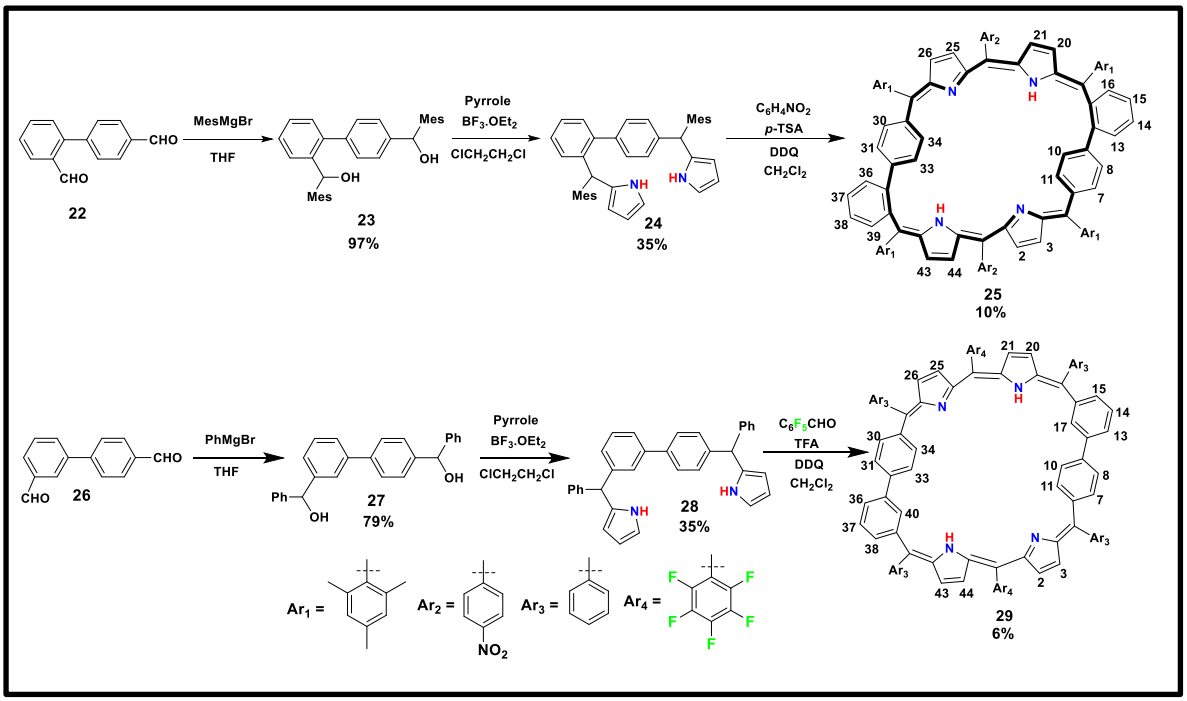

Scheme 3.5: Synthesis of **25** and **29**.

3.3.2 Spectral characterisation

3.3.2.1 Mass spectrometric analysis

The electrospray ionization (ESI) mass spectrometric analysis of **25** and **29** showed molecular ion peaks at *m/z*=1355.6183 (M+1) for hexaphyrin (**25**) and *m/z*=1277.3625 (M+1) for octaphyrin (**29**) respectively, which are consistent with the exact composition of the macrocycle (Figures 3.5 and 3.6).

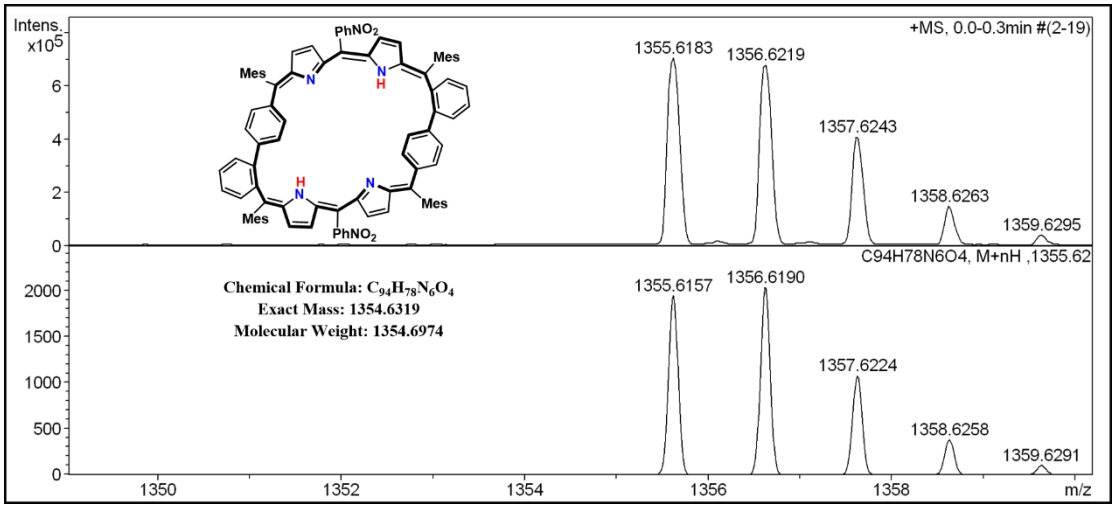

Figure 3.5: HR-MS spectrum of **25**.

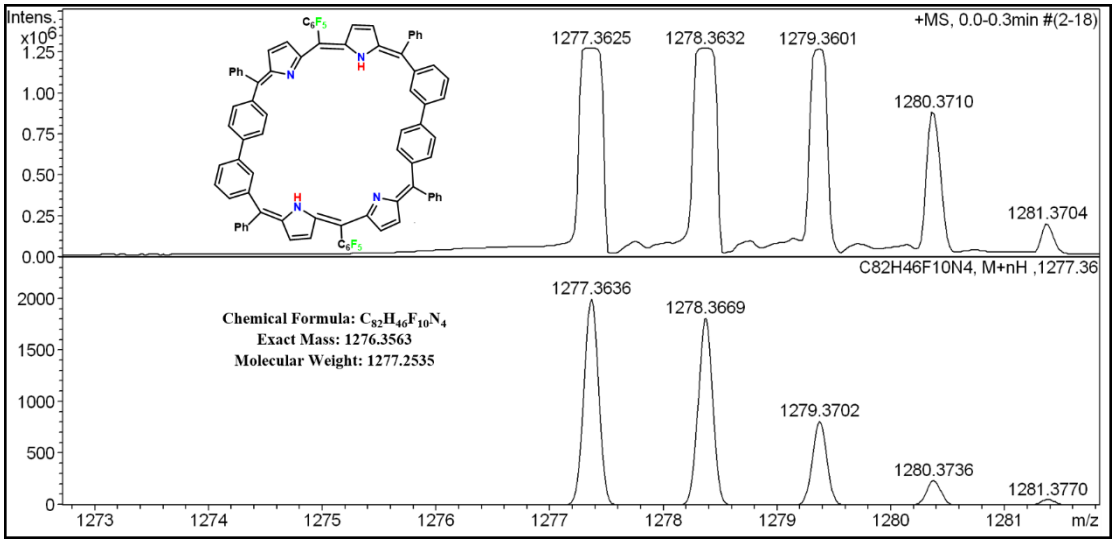

Figure 3.6: HR-MS spectrum of **29**.

3.3.2.2 NMR Analysis

The ^{1}H NMR spectra of **25** and **29** were recorded in CD_2Cl_2 at 298 K and are shown in Figure 3.7. The *β*-CH protons of amine pyrrole units in **25** (Figure 3.7a) resonated as a set of doublets at 6.58 ppm [H(21,44)] and 6.35 ppm [H(20,43)], whereas the imine pyrrole units are observed at 6.33 ppm [H(2,3,25,26)]. The inner NH signal is observed as a broad singlet at 14.05 ppm, which suggests the intramolecular hydrogen bonding interactions, and the signal was further confirmed by D_2O exchange

experiments. The *o*-phenylene protons appeared as a multiplet between 6.99 and 6.89 ppm. The peripheral *p*-phenylene CH protons resonated at 6.97 and 6.85 ppm, whereas the set of inner core CH protons [H(11,10/34,33)] is observed as a doublet at 8.00 ppm; another set of protons can be seen as a broad signal at 8.59 ppm. Thus, variable temperature ^{1}H NMR was further performed. At 253 K, the respective signals became sharp and resonated as a doublet at 8.52 ppm. In addition, at 203 K, the pyrrolic NH signal is bifurcated and resonated at 14.35 and 14.25 ppm (Figure 3.9), which suggests the unsymmetrical nature of the macrocycle. Overall, the spectral pattern resembles typical nonaromatic characteristics; however, the observed results are contrary to those for Möbius aromatic di-*p*-benzihexaphyrin[28] and antiaromatic *p*-benzihexaphyrin.[29] In addition, the protonation experiment was performed with increasing concentrations of TFA in **25**. At 20 equiv of TFA, two different NH signals were observed at 9.14 and 9.91 ppm, which suggested that two of the pyrrolic rings were inverted (Figure 3.10).

At 298 K, the spectral pattern of **29** in CD_2Cl_2 is observed between 7.81 and 6.17 ppm (Figure 3.7b). The amine pyrrolic *β*-CH protons resonated as a doublet at 6.92 ppm [H(20,43)] and a triplet at 6.43 ppm [H(21,44)], whereas the imine pyrrolic *β*-CH protons are observed as individual signals from 6.62 to 6.17 ppm [H(2,3,25,26)]. The inner CH protons of the *m*-phenyl rings are observed at 7.10 ppm [H(40)] and 6.87 ppm [H(17)], and the remaining peripheral protons appeared between 7.48 and 7.21 ppm; on the contrary, the *p*-phenyl protons are observed as doublets at 7.81 ppm [H(34,8)], 7.69 ppm [H(10,30)], 7.07 ppm [H(11,31)] and 7.06 ppm [H(7,33)]. All of these proton signals were further confirmed by ^{1}H–^{1}H COSY spectral analysis (Figure 3.11). At 233 K, the pyrrolic NH signals were observed as a broad signal at 13.13 ppm (Figure 3.12). In addition, the ^{1}H NMR spectrum of **29** with 20 equiv of TFA in CD_2Cl_2 at 298 K showed the inner NH protons and the protonated imine NH signals resonated at 10.80

ppm (Figure 3.13). Overall, the intrinsic property of the *m*-phenyl ring in the core (**29**) restricts the macrocyclic aromatization; thus, the spectral patterns are similar to those of *m*-arene unit-incorporated expanded porphyrinoids.[30, 31-36]

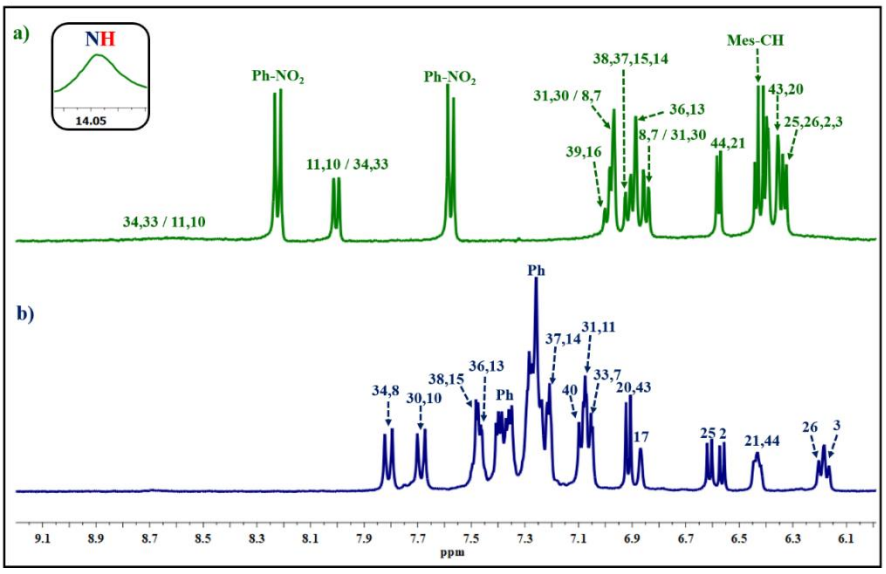

Figure 3.7: ^{1}H NMR spectra of **25** (a) and **29** (b) in CD_2Cl_2 at 298K.

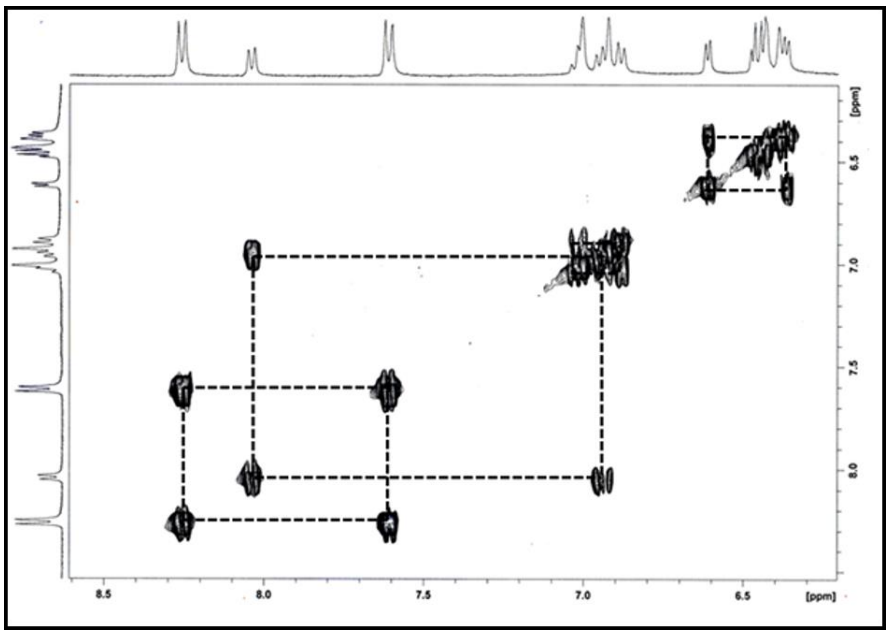

Figure 3.8: ^{1}H –^{1}H COSY spectrum of **25** in CD_2Cl_2.

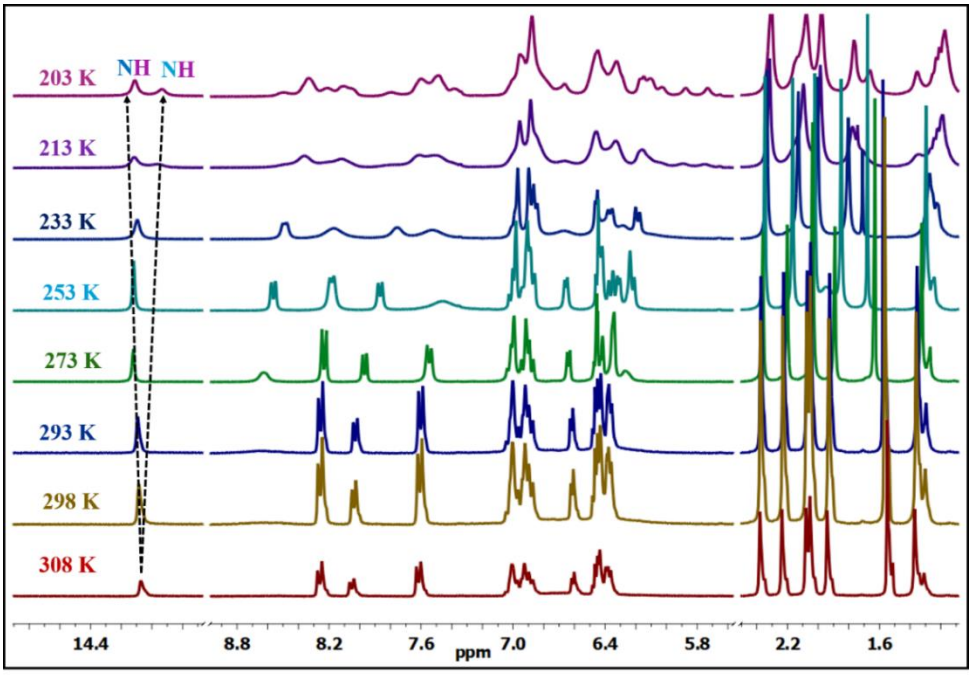

Figure 3.9: Variable temperature ^{1}H-NMR spectara of **25** in CD_2Cl_2.

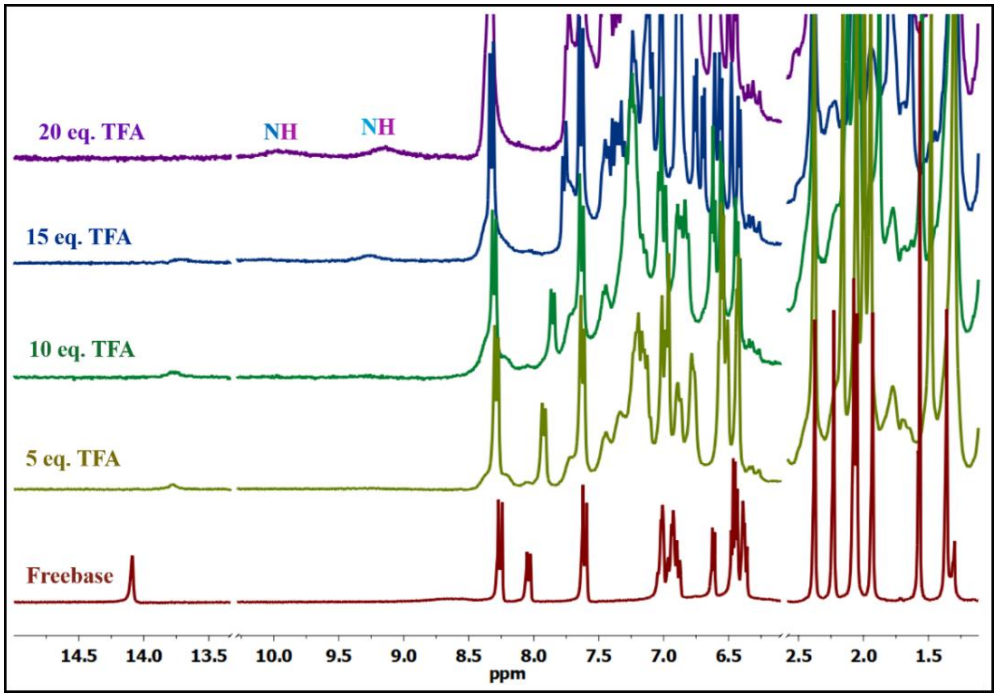

Figure 3.10: ^{1}H-NMR spectra of **25** with increasing conc. of TFA in CD_2Cl_2 at 298K.

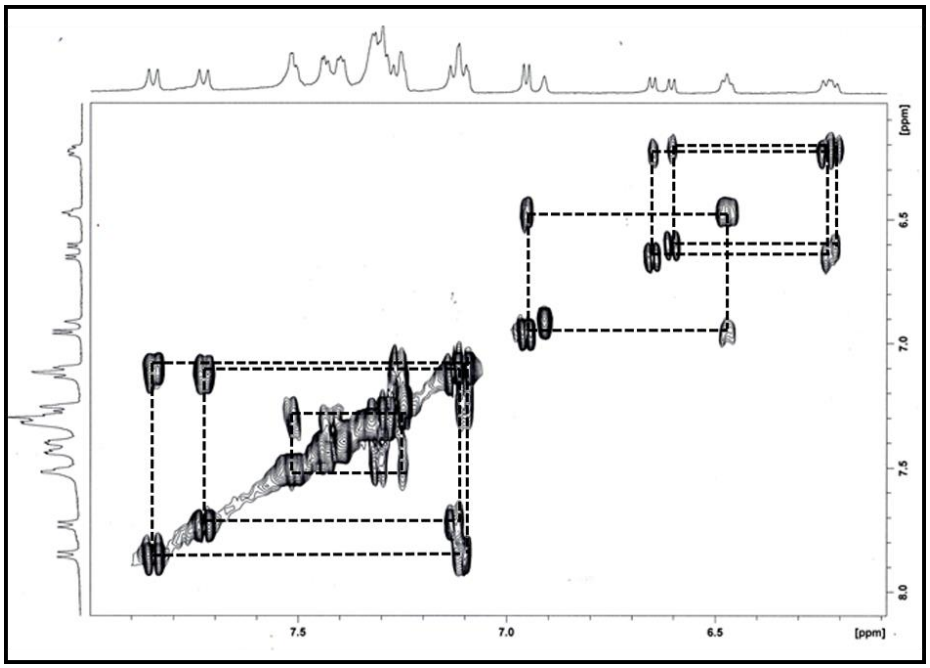

Figure 3.11: ^{1}H –^{1}H COSY spectrum of **29** in CD_2Cl_2.

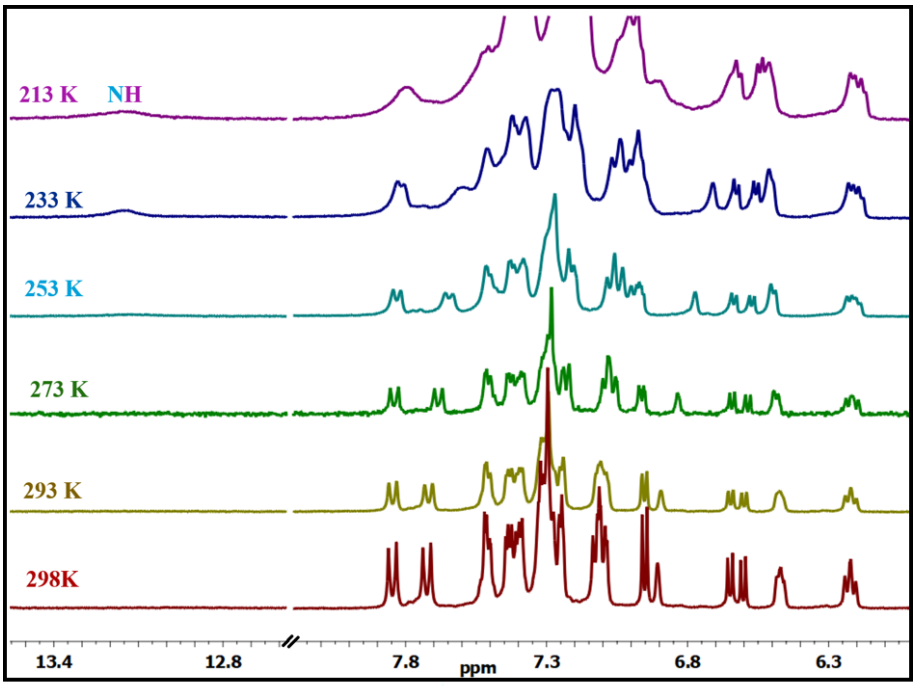

Figure 3.12: Variable temperature ^{1}H-NMR spectra of **29** in CD_2Cl_2.

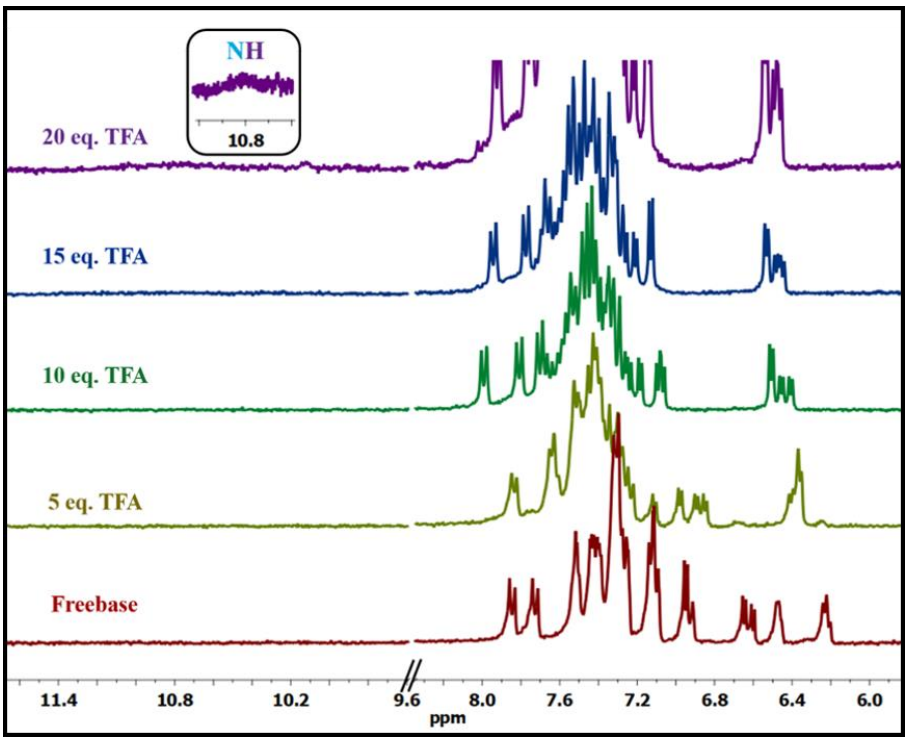

Figure 3.13: ^{1}H-NMR spectra of **29** with increasing conc. of TFA in CD_2Cl_2 at 298K.

3.3.2.3 Single crystal X-ray analysis:

The final confirmation of **25** has come from the single-crystal X-ray analysis, which is shown in Figure 3.14a and d (Table 3.1). The crystals were grown in a CH_2Cl_2/*n*-hexane solvent mixture. The unit cell contains two crystallographically independent molecules with a triclinic crystal lattice and a *P*-1 space group. The crystal structure reveals that two molecules of *o*-*p*-biphenyl dipyrromethene units are connected by *meso*-carbon atoms with *p*-nitrophenyl groups and adopt a bowl-like conformation in the solid state. The crystal analyses reveal a series of weak intramolecular hydrogen bonding interactions between imine nitrogens (N2/N3) and (i) the amine pyrrole nitrogens (N1−H1/N4−H4) and (ii) one of the *p*-phenyl CH (C5−H5/C28−H28) units. The bond distances and angles are 2.02(4) Å and 125.48(2)° (N1−H1···N2), 2.06(4) Å

and 125.3(3)° (N4−H4···N3), 2.33(3) Å and 120.0(3)° (C5−H5···N2), and 2.43(3) Å and 118.8(3)° (C28−H8···N3), respectively. In addition, π-π interactions are observed between π-clouds of *o*- and *p*-phenylene units with distances of 4.083(4) Å (*o*1···*p*2) and 4.236(5) Å (*p*1···*o*2), respectively.

The molecular structure of **25.2H**$^+$ is unambiguously confirmed by crystal analysis and is shown in Figure 3.14b and e (Table 3.1). The molecule is in a monoclinic crystal lattice and space group $P2_1/c$ and located on a crystallographic 2-fold axis. Crystal analyses reveal the following. (i) The imine nitrogen is protonated in the presence of TFA anions. (ii) The bowl-like conformation in **25** changes to an open conformation in **25.2H**$^+$. (iii) Of four pyrrolic units, two are inverted. The respective NHs (N4−H4) are in intermolecular hydrogen bonding interaction with the oxygen atom (O5) of the TFA anions with a bond distance and a bond angle (N4−H4···O5) of 2.166(5) Å and 135.60(3)°, respectively. The anions are located above and below the mean plane containing *meso*-carbon atoms with distances of 3.01 Å.

The aromatic character in **25** and **25.2H**$^+$ is further verified from the crystal analyses, where(i) the bond lengths in the *p*-phenylene units (1.359−1.442 Å) (Figures 3.17−3.19) are within sp^2-sp^2 double bond character and maintain individual aromaticity and (ii) the *o*- and *p*-phenylene units in **25** [58.71(1)° (*o*1), 66.87(1)° (*o*2), 61.78(1)° (*p*1), and 66.87(1)° (*p*2)] and **25.2H**$^+$ [40.11(8)° (*o*) and 33.07(8)° (*p*)] deviate from the respective mean macrocyclic plane. Thus, these compounds are restricted from the overall macrocyclic aromatization and adopts nonaromatic characteristics. A similar trend was observed in *p*-arene unit-incorporated nonaromatic expanded porphyrinoids.[24,37]

The structure of **29** was further confirmed by single-crystal analysis and is shown in Figure 3.14c and f (Table 3.1). The conjugation allowed in **29** was restricted by the

presence of an *m*-arene unit in the macrocyclic core, thus maintaining the nonaromatic character. The molecule crystallizes in a monoclinic crystal lattice in space group $P2_1/c$ and adopts a figure-eight conformation in the solid state. As observed in **25**, the amine pyrrole units (N1−H1/N4−H4) are in intramolecular hydrogen bonding interaction with imine nitrogens (N2/N3) with the bond distances and angles of N1−H1···N2 and N4−H4···N3 being 2.049(6) Å and 124.7(4)° and 2.110(6) Å and 123.3(4)°, respectively. The presence of fluorine atoms in the *meso*-pentafluorophenyl groups are in intermolecular hydrogen bonding interactions and generates series of 1-D arrays and a self-assembled dimer in the solid state (Figure 3.15-3.16).

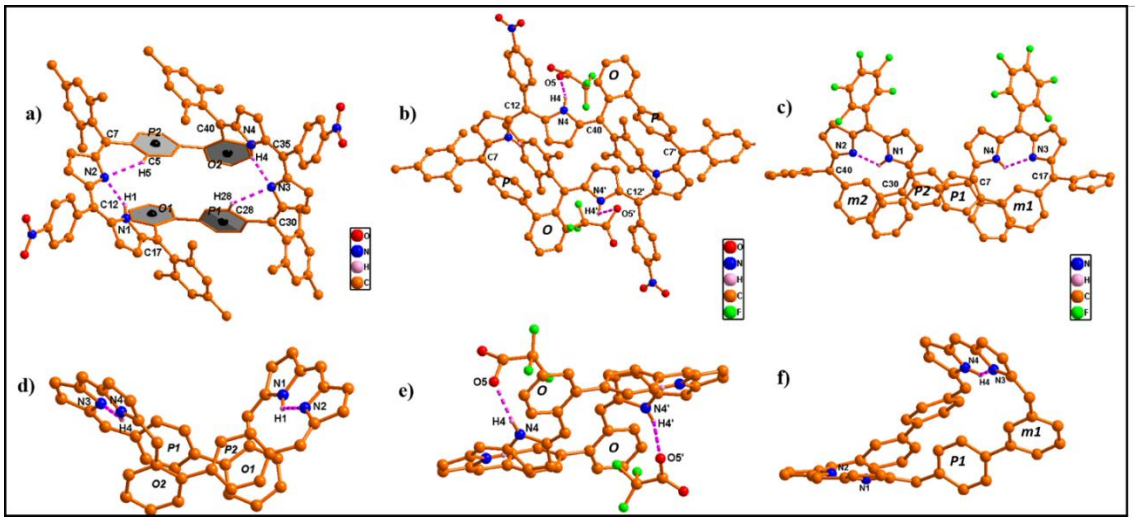

Figure 3.14: Single-crystal X-ray structures of **25**, **25.2H**$^+$, and **29**: top views in panels a-c and side views in panels d-f, respectively. The peripheral hydrogens in panels a-f and the *meso*-aryl groups in panels d-f have been omitted for the sake of clarity.

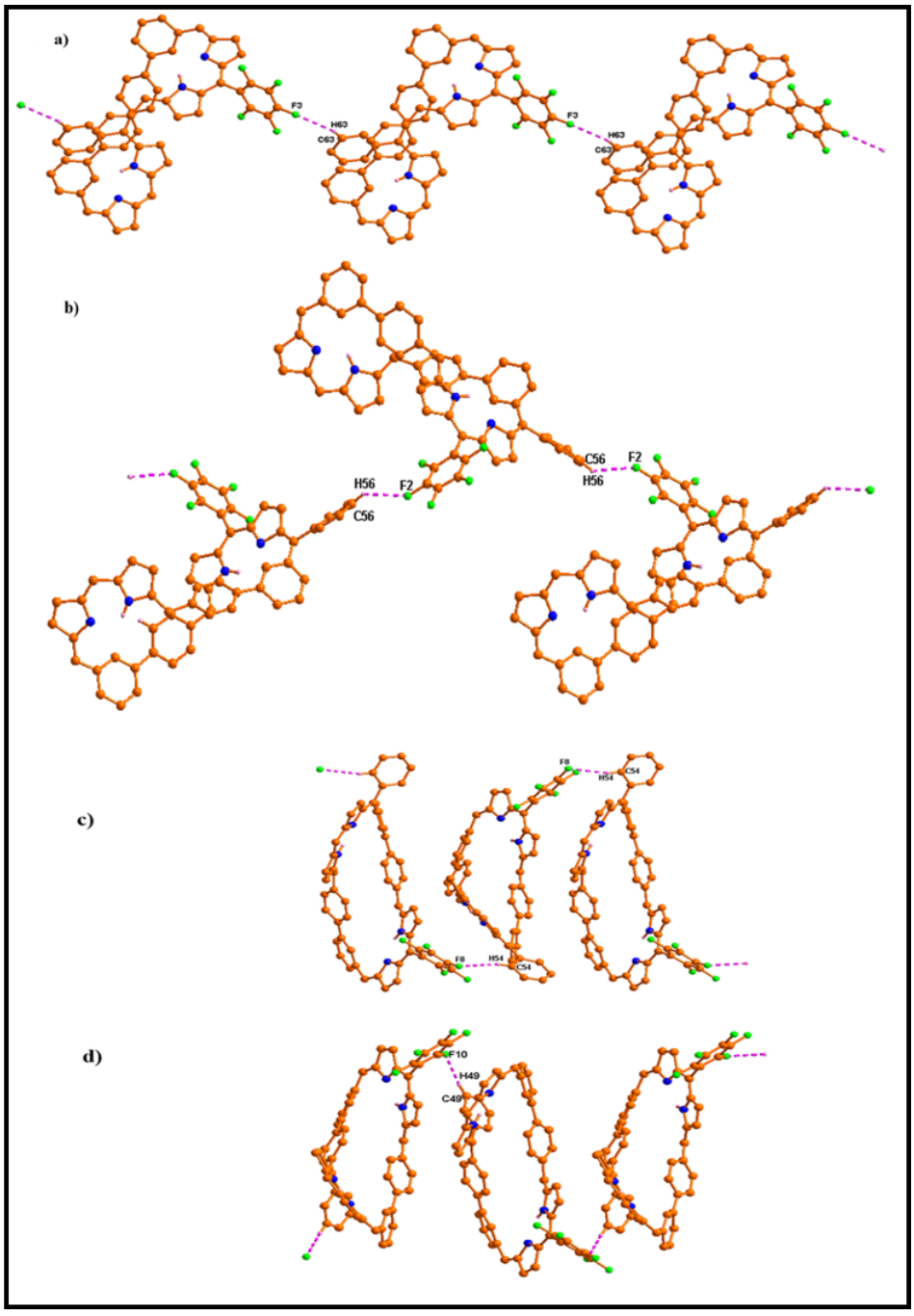

Figure 3.15: 1-D arrays in **29**. The bond distances and angles are a) C63-H63…F3: 2.777(6) Å and 147.36(5)°; b) C56-H56…F2: 2.777(5) Å and 141.10(7)°; c) C54-H54…F8: 2.789(7) Å and 165.50(6)°; d) C49-H49…F10: 2.659(4) Å and 166.37(5)° respectively. The hydrogen atoms and the *meso*-aryl groups which are not in hydrogen bonding interactions are omitted for clarity.

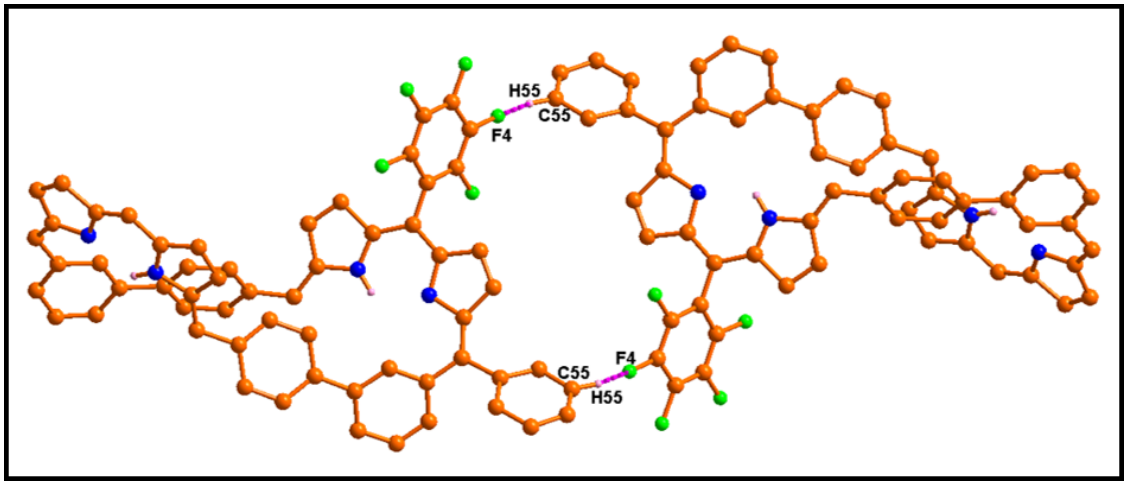

Figure 3.16: Self-assembled dimer in **29**. The bond distance and angle are: a) C55-H55…F4: 2.613(6) Å and 135.85(7)°. The hydrogen atoms, TFA anions and *meso*-aryl groups.

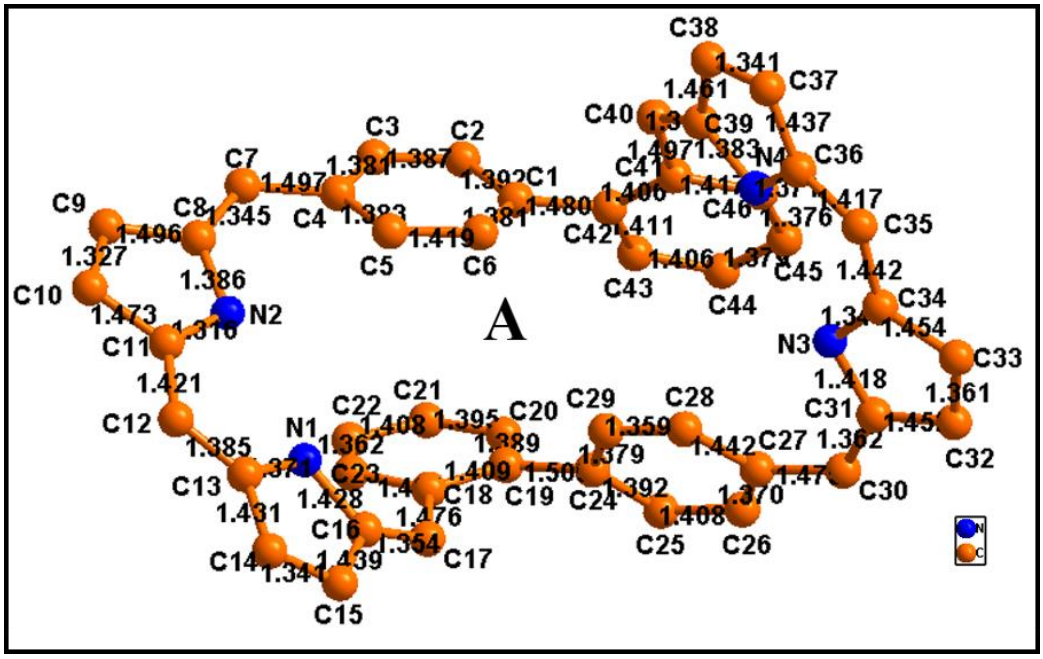

Figure 3.17: Bond lengths in **25 (A)** (Å).

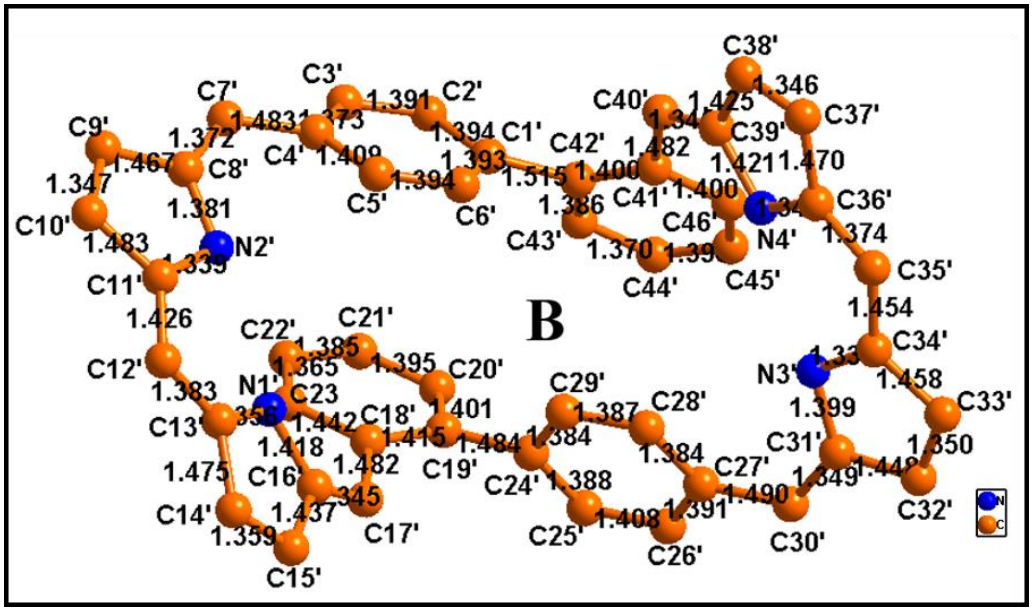

Figure 3.18: Bond lengths in **25 (B)** (Å).

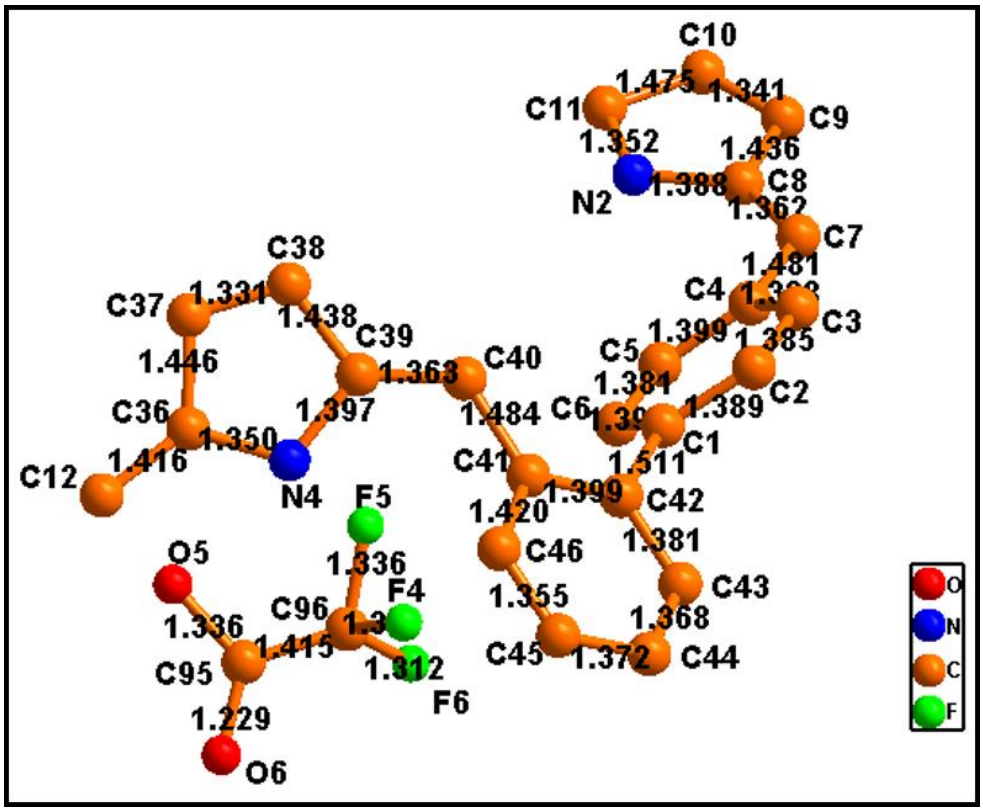

Figure 3.19: Bond lengths in **25.2H**$^{+}$ (Å).

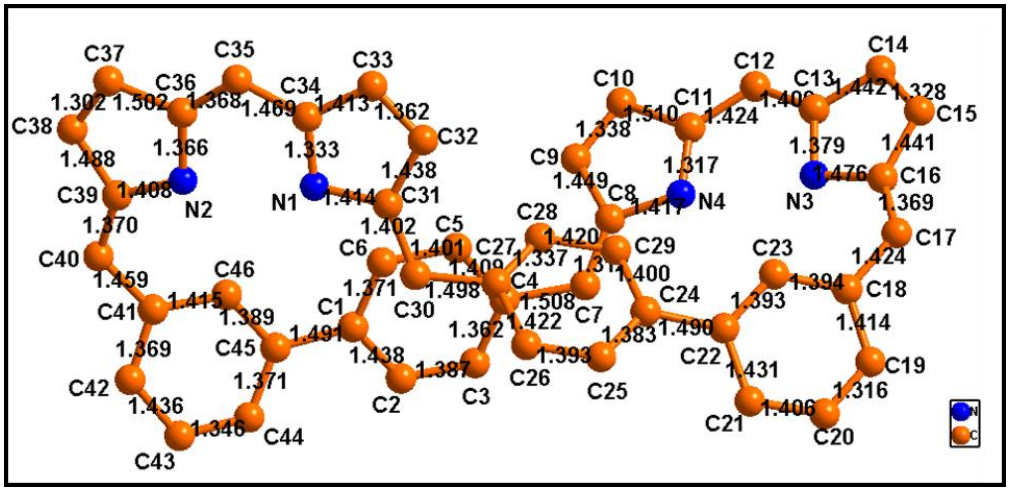

Figure 3.20: Bond lengths in **29** (Å).

Table 3.1: Crystal data for **25**, **25.2H**$^+$ and **29**

Crystal parameters	**25**	**25.2H**$^+$	**29**
Formula	$C_{188}H_{156}N_{12}O_8$	$C_{49}H_{40}F_3N_3O_4$	$C_{82}H_{46}F_{10}N_4$
M/g mol^{-1}	2711.24	791.84	1277.23
T/K	100(2)	296.15	100(2)
Crystal dimensions/mm^3	0.19 × 0.15 × 0.12	0.35 × 0.23 × 0.12	0.18 × 0.14 × 0.12
Crystal system	triclinic	monoclinic	monoclinic
Space group	P-1	$P2_1/c$	$P2_1/c$
a/Å	16.6229(19)	17.5240(10)	17.621(2)
b/Å	18.0863(18)	27.5810(15)	27.685(4)
c/Å	33.294(4)	11.6876(6)	16.722(2)
α/°	90.594(3)	90	90
β/°	97.966(3)	98.894(3)	109.514(8)
γ/°	111.858(3)	90	90
V/Å^3	9179.5(18)	5581.0(5)	7689.0(17)
Z	2	4	4
ρcalcd/mg m^{-3}	0.981	0.942	1.103
μ/mm^{-1}	0.060	0.067	0.081
F(000)	2864.0	1656.0	2624.0
Reflns. collected	33701	70717	71766
Indep.reflns.[R(int)]	33701 [0.1675]	10263 [0.0841]	13477 [0.3214]
Max/min transmission	0.993, 0.989	0.992, 0.982	0.990, 0.986
Data/restraints/parameters	33701/0/1871	10263/33/602	13477/0/799
GOF on F^2	0.988	1.048	0.903
Final R indices[I > 2σ(I)]	R_1 = 0.0816, wR_2 = 0.1066	R_1 = 0.0769, wR_2 = 0.2367	R_1 = 0.0984, wR_2 = 0.2242
R indices (all data)	R_1 = 0.2201, wR_2 = 0.1225	R_1 = 0.1306, wR_2 = 0.2676	R_1 = 0.2738, wR_2 = 0.3033
Largest diff peak and hole [e Å^{-3}]	0.36 and -0.40	0.34 and -0.32	0.31 and -0.33

The crystals have been deposited in the Cambridge Crystallographic Data Centre with reference no. CCDC 1972788 (**25**), CCDC 1972789 (**25.2H**$^+$) and CCDC 1972790 (**29**). These data can be obtained free of charge from the Cambridge Crystallographic Data Centre via www.ccdc.cam.ac.uk/data_request/cif. The crystals of **29** are very weakly diffracting, so that the higher angle reflections are essentially unobserved. This results in overall poor-quality data and high R_{int} value. In spite of several attempts, we could not obtain better quality data of **29**.

3.3.2.4 Electronic absorption spectral analyses

The electronic absorption spectra of **25**, **25.2H**$^+$, **29**, and **29.2H**$^+$ were recorded in CH_2Cl_2 and are shown in Figure 3.21 and the spectral data are presented in Table 3.2. Compound **25** showed an intense band at 394 nm and a comparatively less intense band at 629 nm with molar absorption coefficient values on the order of 10^4. Upon gradual addition of TFA in CH_2Cl_2 solution of **25**, the color of the solution changes from blue to green with isosbestic points at 405, 480 and 590 nm and the solution showed two less intense bands at 362 and 435 nm and a highly intense band at 652 nm (Figure 3.21). Compound **29** showed an almost similar spectral pattern as observed in **25** with less intense bands at 394 and 632 nm. However, upon protonation, the respective bands were red- shifted and observed at 418 and 634 nm. As observed in **25.2H**$^+$, the isosbestic points in **29.2H**$^+$ were appeared at 410 and 480 nm (Figure 3.23). Overall, the spectral pattern in **25**, **25.2H**$^+$, **29**, and **29.2H**$^+$ resembles typical nonaromatic characteristics as observed in *m*/*p*-arene expanded analogues.[24,30,33-37]

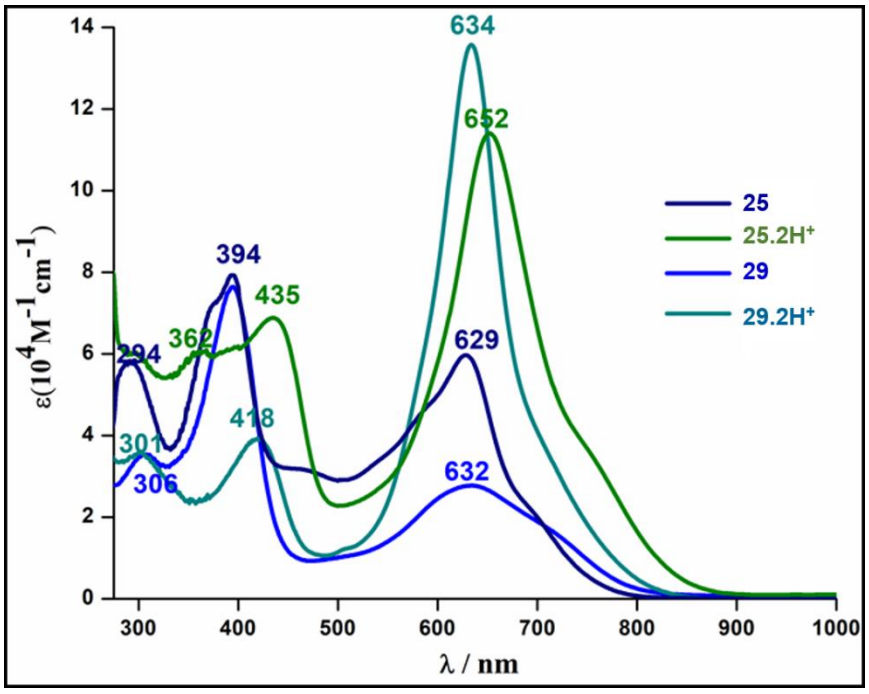

Figure 3.21: Electronic absorption spectra of **25**, **25.2H**$^+$, **29** and **29.2H**$^+$ in CH_2Cl_2.

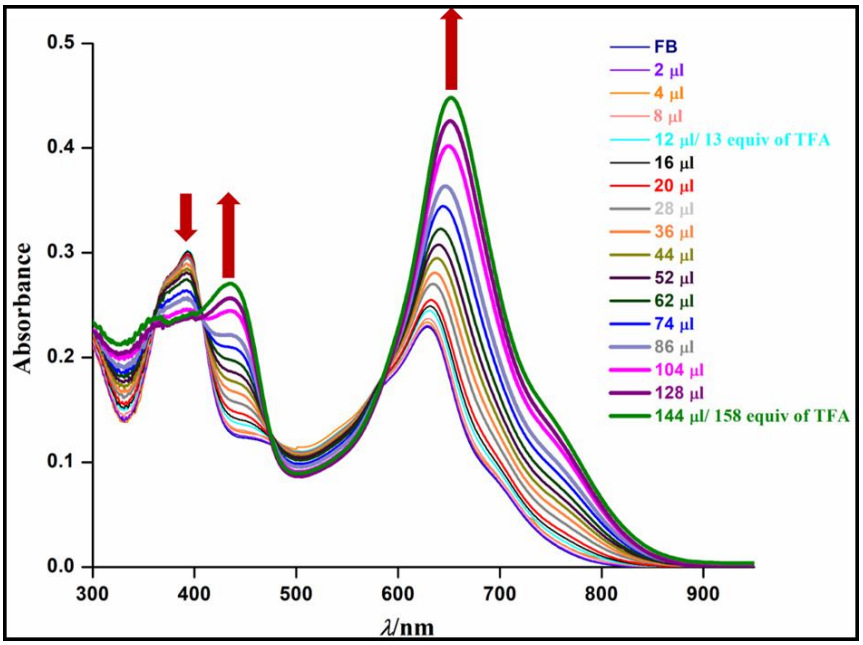

Figure 3.22: Electronic absorption spectra of **25** with various equivalents of TFA in CH_2Cl_2.

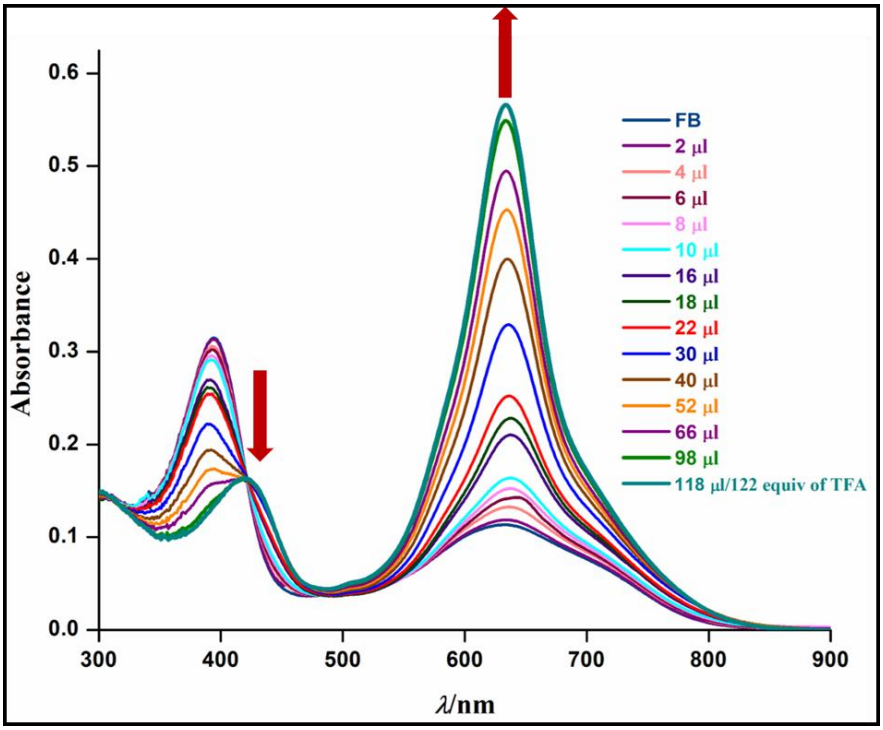

Figure 3.23: Electronic absorption spectra of **29** with various equivalents of TFA in CH_2Cl_2.

Table 3.2: Electronic absorption spectral data of **25, 25.2H**$^+$, **29** and **29.2H**$^+$

Compounds	λ_{max}/nm (ε[$M^{-1}cm^{-1}$]x10^4)
25	294 (5.54), 394 (7.50), 629 (5.82)
25.2H$^+$	362 (6.04), 435 (6.88), 652 (11.39)
29	306 (3.51), 394 (7.52), 632 (2.71)
29.2H$^+$	301 (3.56), 418 (3.88), 634 (13.54)

3.3.2.5 Theoretical calculation

To determine the aromaticity of **25** and **25.2H**$^+$, computational studies such as NICS(0) calculation and ACID plots were performed using the B3LYP/6-31g(d) level of density functional theory (Figures 3.24−3.25).[32,33] The NICS(0) values at the global centre for **25** and **25.2H**$^+$ were found to be 0.03 and −2.12 ppm, respectively (Table 3.3−3.4). The BLA values were calculated from the crystal structures of **25** and **25.2H**$^+$ and found to be 0.146 Å each (Table 3.3). In addition, the random current density flow of the ACID plots of **25** and **25.2H**$^+$ consolidated the nonaromatic character of the molecules (Figure 3.25). Overall, as reflected from spectral and structural analyses, the observed results further corroborate typical nonaromatic character rather than 32π antiaromatic character.

Table 3.3: NICS(0) [ppm] and BLA [Å] values of **25** and **25.2H**$^+$:

Calculation	25	25.2H$^+$
NICS(0)	0.03	-2.12
BLA (Å)	0.146	0.146

Table 3.4: NICS(0) [ppm] values of **25** and **25.2H**$^+$:

	A	B	C	D	E	F	G	H	Center
25	-8.08	-8.48	-4.15	-2.04	-8.08	-8.48	-4.15	-2.04	0.03
25.2H$^+$	-7.25	-7.95	-4.31	-4.59	-7.25	-7.95	-4.31	-4.59	-2.12

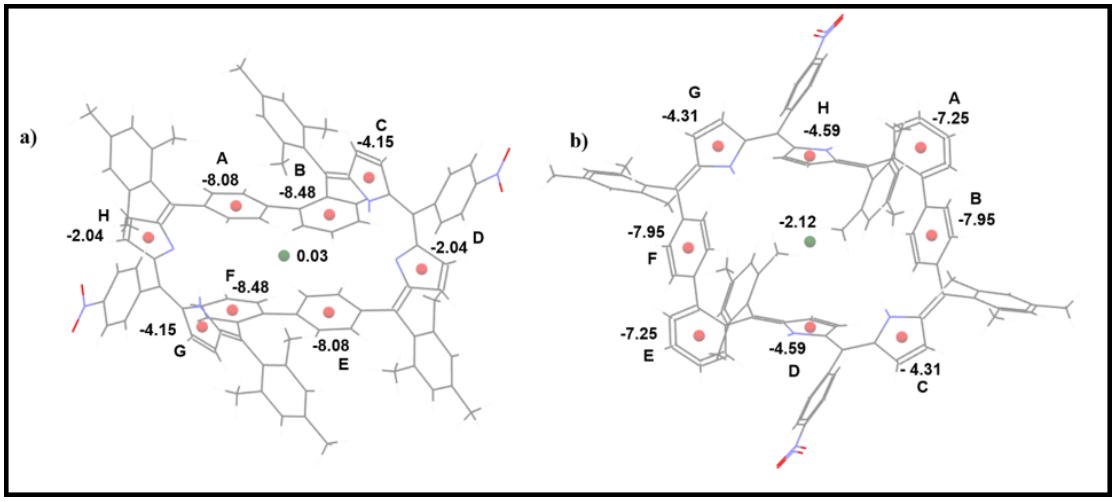

Figure 3.24: NICS(0) values for individual rings and center of the macrocycles of **25** and **25.2H**$^{+}$.

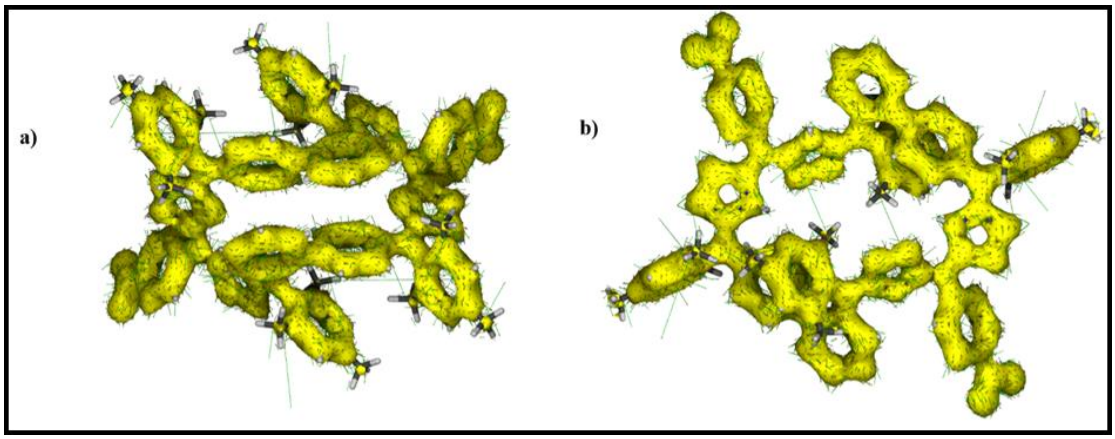

Figure 3.25: ACID Plots of **25** and **25**.**2H**$^{+}$.

3.4 Conclusion

In conclusion, structural isomers such as bis-*o*-*p*-biphenyl and bis-*m*-*p*-biphenyl units are incorporated into the macrocyclic core for the first time to form different expanded porphyrinoids such as hexaphyrin(3.1.1.3.1.1) and octaphyrin (1.1.1.0.1.1.1.0). The bowl-like conformation in hexaphyrin turned into an open conformation upon protonation. The conjugation allowed in the hexaphyrin is restricted

by the individual aromaticity and nonplanarity of the *p*-arene units, and the restricted conjugation in the presence of *m*-arene units in the octaphyrin core exhibited overall nonaromatic character.

3.5 Experimental Section

3.5.1 General Information

The reagents dried by standard grown by slow diffusion of *n*-hexane over CH_2Cl_2 solution. Single-crystal diffraction of **25**, **25.2H**$^+$ and **29** were collected in a APEX-II rotation system, Mo-Kα.

3.6 Synthetic procedure and spectral characterization of 22-29

3.6.1 Synthesis of 22 and **26:** Compounds **22** and **26** were synthesized as per the literature procedure.[24]

protonNMR (400 MHz, $CDCl_3$) of 22: δ = 10.11 (s, 1H), 9.97 (s, 1H), 8.06 (d, *J* = 7.8 Hz, 1H), 8.01 (d, *J* = 7.99 Hz, 1H), 7.99 (d, *J* =8.1 Hz, 1H), 7.80 (d, *J* = 8.2 Hz, 1H), 7.69 (m, 1H), 7.57 (m, 1H), 7.55 (d, *J* = 8.0 Hz, 1H), 7.45 (d, *J* = 7.6 Hz, 1H).

13C NMR (101 MHz, $CDCl_3$) of 22: δ = 191.75, 191.71, 191.55, 144.26, 144.14, 136.00, 135.84, 133.79, 133.67, 130.73, 130.61, 130.38, 129.73, 128.71, 128.28, 128.05.

HighResMassSp (ESI-TOF) *m/z* of 22: *m/z* calculated for $C_{14}H_{10}O_2$ = 210.0681; found = 211.0748 (M+1).

1H NMR (400 MHz, $CDCl_3$) of 26: δ = 10.08 (s, 1H), 10.06 (s, 1H), 8.13 (s, 1H), 7.97 (d, *J* = 5.3 Hz, 2H), 7.90 (m, 2H), 7.78 (d, *J* = 5.6 Hz, 2H), 7.64 (s, 1H).

13C NMR (176 MHz, $CDCl_3$) of 26: δ = 192.10, 191.91, 191.88, 145.69, 140.84, 137.19, 136.11, 135.86, 133.29, 130.56, 130.50, 130.00, 129.93, 128.31, 128.16, 127.91.

HighResMassSp (ESI-TOF) *m/z* of 26: *m/z* calculated for $C_{14}H_{10}O_2$ = 211.0754; found = 211.0763 (M+1).

3.6.2 Synthesis of 23:

1H NMR (400 MHz, $CDCl_3$): δ = 7.52 – 7.50 (m, 1H), 7.38 (t, *J* = 9.0 Hz, 2H), 7.32 (s, 1H), 7.30 (s, 1H), 7.28 (s, 1H), 7.24 (s, 1H), 6.98 (s, 2H), 6.80 (d, *J* = 8 Hz, 1H), 6.40 (s, 1H), 6.29 (d, *J* = 7.9 Hz, 1H), 2.40 (s, 6H), 2.37 (s, 6H), 2.32 (s, 1H), 2.29 (s, 1H), 2.16 (s, 6H), 2.11 (s, 2H).

13C NMR (101 MHz, $CDCl_3$): δ = 141.95, 141.93, 141.70, 141.66, 140.21, 140.18, 139.82, 139.78, 137.40, 137.07, 137.03, 136.82, 136.78, 136.75, 136.46, 136.42, 135.61, 135.57, 130.57, 130.54, 130.14, 129.99, 128.63, 128.58, 127.30, 127.11, 126.99, 125.31, 125.30, 71.03, 70.88, 70.87, 21.18, 21.17, 20.95, 20.84, 20.80, 20.77, 20.73.

HighResMassSp (ESI-TOF) *m/z*: *m/z* calculated for $C_{32}H_{34}O_2$ = 473.2451; found = 473.2469 (M+Na).

3.6.3 Synthesis of 24: [1,1'-biphenyl]-2,4'-diylbis(mesitylmethanol) (**23**) (0.5 g, 1.11 mmol) and pyrrole (7.68 mL) was dissolved in 40 ml 1,2-dichloroethane under N_2 atmosphere. After 10 min, 0.2 mL $BF_3.OEt_2$ solution was added and the resulting mixture was stirred for 3 h. The compound was extracted with CH_2Cl_2 dried over Na_2SO_4 and concentrated by rotary evaporator. The crude mixture was purified by silica gel (100-200 mesh) column chromatography in 7% EtOAC/*n*-Hexane mixture to afford **24** as a white solid in 35% yield (0.209 g, 0.37 mmol).

1H NMR (400 MHz, $CDCl_3$): δ = 7.73 (s, 2H), 7.20 (d, *J* = 7.5 Hz, 1H), 7.17 (d, *J* = 7.8 Hz, 1H), 7.13 (d, *J* = 7.5 Hz, 1H), 7.11 (d, *J* = 7.4 Hz, 1H), 7.03 (d, *J* = 7.6 Hz, 1H),

7.01 (d, *J* = 3.8 Hz, 1H), 6.95 (d, *J* = 1.5 Hz, 1H), 6.94 (m, 1H), 6.86 (d, *J* = 7.2 Hz, 1H), 6.69 (s,1H), 6.66 (s, 2H), 6.17 (d, *J* = 4.6 Hz, 1H), 6.12 (d, *J* = 4.5 Hz,1H), 5.89 (d, *J* = 4.4 Hz, 1H), 5.86 (s, 1H), 5.82 (s, 1H), 5.74 (m, 1H), 5.73 (s, 1H), 5.70 (s, 1H), 2.29 (s, 3H), 2.18 (s, 3H), 2.03 (s, 6H),1.79 (s, 3H), 1.77 (s, 3H).

13C NMR (101 MHz, $CDCl_3$): δ = 142.39, 142.38, 140.61, 140.36, 139.64, 139.43, 139.06, 137.65, 137.61, 137.23, 137.19, 136.58, 136.42, 136.24, 135.78, 135.76, 135.74, 133.17, 132.91, 132.68, 130.34, 130.29, 130.20, 130.03, 129.23, 129.20, 128.59, 128.53, 127.92, 127.90, 127.35, 127.33, 126.36, 126.34, 116.31, 116.28, 116.08, 116.04, 108.50, 108.38, 108.37, 108.20, 107.24, 107.21, 44.31, 44.23, 43.59, 43.58, 21.13, 21.12, 21.03, 20.80, 20.68, 20.65.

HighResMassSp (ESI-TOF) *m/z*: *m/z* calculated for $C_{40}H_{40}N_2$ = 571.3084; found = 571.3084 (M+Na).

3.6.4 Synthesis of 25:

1H NMR (400 MHz, CD_2Cl_2): δ = 14.05 (s, 2H), 8.59 (s, 2H), 8.22 (d, *J* = 8.8 Hz, 4H), 8.00 (d, *J* = 7.9 Hz, 2H), 7.57 (d, *J* = 8.6 Hz, 4H), 6.99 (m, 2H), 6.97 (s, 2H), 6.92 (m, 4H), 6.89 (m, 2H), 6.85 (d, *J* = 7.5 Hz, 2H), 6.58 (d, *J* = 5.3 Hz, 2H), 6.44 (s, 1H), 6.43 (s, 1H), 6.41 (s, 2H), 6.40 (s, 4H), 6.35 (d, *J* = 5.1 Hz, 2H), 6.33 (d, *J* = 5.2 Hz, 4H), 2.34 (s, 6H), 2.19 (s, 6H), 2.04 (s, 6H), 2.01 (s, 6H), 1.89 (s, 6H), 1.32 (s, 6H).

13C NMR (101 MHz, CD_2Cl_2): δ = 165.68, 152.07, 137.52, 137.47, 137.45, 137.28, 137.05, 136.70, 136.20, 135.92, 134.54, 134.17, 132.50, 131.66, 131.59, 128.76, 128.56, 128.39, 127.87, 127.65, 127.58, 126.94, 126.77, 126.52, 123.44, 22.40, 21.00, 20.83, 20.47, 20.31, 19.86.

HighResMS (ESI-TOF) *m/z*: *m/z* calculated for $C_{94}H_{78}N_6O_4$ = 1355.6157; found = 1355.6183 (M+1).

UV-Visble (CH_2Cl_2): λ_{max}/nm ($\varepsilon/M^{-1}cm^{-1}$) = 294 ($5.54 \times 10^4$), 394 ($7.50 \times 10^4$), 629 ($5.82 \times 10^4$).

3.6.5 Spectral analysis of $25.2H^+$

1H NMR (300 MHz, CD_2Cl_2): δ = 9.85 (s, 2H), 9.06 (s, 2H), 8.30 (d, *J* = 8.0 Hz, 4H), 7.71- 7.69 (m, 2H), 7.59 (d, *J* = 7.9 Hz, 2H), 7.43- 7.40 (m, 4H), 7.28- 7.26 (m, 2H), 7.20 (m, 4H), 7.09 (d, *J* = 7.0 Hz, 4H), 7.00 (m, 4H), 6.86 (m, 4H), 6.80 (d, *J* = 4.3 Hz, 2H), 6.72 (d, *J* = 5.3 Hz, 2H), 6.59 (m, 2H), 6.47 (s, 2H), 6.42 (d, *J* = 5.2 Hz, 2H), 2.34 (s, 6H), 2.21 (s, 6H), 2.07 (s, 6H), 2.00 (s, 6H), 1.76 (s, 6H), 1.62 (s, 6H).

UV-Visible (CH_2Cl_2): λ_{max}/nm ($\varepsilon/M^{-1}cm^{-1}$) = 362 ($6.04 \times 10^4$), 435 ($6.88 \times 10^4$), 652 ($11.39 \times 10^4$).

3.6.6 Synthesis of 27: The compound **26** (1 g, 4.73 mmol) was dissolved in 30 ml THF and added dropwise to freshly prepared phenylmagnesium bromide (5.0 g, 28.45 mmol) under N_2 atmosphere at 0 °C. The reaction mixture was allowed to stir at room temperature for 4 h. After 4 h the reaction was quenched with EtOAc, dried over Na_2SO_4, and concentrated by rotary evaporator. Compound was purified by silica gel column chromatography (100-200 mesh) using 20% EtOAc/*n*-hexane mixture to afford **27** as a white color solid in 79% (1.36 g, 3.71 mmol) yield.

1H NMR (400 MHz, $CDCl_3$): δ = 7.58 (s, 1H), 7.52 (s, 1H), 7.50 (s, 1H), 7.46-7.44 (m, 1H), 7.41 (d, *J* = 7.8 Hz, 2H), 7.39 (d, *J* = 7.2 Hz, 2H), 7.38 (s, 2H), 7.37 (s, 2H), 7.35 (s, 1H), 7.33 (d, *J* = 7.6 Hz, 1H), 7.32 (s, 1H), 7.30 (s, 1H), 7.28 (s, 1H), 7.25-7.23(m, 1H), 5.84 (s, 2H), 2.38 (s, 2H).

13C NMR (101 MHz, $CDCl_3$): δ = 144.37, 143.74, 143.72, 143.96, 142.90, 141.03, 140.29, 140.05, 128.97, 128.59, 127.68, 127.32, 127.20, 127.02, 126.98, 126.59, 126.58, 126.33, 125.56, 125.29, 76.30, 76.04, 76.03.

HighResMS (ESI-TOF) *m/z*: *m/z* calculated for $C_{26}H_{22}O_2$ = 389.1512; found = 389.1524 (M+Na).

3.6.7 Synthesis of 28: 3,4'-Bis(phenylhydroxymethyl) biphenyl (**27**) (1 g, 2.73 mmol) and pyrrole (18.7 mL) was dissolved in 40 ml 1,2-dichloroethane under N_2 atmosphere. After 10 min, 0.6 mL $BF_3.OEt_2$ solution was added and the resulting mixture was stirred for 3 h. The compound was extracted with CH_2Cl_2 dried over Na_2SO_4 and concentrated by rotary evaporator. The crude mixture was purified by silica gel column chromatography (100-200 mesh) in 7% EtOAC/*n*-hexane mixture to afford **28** as a white solid in 35% yield (0.4 g, 0.94 mmol).

1H NMR (400 MHz, $CDCl_3$): δ = 7.84 (s, 2H), 7.51 (d, J = 8.1 Hz, 2H), 7.48 (s, 1H), 7.45 (d, *J* =7.6 Hz, 1H), 7.41 (s, 1H), 7.36 (d, *J* = 7.7 Hz, 1H), 7.34 – 7.30 (m, 6H), 7.24 (m, 4H), 7.22 (s, 1H), 7.17 (d, *J* = 7.5 Hz, 1H), 6.72 (d, *J* = 5.1 Hz, 2H), 6.18 (d, *J* = 4.9 Hz, 2H), 5.85 (s, 2H), 5.51 (t, *J* = 5.6 Hz, 2H).

13C NMR (101 MHz, $CDCl_3$): δ = 143.63, 142.99, 142.96, 142.25, 142.14, 140.97, 139.39, 139.16, 133.53, 133.48, 129.27, 129.24, 128.94, 128.89, 128.57, 127.79, 127.61, 127.25, 127.11, 126.77, 125.41, 117.21, 108.32, 108.06, 107.99, 50.70, 50.27.

HighResMS (ESI-TOF) *m/z*: *m/z* calculated for $C_{34}H_{28}N_2$ = 487.2145; found = 487.2179 (M+Na).

3.6.8 Synthesis of 29:

1H NMR (400 MHz, CD_2Cl_2): δ = 7.81 (d, *J* = 8.2 Hz, 2H), 7.69 (d, *J* = 8.3 Hz, 2H), 7.48 (d, *J* = 8.0 Hz, 2H), 7.47 (d, *J* =7.9, 2H), 7.40 – 7.39 (m, 4H), 7.37 – 7.35 (m, 4H), 7.28 – 7.23 (m, 12H), 7.21 (m, 2H), 7.10 (s, 1H), 7.07 (d, *J* = 8.2 Hz, 2H), 7.06 (d, *J* =8.1 Hz, 2H), 6.92 (d, *J* = 5.0 Hz, 2H), 6.87 (s, 1H), 6.62 (d, *J* = 5.0 Hz, 1H), 6.57 (d,

J = 5.1 Hz, 1H), 6.43 (t, *J* = 4.2 Hz, 2H), 6.20 (d, *J* = 5.1 Hz, 1H), 6.17 (d, *J* = 5.0 Hz, 1H).

13C NMR (101 MHz, CD_2Cl_2): δ = 139.30, 135.51, 135.50, 134.43, 134.42, 132.03, 131.82, 131.76, 131.53, 131.40, 128.08, 128.00, 127.87, 127.86, 127.04, 126.77, 126.19, 126.00.

HighResMS (ESI-TOF) *m/z*: *m/z* calculated for $C_{82}H_{46}F_{10}N_4$ = 1277.3636; found = 1277.3625 (M +1).

UV-Visible (CH_2Cl_2): λ_{max}/nm (ε/$M^{-1}cm^{-1}$) = 306 (3.51 × 10^4), 394 (7.52 × 10^4), 632 (2.71 × 10^4).

3.7 References

1. A. R. Battersby, C. J. R. Fookes, G. W. J. Matcham, E. McDonald, *Nature* **1980**, *285*, 17-21.
2. J. L. Sessler, A. Gebauer, E. Vogel, In The Porphyrin Handbook, Vol. 2. K. M. Kadish, K. M. Smith, R. Guilard (eds). Academic Press: San Diego, CA, **1999**, 1-54.
3. E. Vogel, M. Köcher, H. Schmickler, J. Lex, *Angew. Chem. Int. Ed. Engl.* **1986**, *25*, 257-259.
4. J. L. Sessler, E. A. Brucker, S. J. Weghorn, M. Kisters, M. Schäfer, J. Lex, E. Vogel, *Angew. Chem. Int. Ed. Engl.* **1994**, *33*, 2308-2312.
5. H. Callot, A. Rohrer, T. Tschamber, B. Metz, *New J. Chem.* **1995**, *19*, 155-159.
6. E. Vogel, *J. Heterocycl. Chem.* **1996**, *33*, 1461-1487.
7. H. Furuta, T. Asano, T. Ogawa, *J. Am. Chem. Soc.* **1994**, *116*, 767-768.
8. P. J. Chmielewski, L. Latos-Grażyński, K. Rachlewicz, T. Glowiak, *Angew. Chem., Int. Ed. Engl.* **1994**, *33*, 779-781.

9. L. Ruoshi, G. M. Ferrence, T. D. Lash, *Chem. Commun.* **2013**, *49*, 7537-7539.
10. T. Tanaka, A. Osuka, *Chem. Rev.* **2017**, *117*, 2584-2640.
11. S. Saito, A. Osuka, *Angew. Chem., Int. Ed. Engl.* **2011**, *50*, 4342-4373.
12. M. Stępień, N. Sprutta, L. Latos-Grażyński, *Angew. Chem., Int. Ed.* **2011**, *50*, 4288-4340.
13. Y. Tanaka, J.-Y. Shin, A. Osuka, *Eur. J. Org. Chem.* **2008**, 1303-1308.
14. S. Shimizu, N. Aratani, A. Osuka, *Chem. Eur. J.* **2006**, *12*, 4909-4918.
15. P. J. Chmielewski, L. Latos-Grażyński, K. Rachlewicz, *Chem. Eur. J.* **1995**, *1*, 68-73.
16. I. Gupta, A. Srinivasan, T. Morimoto, M. Toganoh, H. Furuta, *Angew. Chem. Int. Ed. Engl.* **2008**, *47*, 4563-4567.
17. D. Xie, Y. Liu, Y. Rao, G. Kim, M. Zhou, D. Yu, L. Xu, B. Yin, S. Liu, T. Tanaka, N. Aratani, A. Osuka, Q. Liu, D. Kim, J. Song, *J. Am. Chem. Soc.* **2018**, *140*, 16553-16559.
18. Y. Rao, W. Zhou, L. Xu, M. Zhou, B. Yin, T. Tanaka, A. Osuka, J. Song, *J. Am. Chem. Soc.* **2019**, *141*, 18836-18844.
19. M. G. P. M. S. Neves, R. M. Martins, A. C. Tomé, A. J. D. Silvestre, A. M. S. Silva, V. Félix, M. G. B. Drewb, J. A. S. Cavaleiro, *Chem. Commun.* **1999**, 385-386.
20. A. Srinivasan, T. Ishizuka, A. Osuka, H. Furuta, *J. Am. Chem. Soc.* **2003**, *125*, 878-879.
21. Y.-S. Xie, K. Yamaguchi, M. Toganoh, H. Uno, M. Suzuki, S. Mori, S. Saito, A. Osuka, H. Furuta, *Angew. Chem. Int. Ed. Engl.* **2009**, *48*, 5496-5499.
22. J.-Y. Shin, H. Furuta, K. Yoza, S. Igarashi, A. Osuka, *J. Am. Chem. Soc.* **2001**, *123*, 7190-7191.

23. K. Zhang, J. Zhang, X. Li, R. Guo, H. Ågren, Z. Ou, M. Ishida, H. Furuta, Y. Xie, *Org. Lett.* **2015**, *17*, 4806-4809.

24. B. Adinarayana, M. Das, C. H. Suresh, A. Srinivasan, *Chem. Eur. J.* **2019**, *25*, 4683-4687.

25. S. K. Pushpan, S. Venkatraman, V. G. Anand, J. Sankar, H. Rath, T. K. Chandrashekhar, *Proc. Indian Acad. Sci. (Chem. Sci.).* **2002**, *114*, 311-338.

26. S. Chitranshi, M. Das, B. Adinarayana, W.-Y. Cha, D. Kim, A. Srinivasan, *Org. Lett.* **2020**, *22*, 1081-1085.

27. B. Saikia, P. R. Boruah, A. A. Ali, D. Sarma, *Tetrahedron Lett*. **2015**, *56*, 633-635.

28. M. Stępień, L. Latos-Grażyński, N. Sprutta, P. Chwalisz, L. Szterenberg, *Angew. Chem. Int. Ed*. **2007**, *46*, 7869-7873.

29. M. Stępień, B. Szyszko, L. Latos-Grażyński, *Org. Lett*. **2009**, *11*, 3930-3933.

30. S. Kumar, M. Ravikanth, *J. Org. Chem*. **2017**, *82*, 12359-12365.

31. T. D. Lash, *Chem. Rev*. **2017**, *117*, 2313-2446.

32. B. Szyszko, L. Latos-Grażyński, *Angew. Chem. Int. Ed*. **2019**, DOI: 10.1002/anie.201914840.

33. R. Sengupta, K. G. Thorat, M. Ravikanth, *J. Org. Chem*. **2018**, *83*, 11794-11803.

34. S. Kumar, M. R. Rao, M. Ravikanth, *J. Org. Chem*. **2018**, 83, 1584-1590.

35. S. Kumar, K. G. Thorat, M. Ravikanth, *J. Org. Chem.* **2018**, *83*, 14277-14285.

36. M. Das, B. Adinarayana, M. Murugavel, S. Nayak, A. Srinivasan, *Org. Lett.* **2019**, *21*, 2867-2871.

37. S. Chitranshi, B. Adinarayana, M. Das, W.-Y. Cha, D. Kim, A. Srinivasan, *Chem. Eur. J.* **2019**, *25*, 12911-12915.

38. A. D. Becke, *J. Chem. Phys.* **1993**, *98*, 1372-1377.

39. C. Lee, W. Yang, R. G. Parr, *Phys. Rev. B: Condens. Matter Mater. Phys.* **1988**, *37*, 785-789.

CHAPTER 4

Bis-4,4′-biphenyl Ring Embedded Octaphyrin with Three Distinct Conformational Structures

4.1 Introduction

Octaphyrins are expanded porphyrns consist of eight pyrrole/heterocyclic rings which are connected with/without *meso*-carbon bridge.[1-3] In general, structural diversity and conformational flexiblity of octaphyrins predominantly based on the no. of *meso*-carbon and type of heterocyclic ring.[1,4,5] The structural diversity in octaphyrin exhibits in various forms which includes; planar, figure-eight, inverted, fused, bridged and Möbius twist.[6-20] In this chapter, the octaphyrins are arranged in the increasing order of *meso*-carbon bridges and their synthetic methodologies and salient features are described.

The first meso free octaphyrin **2** was synthesized by Sessler and co-workers.[21] The acid-catalysed oxidative coupling of bipyrrole **1** in the presence of $FeCl_3$ afforded [30]π octaphyrin(0.0.0.0.0.0.0.0) **2** (Scheme 4.1). The crystal analyses revealed that the sulphate ion is trapped inside the macrocyclic framework and bound with eight intermolecular hydrogen bonding interaction with N-H…O bonding distance of 1.91 to 2.49 Å and thus making the molecule planar. The aromatic character of **2** was reflected from ^{1}H NMR analysis, where the inner NH proton was resonated at 0.64 ppm at room temperature.

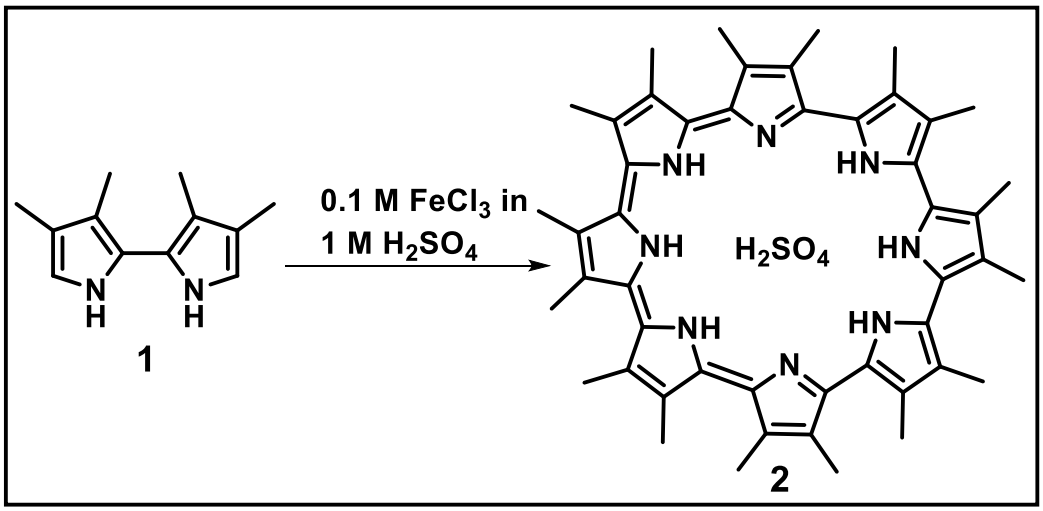

Scheme 4.1: Synthesis of octaphyrin **2**.

[32]π octaphyrin (1.0.1.0.1.0.1.0) **3** with four meso carbons was reported by the Vogel and co-workers.[22] The linear tetrapyrrole (**3a**) and its α, ω-dialdehyde (**3b**) were mixed in 1:1 ratio under acidic condition followed by open-air oxidation to form the octaphyrin **3**. (Scheme 4.2). Alternatively, the reaction was also performed with **2** equivalents of bipyrrole (**3c**) and its diformyl derivative (**3d**) to obtain the octaphyrin **3**. The compound **3** was in figure-eight conformation as revealed by crystal analysis and attained the nonaromatic character.

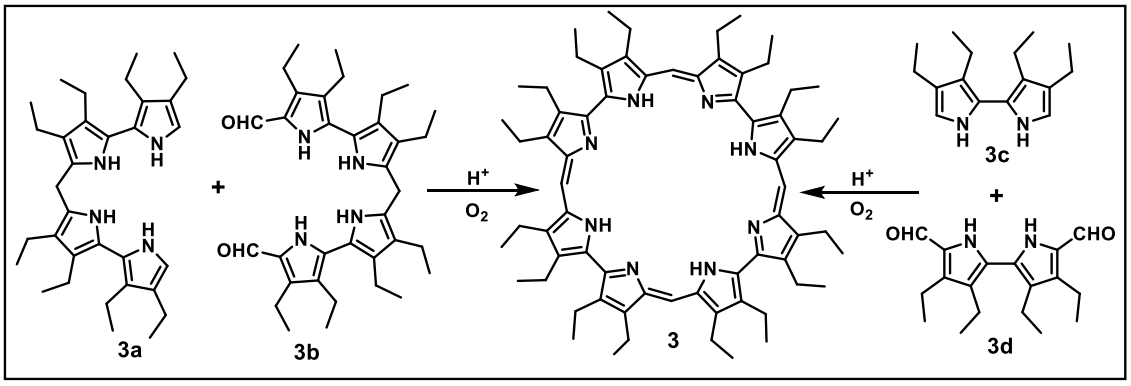

Scheme 4.2: Synthesis of octaphyrin **3**.

The core-modified [34] octaphyrin with six *meso*-carbons was reported by Chandrashekar and co-workers, where the macrocycle was achieved by introducing thiophene units in the core.[23] The compound **4** was synthesized by using two methodologies; (i) by an oxidative coupling reaction of tetrapyrrane (**4a**) with pentafluoro benzaldehyde and 2,3-bischloro-5,6-dicyno-*p*-benzoqunone (DDQ) as a oxidation agent and (ii) [4+4] acid catalysed condensation of **4a** in the presence of *p*-TSA followed by chloranil oxidation (Scheme 4.3). The crystal X-ray analysis reflected the figure-8 confomation of **4** in solid.

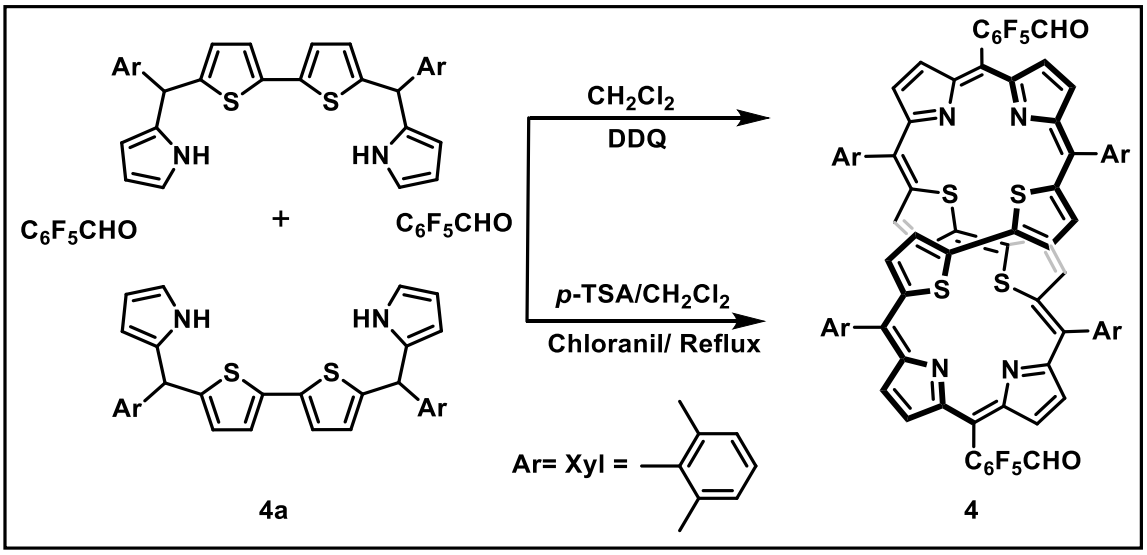

Scheme 4.3: Synthesis of octaphyrin **4**.

The neo-confused octaphyrn (1.1.1.1.1.1.1.0) with seven meso carbons was reported by Furuta and co-workers.[24] The compound **6** was synthesized through a ring closur reaction of an octapyrane derivative implanted with two terminal confused pyrrole (**5**). Precursor **5** as synthesized by acid-catalyzed condensation of hexapyrrane (**5a**) with N-triisopropylsilyl β-pyrrole carbinol (**5b**), succeeded by deprotection with tetra-*n*-butylammonium fluoride. The ring-closure reaction was further executed in the presence of **5** with 5.5 equiv. of DDQ to obtain **6** (Scheme 4.4). The spectral features suggested that the macrocycle **6** is a nonaromatic figure-eight octaphyrin.

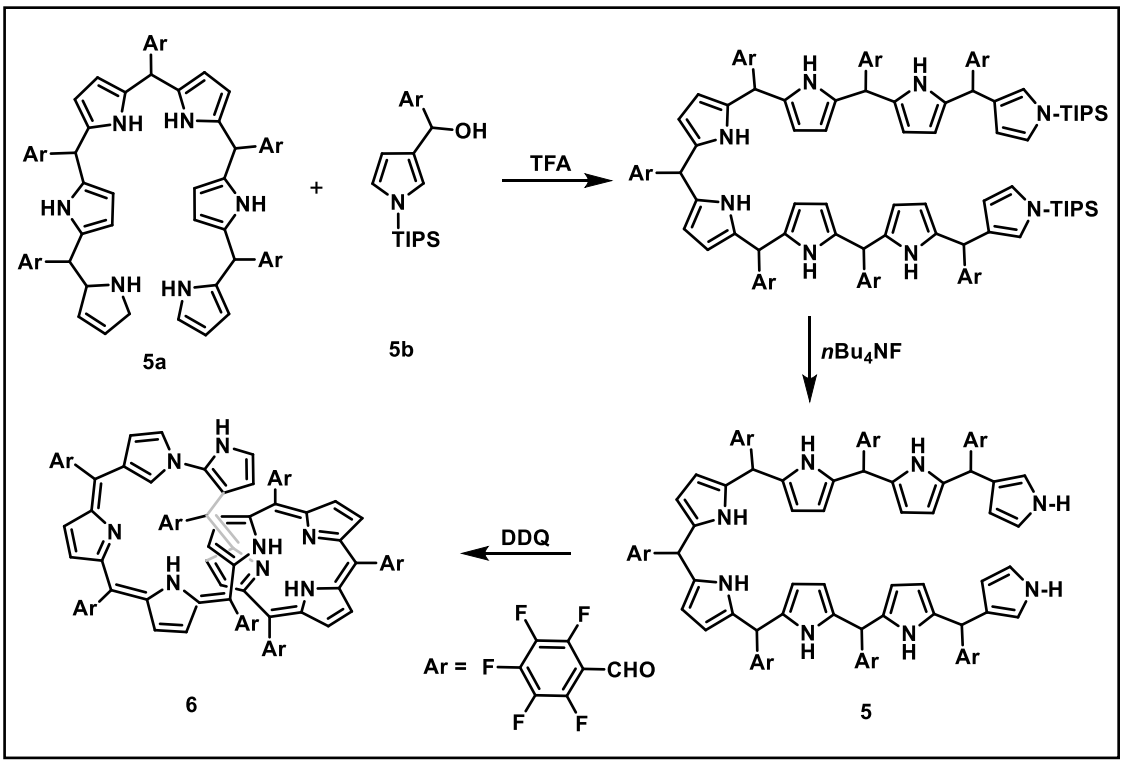

Scheme 4.4: Synthesis of octaphyrin **6**.

The *meso*-aryl octaphyrin with eight meso links **7** was reported by Osuka and co-workers.[25] They adopted modified Lindsey conditions for the synthesis of nonaromatic [36]octaphyrin(1.1.1.1.1.1.1.1) **7** by using pyrole and pentafluorobenzaldehyde follow up by oxidisation with DDQ in 6% yield (Scheme 4.5). The figure-eight conformation was reflected from crystal analyses. Two porphyrin-like pockets in the core of the macrocycle was utilized to stabilize mono and bis-metal ions in the core (**8-14**) and shown in Figure 4.1. Most of protonation experiment were done by using trifluoroacetic acid (TFA) and deprotonation experiment by TBAF salts. The free-ligands, coordinated complexes, protonated and deprotonated macrocycles were identified by various spectral analyses and Möbius and Hückel aromatic characteristics were explored.[5,19] The deprotonation experiment of **7** was further performed with tetrabutylammonium fluoride (TBAF) salt and afforded the monoanionic twisted Möbius aromatic and dianionic Hückel anti-aromatic [36]octaphyrin.[20]

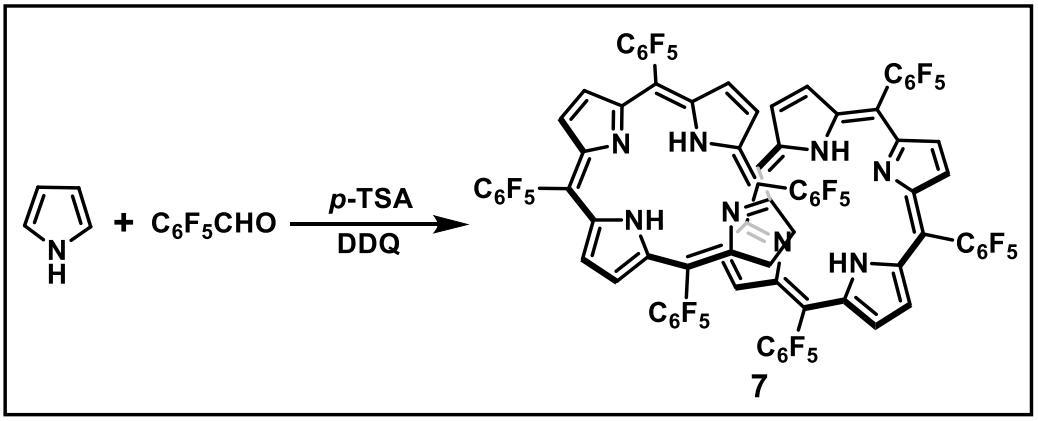

Scheme 4.5: Synthesis of octaphyrin **7**.

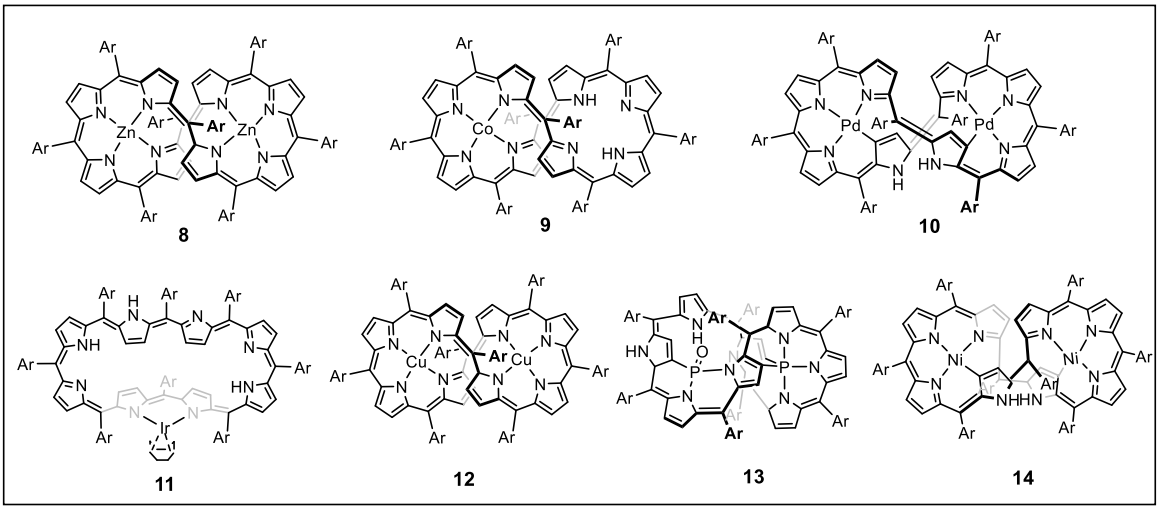

Figure 4.1: Structures of metal complexes of **7**.

The octaphyrin with *meso*-aryl and β-alkyl substituents were discussed so far. The absence of such substituents in the octaphyrin was reported by Vogel and co-workers.[26] Tetrahydroocaphyrin(2.1.0.1.2.1.0.1) was syntheszed by acd-catalytic condensaton of bipyrrole dialdehyde **15** with dipyrroethane dicarboxylic acid **16**. The thermal dehydrogenation of **17a** with 10% Pd / C under reflux condition resulted in the formation of conjugated product **17**. (Scheme 4.6). In addition, the octaphyrin(1.1.1.0.1.1.1.0) **19** was also obtained under similar reaction conditions using dipyrromethane dicarboxylic acid **18** and dialdehyde **15** (Scheme 4.7). Both **17** and **19** attained figure-eight conformation and exhibited nonaromatic character.

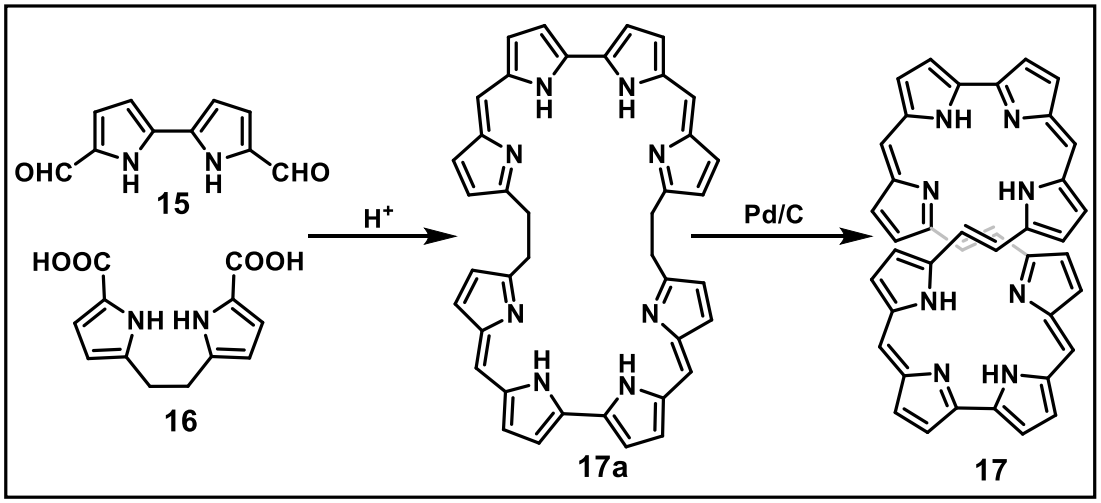

Scheme 4.6: Synthesis of octaphyrin **17**.

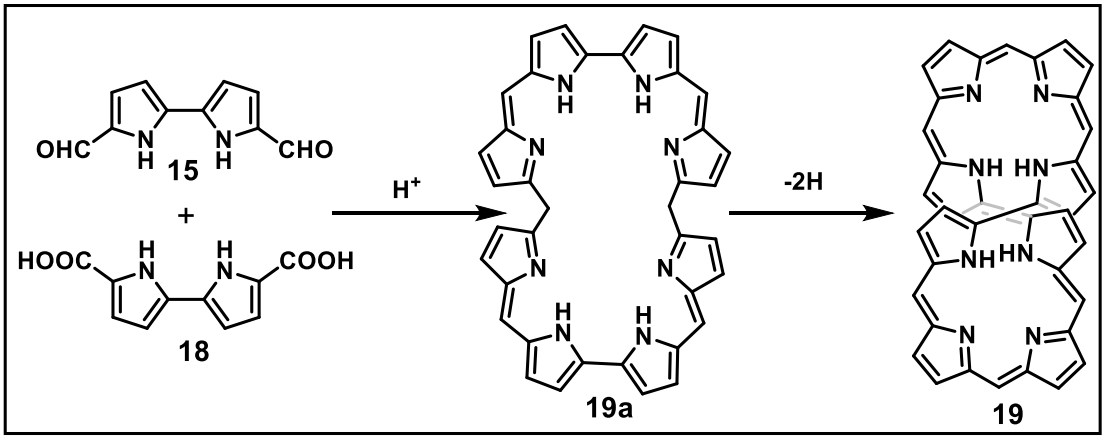

Scheme 4.7: Synthesis of octaphyrin **19**.

The octaphyrin with more than eight *meso*-carbons was reported by Rath and co-workers, where the octaphyrin(2.1.1.1.2.1.1.1) (**21**) contained two conjugated ethyne bridges.[27] The macrocycle **21** was achieved by an acid catalysed condensation of tetrapyrrane moiety **20** with pentaflourobenzaldehyde which was then oxidised with chloranil (Scheme 4.8). Spectral assignment established that the conformation of **21** in solution is figure-eight and maintained same structure in the solid state.

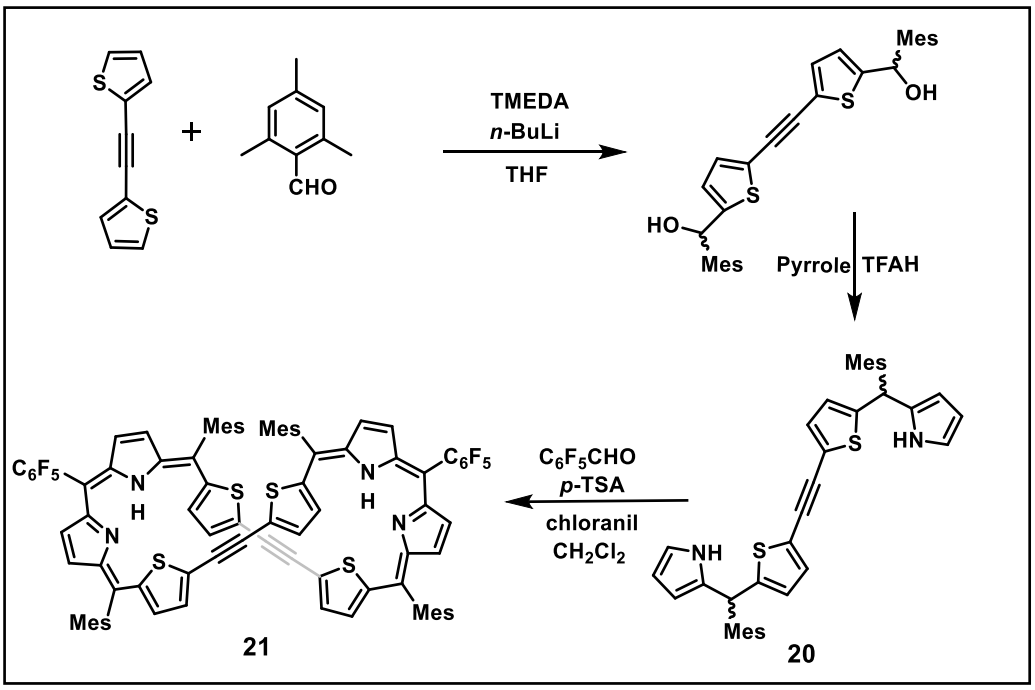

Scheme 4.8: Synthesis of octaphyrin **21**.

4.2 Objective of our work

Initially, octaphyrins were mainly confined to polypyrrolic units, however with due time it has been tuned by modifying; i) the core with heterocyclic units other than pyrrole and ii) by increasing or decreasing the number of *meso*-carbon atoms. These factors impart conformational and structural diversity to the macrocycle. However, carbocyclic octaphyrin is unknown in the literature and such porphyrin analogues provides a deeper insight into their rich coordination chemistry, conformational flexibility and higher oxidation state organometallic complexes.[28] To explore such chemistry, in our initial effort, biphenyl unit has been incorporated in the octaphyrin framework for the first time. Hence, the main objective of this chapter is to; (i) introduce higher arene units in the octaphyrin macrocycle (**25**) and (ii) also explore its coordination chemistry and structural diversity (**26**).

4.3 Results and discussions

4.3.1 Synthesis

The synthesis of bis-*p,p′*-biphenyl unit incorporated octaphyrin(1.1.1.0.1.1.1.0) and its bis-Rh(I) complex in Scheme 4.9. The initial, 4,4′-diformyl biphenyl (**22**) was synthesized as per the literature procedure.[34] The Grignard reaction of **22** in the presence of phenylmagnesium bromide in THF to form respectiv diol **23** in 88%. The required precursor to synthesize the target macrocycle was achieved by Lewis acid-catalyzd condensaton of **23** with excess pyrole reflux to form 4,4'- bis(phenyl(1H-pyrrol-2-yl)methyl)-1,1'-biphenyl (**24**) in 64% yield. The final condensation of of 4,4'-bis(phenyl(1H-pyrrol-2-yl)methyl)-1,1'-biphenyl **24** and pentafluorobenzaldehyde in the presence of *p*-TSA followed by oxidation with 2,3-dichloro-5,6-dicyano-*p*-benzoquinone (DDQ) (Scheme 4.9). The crude reaction mixture was purified by silica gel (100-200 mesh) colun separation by using 20% DCM /hexane mxture, where the desired product was eluted as a green fraction and identified as **25** in 9% yield. The coordination chemistry of **25** was performed by reaction with $[Rh(CO)_2Cl]_2$ in CH_2Cl_2 / CH_3OH solution at room temperature followed by column chromatographic purification to afford **26** as blue color solid in 7% yield.

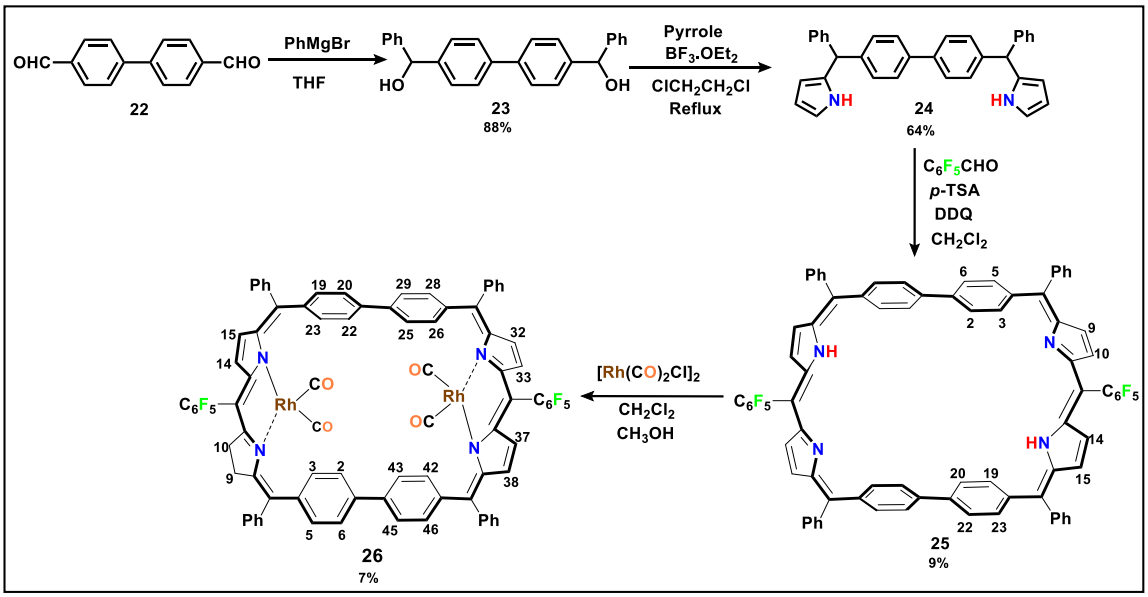

Scheme 4.9: Synthesis of **25** and its bis-Rh(I) complex (**26**).

4.3.2 Spectral Characterization

4.3.2.1 Mass spectral analyses

The formation of compound **25** was confirmed by electrospray ionization (ESI) mass spectrometric analysis with molecular ion peak at 1277.3657 (*m/z*) (Figure 4.2), whereas the molecular ion peak at 1592.1300 (*m/z*) (Figure 4.3) confirmed the exact composition of the complex **26**.

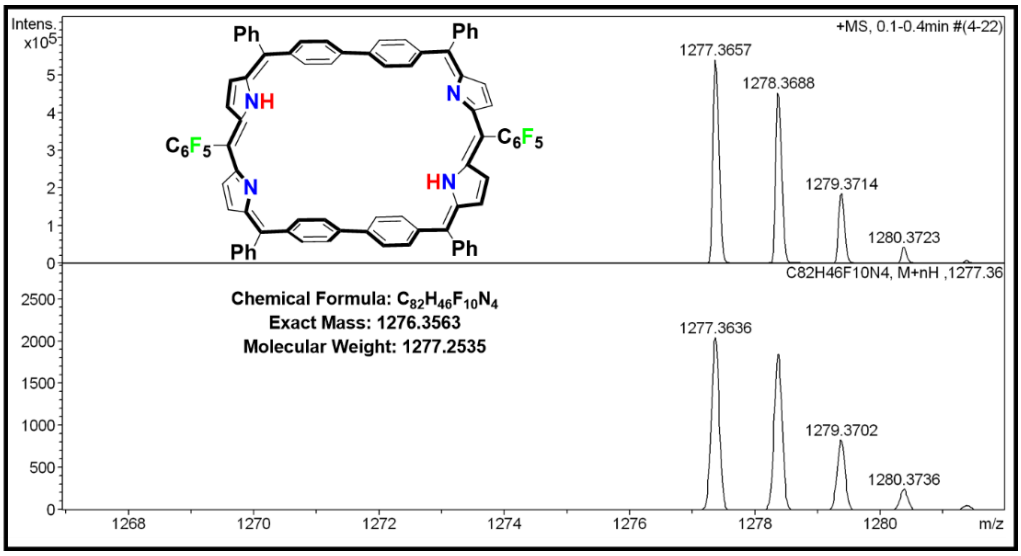

Figure 4.2: HR-MS spectrum of **25**.

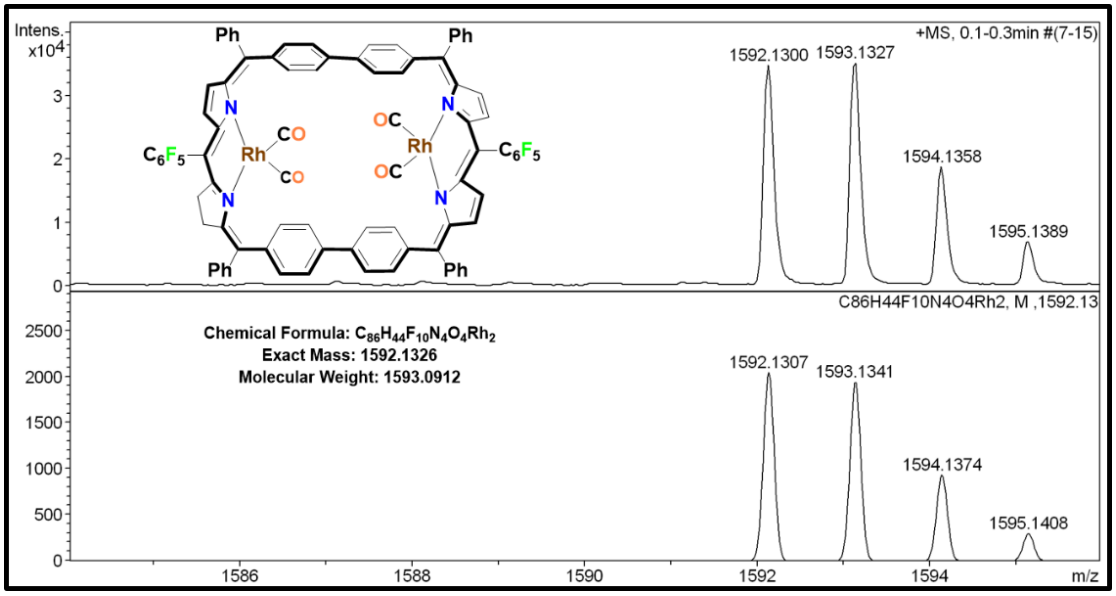

Figure 4.3: HR-MS spectrum of **26**.

4.3.2.2 NMR Analyses

The proton spectrum of **25** at 297 K is shown in Figure 4.4a with two set of doublets and a set of multiplet signals. The doublet signal resonated at 6.56 [H(10,14)] and 6.12 ppm [H(9,15)] corresponds to pyrrolic *β*-CH protons. The inner and peripheral-CH protons of biphenyl ring are resonated as another set of doublet signals at 7.35 [H(2,3,19,20)] and 7.93 ppm [H(5,6,22,23)]. The *meso*- phenyl protons are observed as multiplets at 7.20 and 7.40 ppm. The broad NH signal observed at 13.80 ppm was further confirmed by D_2O exchange experiments, suggesting the strong intramolecular hydrogen bonding interactions. All these signals were further confirmed by (Figure 4.5), where the corelation was observed amine and imine pyrrole *β*-CH protons and also between the inner and peripheral-CH protons of biphenyl ring. Upon lowering the temperature, the pyrrolic *β*-CH as well as biphenyl protons are slightly upfield shifted, whereas the NH signal is minutely deshielded **(**Figure 4.6). The Δδ value of inner and outer biphenyl protons is 0.8 ppm which clearly reveals the nonaromatic character in

25.[29,30] The protonation experiment was further conducted by increasing the concentration of trifluoroacetic acid (TFA) in CD_2Cl_2 solution of **25** at 298 K (Figure 4.7). The pyrrolic β-CH protons are upfield shifted by 0.52 and 0.76 ppm and resonated at 6.64 [H(10,14)] and 7.32 ppm [H(9,15)], respectively. However, the pyrrolic NH proton is drastically upfield shifted by 4.85 ppm and appeared as broad signal at 8.95 ppm. At 233 K, two different type of NH signals were observed at 10.07 and 8.78 ppm respectively, which suggests that one of the pyrrole rings in the dipyrromethene unit is inverted as compared to **25** (Figure 4.8). The inner and peripheral biphenyl protons are moderately deshielded. Overall, the spectral analysis of **25**.**2H**$^+$ maintains the nonaromatic character in solution.

Upon metal ion insertion, the following changes were observed in the ^{1}H NMR analysis of **26** in CD_2Cl_2; (i) all the signals were broad at 298 K (Figure 4.9); however, the signals were well resolved upon lowering the temperature at 253 K (Figure 4.4b); (ii) the loss in symmetry results in the appearance of individual signals for pyrrolic and biphenylene units between 6.32 ppm and 8.06 ppm. Interestingly, the biphenyl protons [H(3,42)], which are in close proximity to the metal ion are deshielded as compared to the other proton signals in the complex reveals the weak M…H–C interaction; and (iii) the disappearance of NH signal further confirms the metal ion insertion only in the dipyrromethene units. All these proton signals were also assigned by ^{1}H-^{1}H COSY analysis (Figure 4.10). Overall, spectral analysis suggests that the nonaromatic character is retained as such in complex **26**.[29, 30]

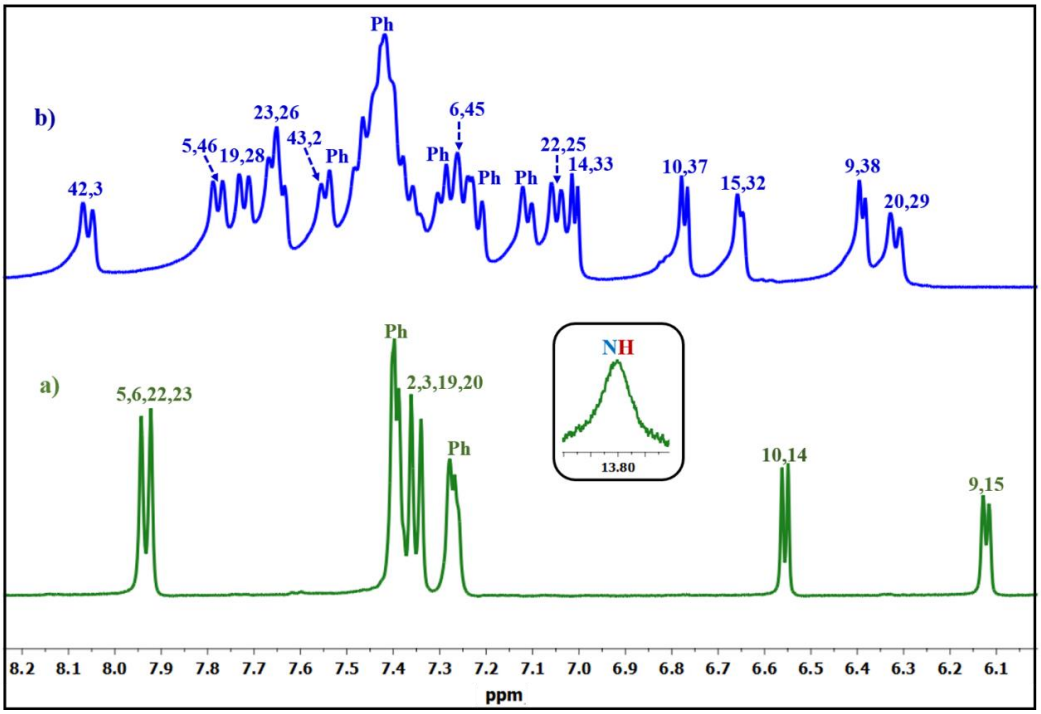

Figure 4.4: Proton NMR spectra of **25** (a) 298 K and **26** (b) 253 K in CD_2Cl_2.

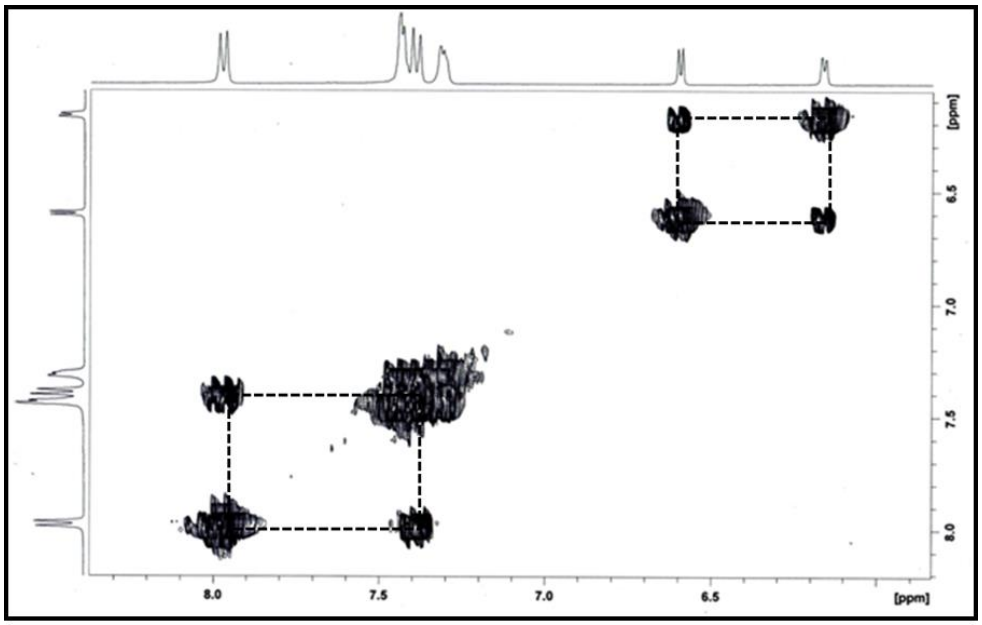

Figure 4.5: ^{1}H –^{1}H COSY spectrum of **25** in CD_2Cl_2 at 298 K.

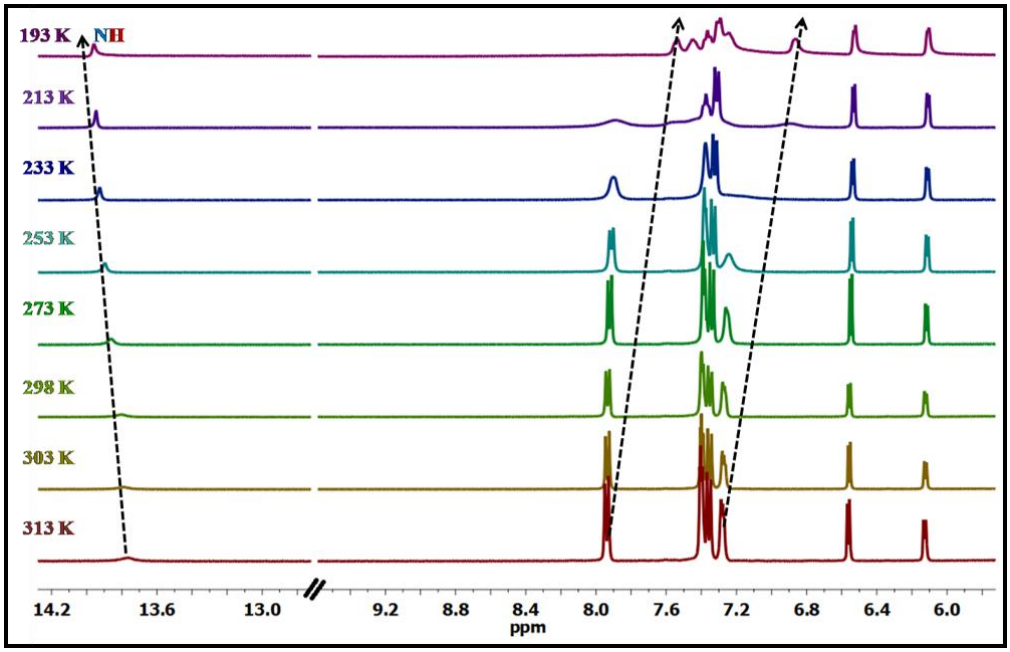

Figure 4.6: Variable temperature ^{1}H NMR spectra of **25** in CD_2Cl_2.

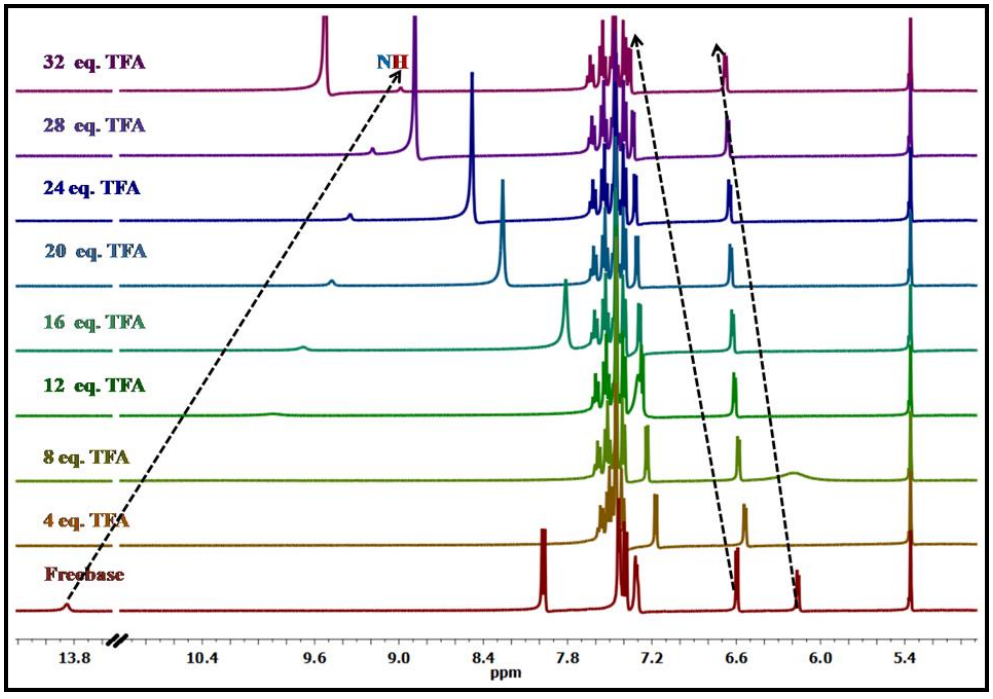

Figure 4.7: ^{1}H NMR spectra of **25** with increasing concentration at 298 K.

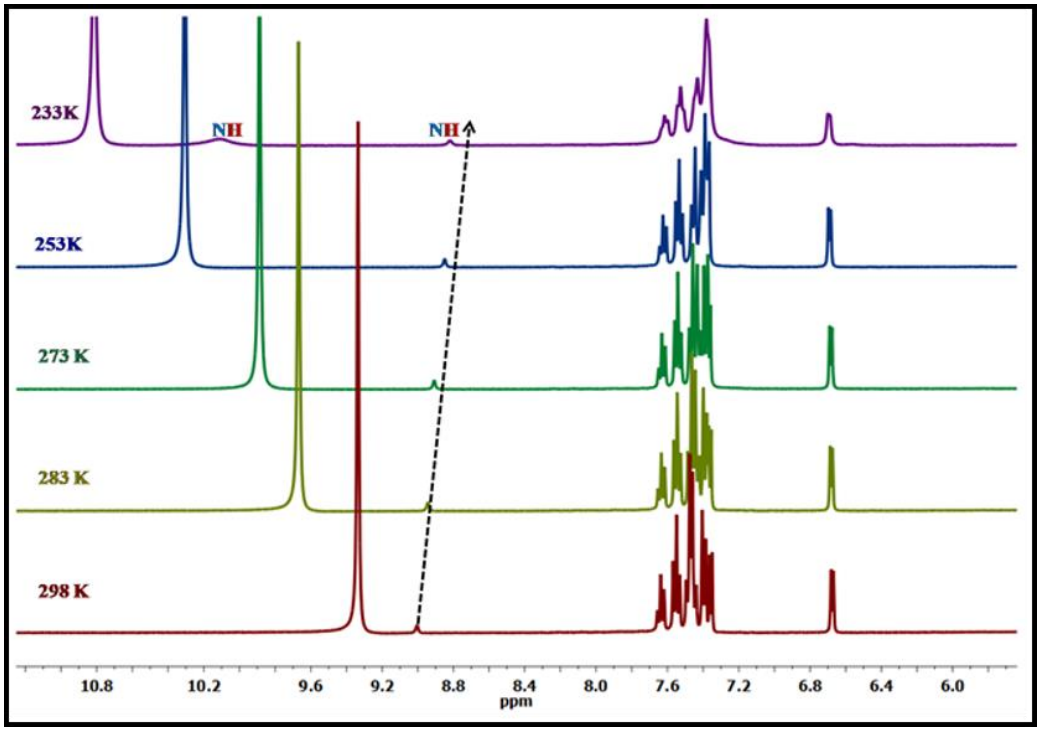

Figure 4.8: Low temperature ^{1}H NMR spectra of **25**.**2H**$^{+}$ with 32 eq. of TFA in CD_2Cl_2.

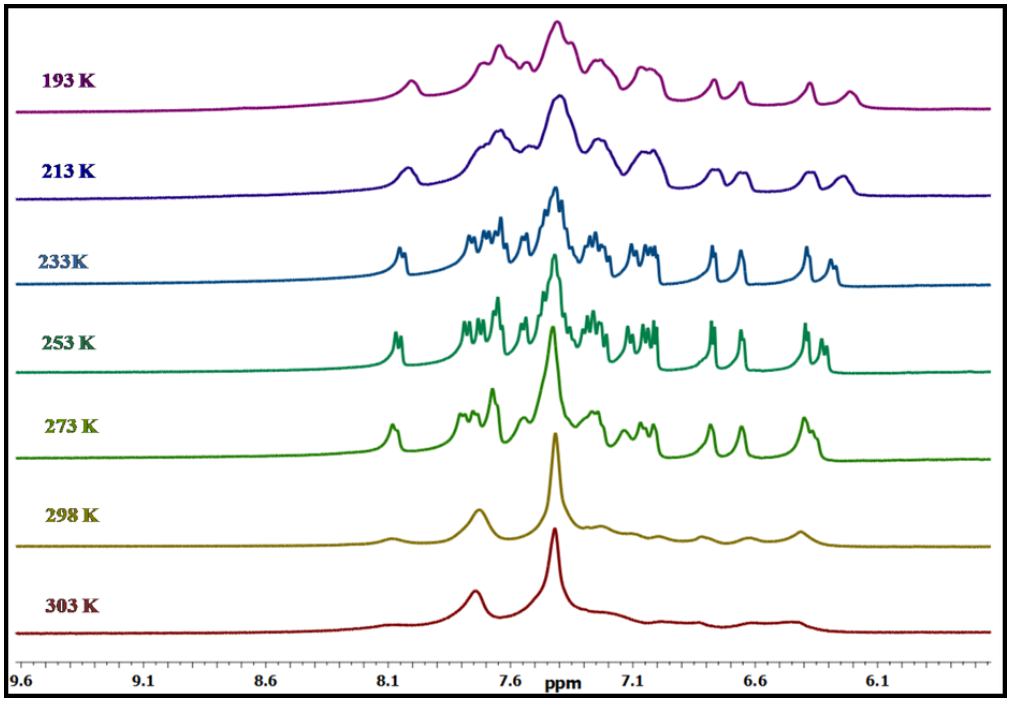

Figure 4.9: Variable temperature ^{1}H NMR spectra of **26** in CD_2Cl_2.

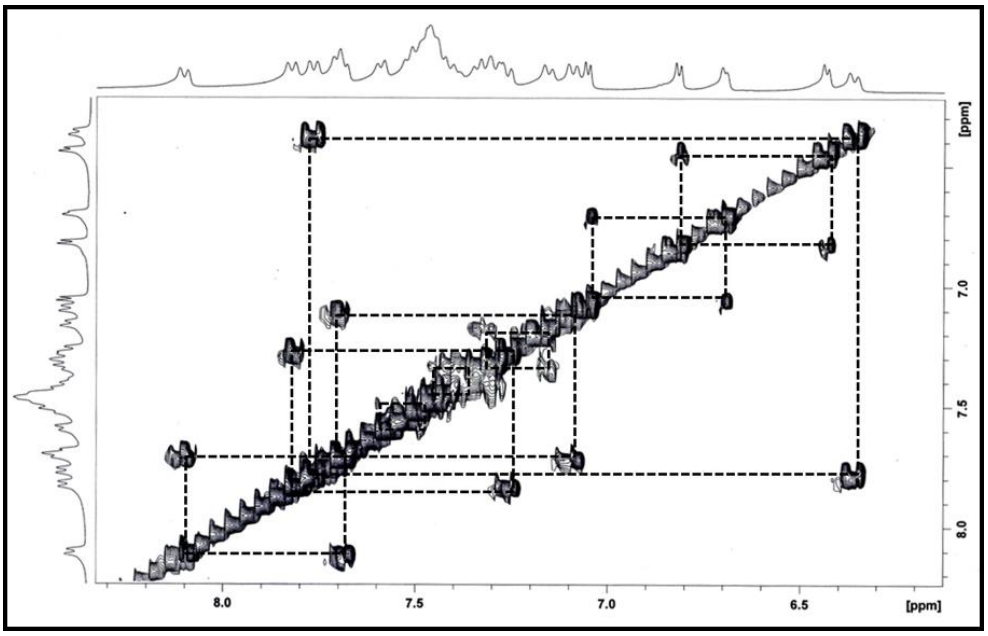

Figure 4.10: ^{1}H –^{1}H COSY spectrum of **26** in CD_2Cl_2 at 253 K.

4.3.2.3 Crystal analyses of 25, 25.2H^{+} and 26

The structure of **25** was characterized by X-ray analysis as shown in Figure 4.11 a & c and the crystal data are in Table 4.1. $P4_2/n$ space group and is located on crystallographic twofold axis. The deshielded NH signal as observed in the NMR spectral analysis of **25** is reflected in the X-ray crystal analysis, in which intramolecular hydrogen-bonding interactions were observed between the pyrrolic amine NH and the imine N with a bond length and angle of N1-H1⋯ N2/N1′-H1′⋯N2′ corresponding to 2.151(4) Å and 122.34(4)°, respectively. The pyrrolic units in the macrocyclic framework (28.86°) are highly tilted from the mean plane containing the *meso*-carbon atoms (C7-C12-C17-C17′-C12′-C7′) compared to the biphenyl unit (6.09°), and the overall structure adopts a figure-eight conformation in the solid state. The crystal analysis also reveals the π–π interaction between the biphenyl units with bond lengths of Ph(π)1-Ph(π)1′ and Ph(π)2-Ph(π)2′ corresponding to 4.03(4) Å (Figure 4.12). In

addition, one of the fluorine atoms in the *meso*-pentafluorophenyl units (F3) is in intermolecular hydrogen bonding interaction with pyrrolic *β*-CH (C10-H10) with bond distance and angle of 2.831 (4) Å and 140.75 (3)° and generate 1-D array in the solid state **(**Figure 4.13).

The structure of **25.2H**$^{+}$ was determined by single-crystal X ray analysis and shown in Figure 4.11 b & d and Table 4.1. Upon interaction with the TFA anion the crystal analysis reveals the following: (i) major conformational change from a twisted figure-eight to an open conformation, (ii) induces the pyrrolic ring inversion as observed in the ^{1}H NMR analysis, and (iii) the inverted pyrrolic *β*-CH protons (C15-H15/C15′-H15′) show intermolecular hydrogen-bonding interactions with the fluorine atoms (F15/F15′) of the trifluoroacetate unit, with a distance and angle of C15-H15 ⋯F15/C15′- H15′⋯F15′) corresponding to 2.80(6) Å and 126.25(3)°, respectively; and trifloroacetate anions are located above and below the mean macrocyclic plane containing the *meso*- carbon atoms (C13-C18-C23-C13′-C18′-C23′) (Figure 4.11 b & d).

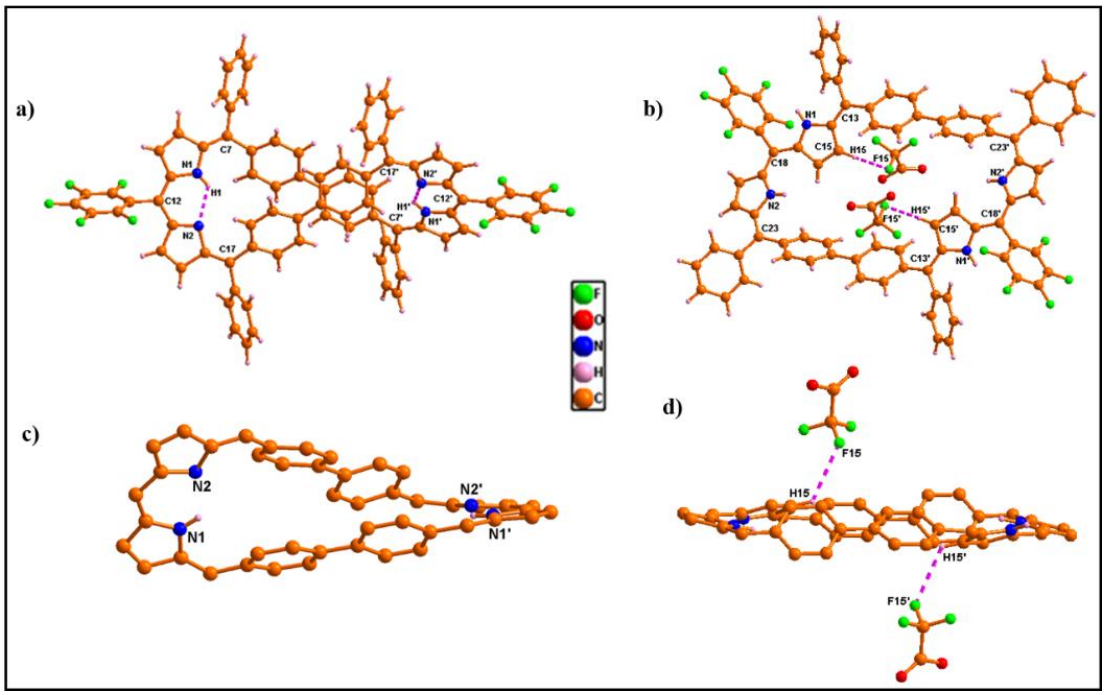

Figure 4.11: Crystal structures of **25** and **25.2H**$^{+}$. a) & b) Top views and c) & d) side views.

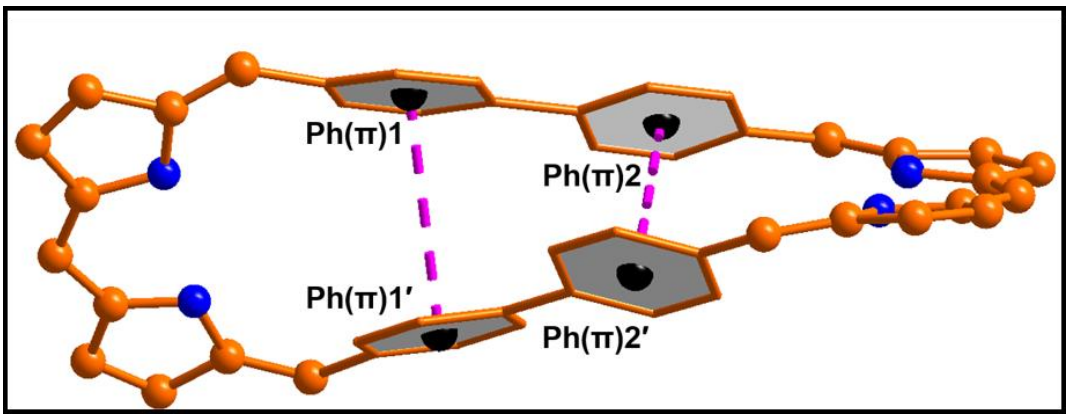

Figure 4.12: Crystal analysis of **25**. The bond distances are Ph(π)1-Ph(π)1′: 4.034(4) Å and Ph(π)2-Ph(π)2′: 4.034(4) Å. The hydrogen atoms and *meso*-aryl groups are omitted for clarity.

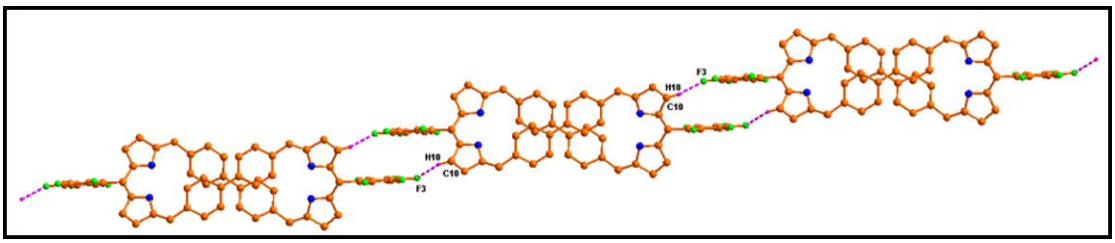

Figure 4.13: Single crystal X-ray analysis of **25** in 1-D array. The bond distances and angles are C10-H10…F3: 2.831(4)Å and 140.75(3)° respectively.

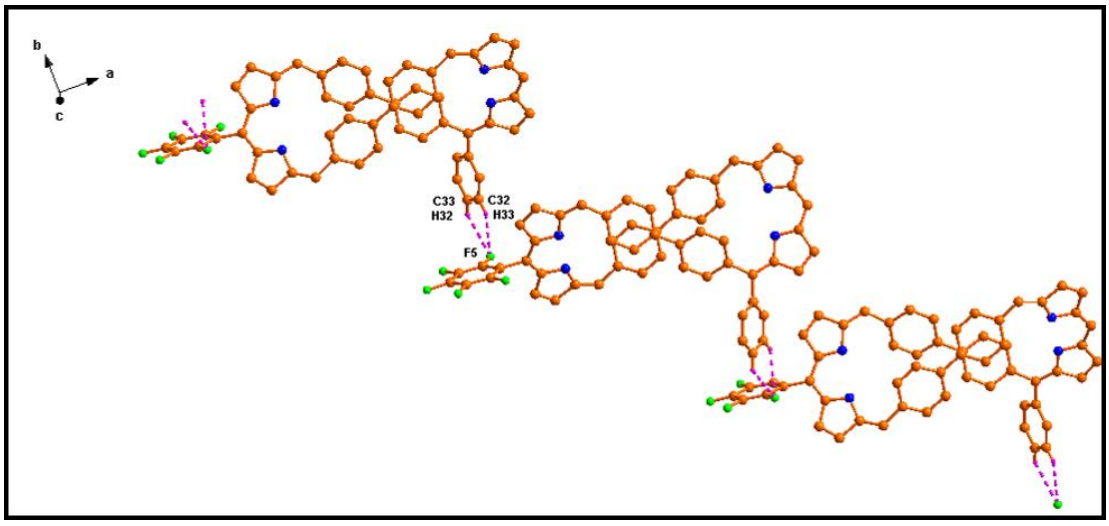

Figure 4.14: Single crystal X-ray analysis of **25** in 2-D array. The bond distances and angles are C33-H33…F5: 2.547(4)Å and 132.23(3)°; C32-H32…F5: 2.674(4)Å and 126.56(3)° respectively.

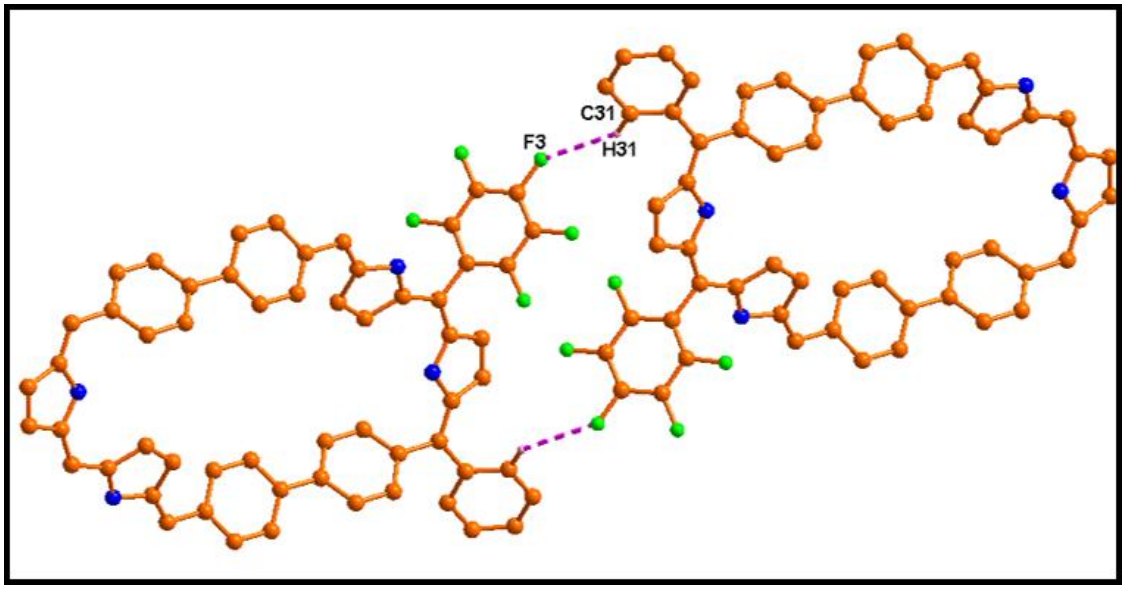

Figure 4.15: Self-assembled dimer in **25.2H**$^{+}$. The bond distance and angle are: a) C31-H31…F3: 2.877(5) Å & 145.51(4)°.

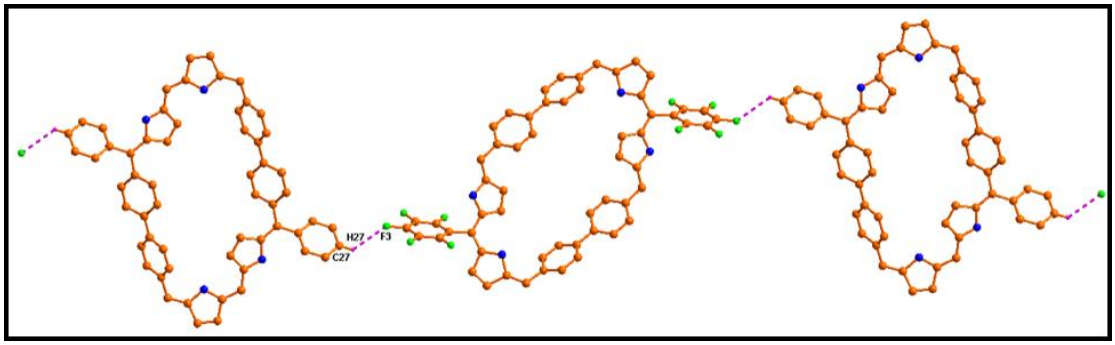

Figure 4.16: 1-D array in **25.2H**$^{+}$.: C27-H27…F3: 2.757(5) Å and 125.59(4)° respectively.

The complex crystallizes in a triclinic crystal lattice with *P*-1 space group. As observed in the spectral analyses, the two Rh(I) ions are coordinated with the dipyrromethene units. The geometry around the Rh(I) ions is square planar. The bond lengths in Rh1-N1, Rh1-N2, Rh2-N3 and Rh2-N4 are between 2.07(4) and 2.09(5) Å; where these values are comparable with those of Rh(I) complex of *p-o-p*

homoporphyrin, albeit larger with respect to Rh complex of rosarin.[29,30] The dihedral angles between the mean plane of the biphenyl and the dipyrromethene units are 88.86(1) and 89.38(9)°, respectively; and provide an unsymmetrical structure with a singly twisted conformation (Figure 4.17b). One of the Rh(I) ions is protruded above the mean dipyrromethene plane with a distance of 1.04(1) Å and the other located below with a distance of 1.06(2) Å. The distance between these Rh(I) ions is 10.327(7) Å. The crystal analyses reveal the following weak non-bonding interactions: (i) one of the CH (C5-H5/C46- H46) protons of the biphenylene units shows weak anagostic type interactions with the metal ions and with a bond length of C5-H5⋯Rh1 and C46-H46⋯Rh2 corresponding to 2.89(4) and 2.89(5) Å, respectively (Figure 4.17b);[31] and (ii) an intermolecular hydrogen-bonding interaction between one of the CH protons (C6-H6/C45-H45) of the biphenyl units with the π-cloud of the other biphenyl unit with a bond length and angle for C6-H6⋯Ph(π)1 of 2.95(1) Å and 143.65(3)°; and for C45-H45⋯Ph(π)2 of 2.89(2) Å and 146.59(4)°, respectively.

.

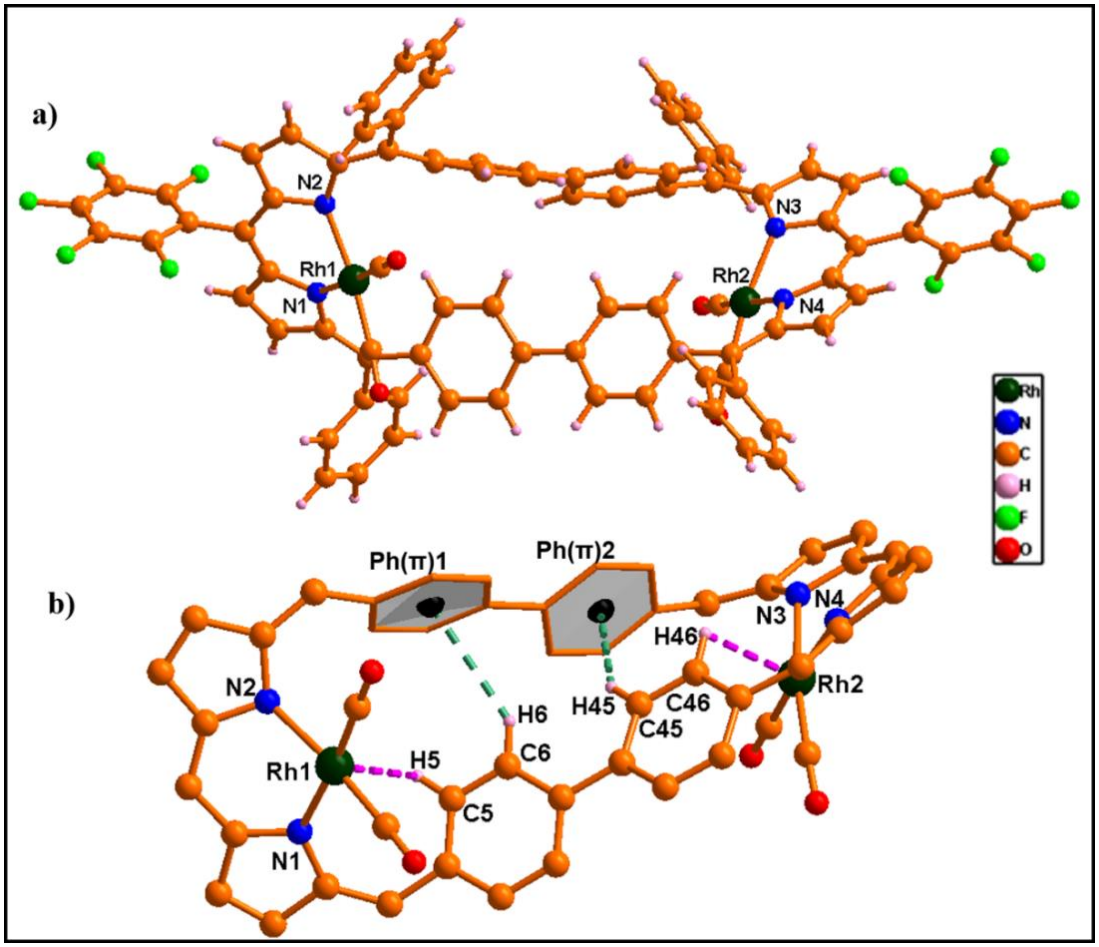

Figure 4.17: Single crystal X-ray structure of **26**. a) Top view and b) side view. Peripheral hydrogen atoms and *meso*-aryl groups in b) are omitted for clarity.

The aromatic properties of **25**, **25.2H**$^{+}$ and **26** have been monitored by X-ray analysis and reveal: (i) the bond lengths across the dipyrromethene units adopt alternatively an sp^2-sp^2 single (1.456(9) Å) and double (1.318(1) Å) bond character and exhibit π delocalization within the dipyrromethene units; (ii) the phenylene units are connected with another phenylene unit and the dipyrromethene units show an sp^2-sp^2 single bond character (1.483(4) Å); and (iii) the bond distances within the phenylene units of the biphenyl moieties exhibit an sp^2-sp^2 double bond character (1.362(4)–1.481(4) Å) and the mentioned bond length values are comparable with those of *p*-*o*-*p* homoporphyrin and Rh(I) complex of rosarin, confirming the individual aromaticity in the biphenyl

moieties.[29, 30] Overall, the allowed π-conjugation bonding mode of the biphenyl unit in the global aromatic macrocycle was dominated by local aromaticity, thus confirming the nonaromatic characteristics in all the forms (Figures 4.19 – 4.21).

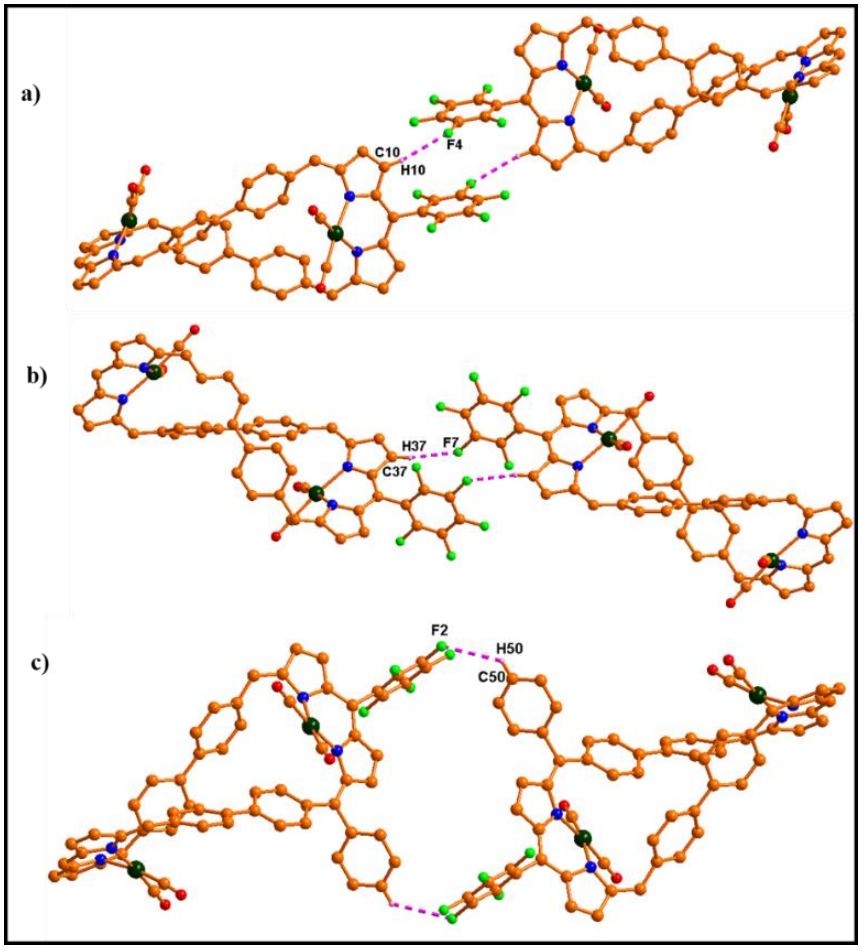

Figure 4.18: Single crystal X-ray analysis of **26**. a), b) and c) are self-assembled dimers. The bond distances and angles are: a) C10-H10…F4: 2.673(6) Å and 167.77(4)° ; b) C37-H37…F7: 2.531(8) Å and 157.06(4)°; c) C50-H50…F2: 2.833(7) Å and 132.27(5)° respectively.

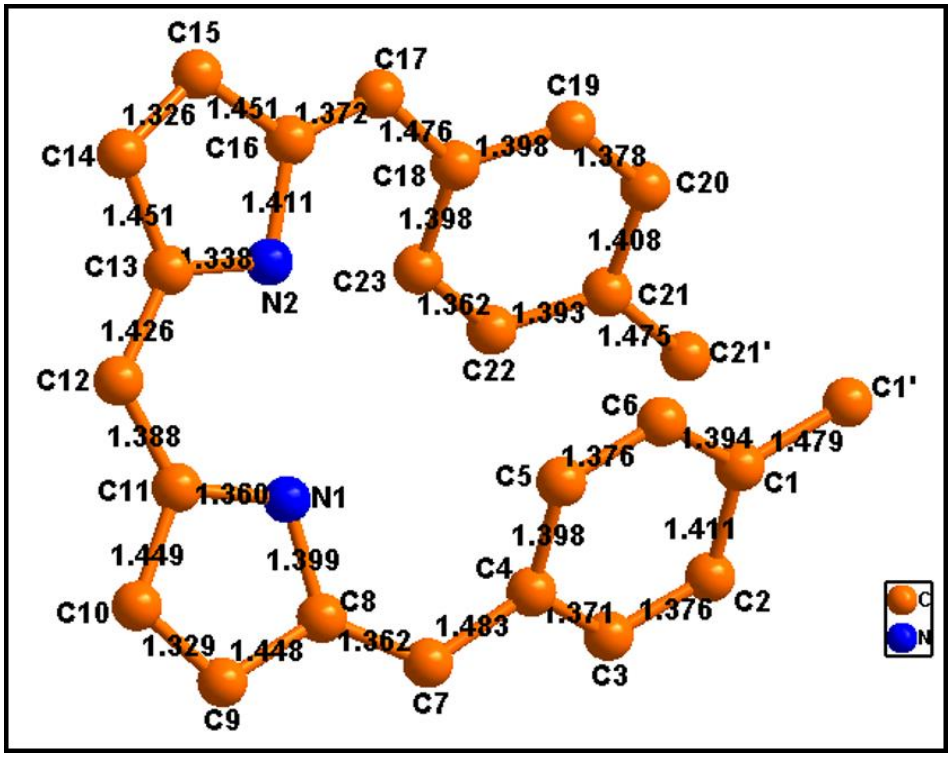

Figure 4.19: Bond lengths in **25** (Å) as present in unit cell.

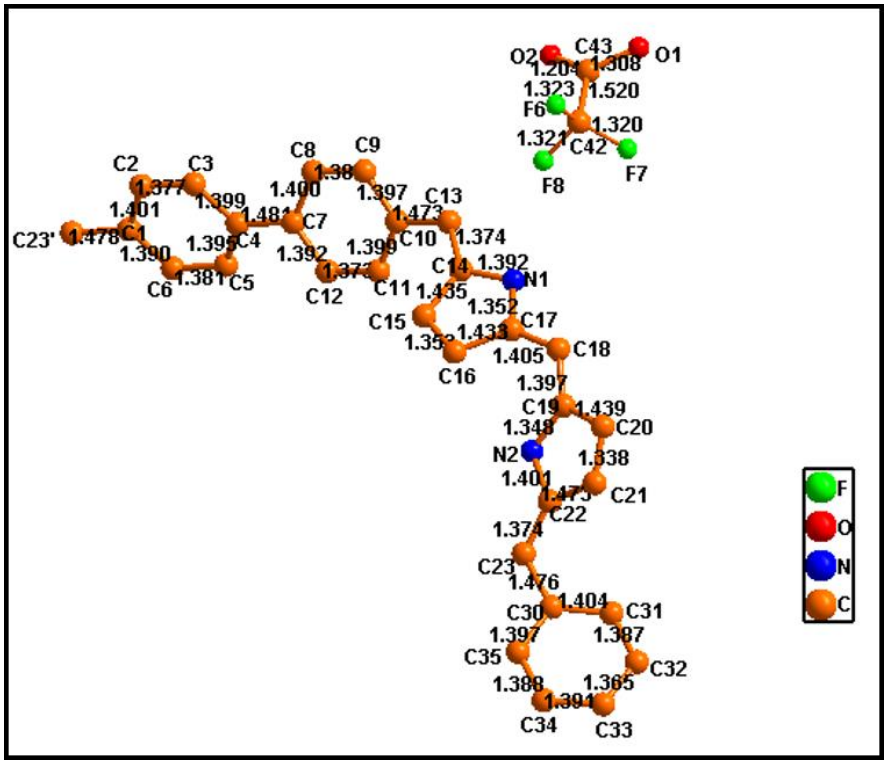

Figure 4.20: Bond lengths in **25.2H**$^{+}$ (Å) as present in unit cell.

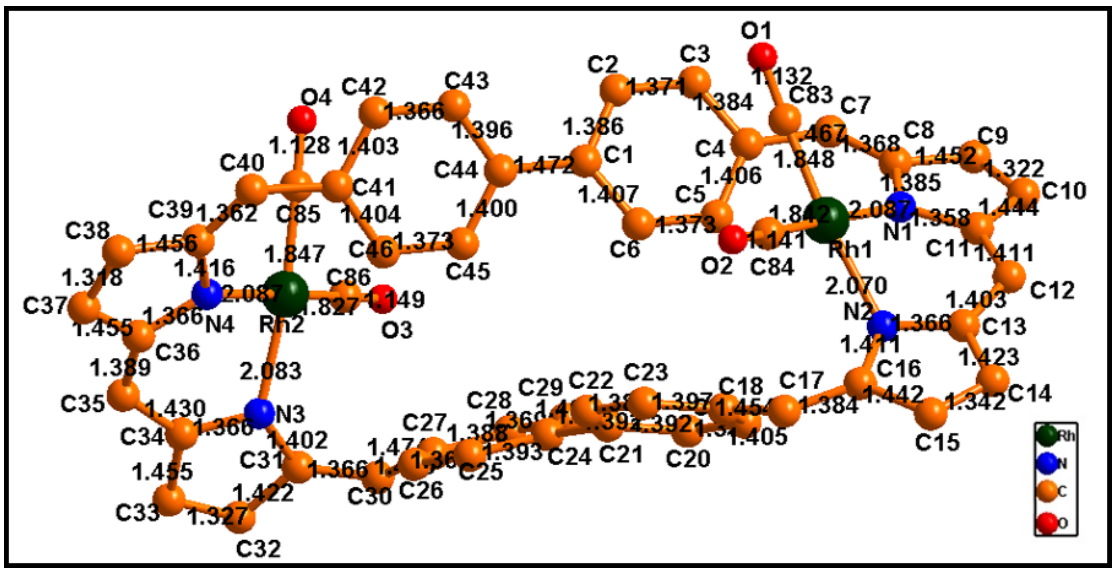

Figure 4.21*:* Bond lengths in **26** (Å) as present in unit cell.

Table 4.1: Crystal data for **25**, **25.2H**$^{+}$ and **26**

Crystal parameters	**25**	**25.2H**$^{+}$	**26**
Formula	$C_{82}H_{46}F_{10}N_4$	$C_{49}H_{26}F_{17}N_2O_8$	$C_{86}H_{44}F_{10}N_4O_4Rh_2$
M/g mol^{-1}	1277.23	1093.73	1593.07
T/K	100 K	100 K	293 K
Crystal dimensions/mm^3	0.1 × 0.07 × 0.05	0.24 × 0.18 ×0.11	0.2 × 0.15 × 0.09
Crystal system	Tetragonal	monoclinic	triclinic
Space group	$P4_2/n$	$P2_1/n$	$P\,1$
a/Å	24.009(3)	14.6076(14)	10.2981(6)
b/Å	24.009(3)	16.5294(15)	22.4414(6)
c/Å	13.199(2)	20.1422(18)	22.9215(3)
α/°	90.00	90	70.038(2)
β/°	90.00	102.787(6)	80.330(4)
γ/°	90.00	90	81.387(4)
V/Å^3	7608.4(2)	4742.8(8)	4883.8(3)
Z	4	4	2
ρcalcd/mg m^{-3}	1.115	1.5316	1.083
μ/mm^{-1}	0.082	0.148	3.245
F(000)	2624.0	2206.1	1600.0
Reflns. collected	77817	55937	59273
Indep.reflns.[R(int)]	7213 [0.1489]	8745 [0.0778]	17229 [0.0723]
Max/min transmission	0.996 and 0.993	0.984 and 0.969	0.747 and 0.585
Data/restraints/parameters	7213/0/513	8745/0/687	17229/0/955
GOF on F^2	1.048	1.103	1.012
Final R indices[$I > 2\sigma(I)$]	R1 = 0.0785, wR2 = 0.2047	R_1 = 0.0663, wR_2 = 0.1619	R1 = 0.0714, wR2 = 0.2280
R indices (all data)	R1 = 0.1207, wR2 = 0.2242	R_1 = 0.1172, wR_2 = 0.1927	R1 = 0.0970, wR2 = 0.2787
Largest diff peak and hole [e Å^{-3}]	0.32 and -0.28	1.14 and -0.64	1.19 and -2.65

The crystals deposited in the Cambridge Crystallographic Data Centre with reference no. CCDC 1936876 (**25**), CCDC 1936880 (**25.2H**$^{+}$) and CCDC 1936890 (**26**). These data can be obtained free from the Cambridge Crystallographic Centre via www.ccdc.cam.ac.uk/data_request/cif.

4.3.2.4 Absorption spectral analysis

The UV spectrum of **25**, **25**.**2H**$^+$ and **26** in CH_2Cl_2 is shown in Figure 4.22 and its molar extinction coefficient values are mentioned in Table 4.2. An intense band was observed between 400 and 490 nm and weak bands between 500 and 900 nm. For example, the intense band in **25** is observed at 431 nm and weak band at 642 nm. Upon protonation (**25**.**2H**$^+$) and metal ion insertion (**26**), the color of the solution changes from green to blue and the intense bands are blue-shifted, whereas the weak bands are redshifted as compared to **25**. Overall, the observed spectral pattern and molar extinction coefficient values are comparable with the reported *p*-*o*-*p* homoporphyrin,[29] which clearly indicates the nonaromatic character in **25**, **25**.**2H**$^+$ and **26**.

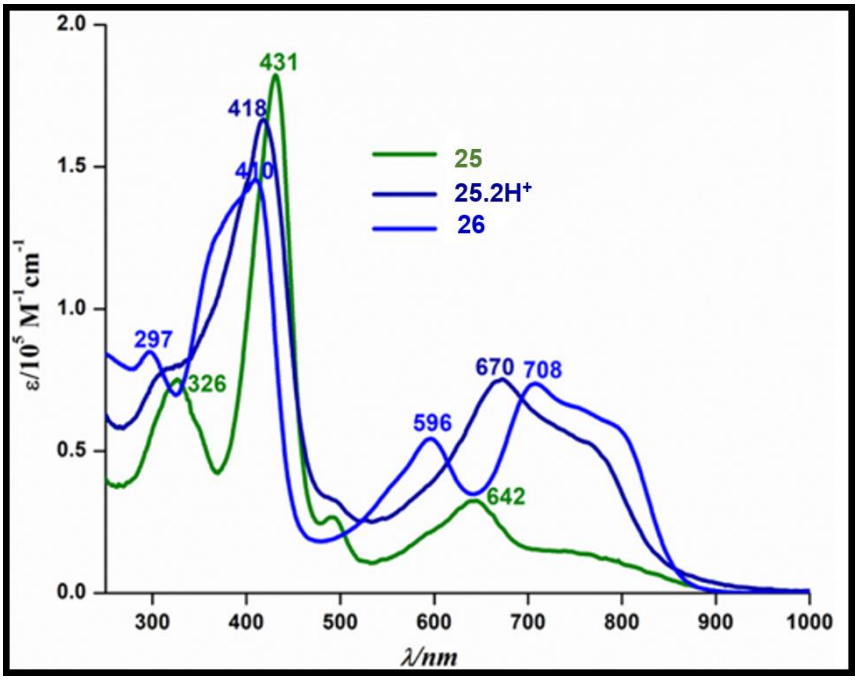

Figure 4.22: The absorption spectra of **25**, **25.2H**$^+$ and **26** in CH_2Cl_2.

Table 4.2: Electronic absorption spectral data of **25**, **25.2H**$^{+}$ and **26** (concentration ≈ 10^{-6} M)

Compounds	λ_{max}/nm (ε[$M^{-1}cm^{-1}$]x10^5)
25	326 (0.75), 431 (1.82), 642 (0.32)
25.2H^{+}	418 (1.66), 670 (0.74)
26	297 (0.84), 410 (1.45), 596 (0.54), 708 (0.73)

4.3.2.5 Theoretical calculation

To further understand the degree of aromaticity, the nucleus-independent chemical shifts (NICS(0)) and anisotropy of the induced current density (ACID) plots were calculated for **25**, **25.2H**$^{+}$ and **26** at the B3LYP/6–31 g(d) level of theory.[32, 33] The NICS(0) values (Tables 4.3, 4.4, and Figure 4.23) at the centre of **25**, **25.2H**$^{+}$ and **26** are 2.54, 1.28 and -1.11 ppm, respectively; confirming the typical nonaromatic character. The bond length alternation (BLA) values were calculated from the crystal structures of **25**, **25.2H**$^{+}$ and **26**, which were found to be between 0.143 and 0.156 Å, further proving their nonaromatic character (Table 4.3). Finally, the random current density flow from the ACID plots corroborate the nonaromaticity of these molecules (Figure 4.24).

Table 4.3: NICS(0) [ppm] and BLA [Å] values of **25**, **25.2H**$^{+}$and **26**:

Calculation	25	25.2H^{+}	26
NICS(0)	-2.54	1.28	-1.11
BLA (Å)	0.154	0.143	0.156

Table 4.4: NICS(0) [ppm] values of individual rings in **25**, **25.2H**$^{+}$ and **26**:

	A	B	C	D	E	F	G	H	Center
25	-7.00	-7.00	-2.26	-4.18	-7.15	-7.15	-4.18	-2.26	-2.54
25.2H^{+}	-6.81	-6.97	-5.67	-5.20	-6.81	-6.97	-5.67	-5.20	1.28
26	-6.82	-6.82	-2.97	-3.07	-6.37	-6.37	-3.07	-2.97	-1.11

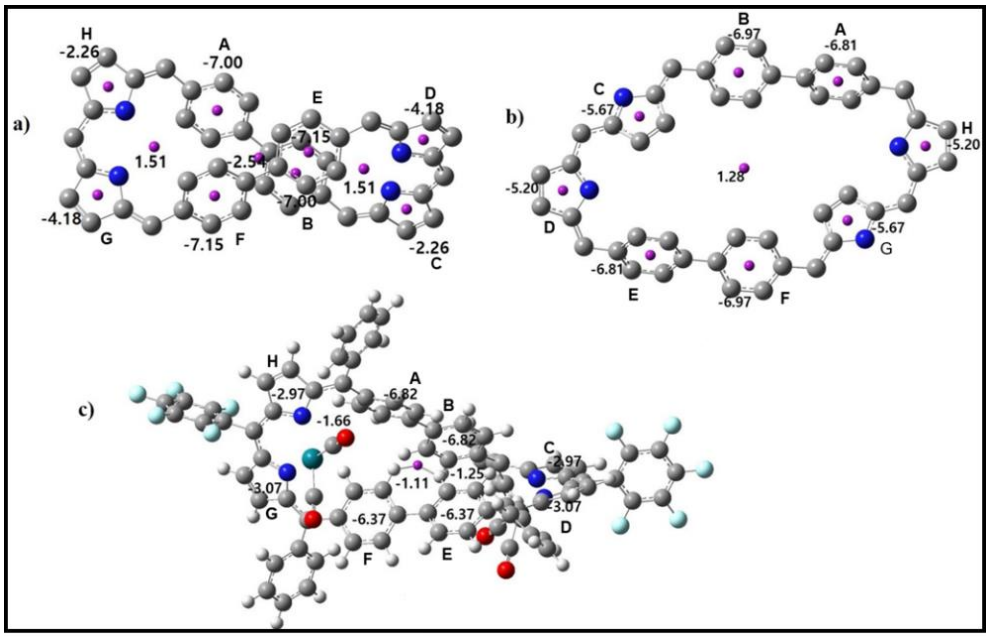

Figure 4.23: NICS(0) values for individual rings and center of the macrocycle of **25** (a), **25.2H**$^{+}$ (b) and **26** (c).

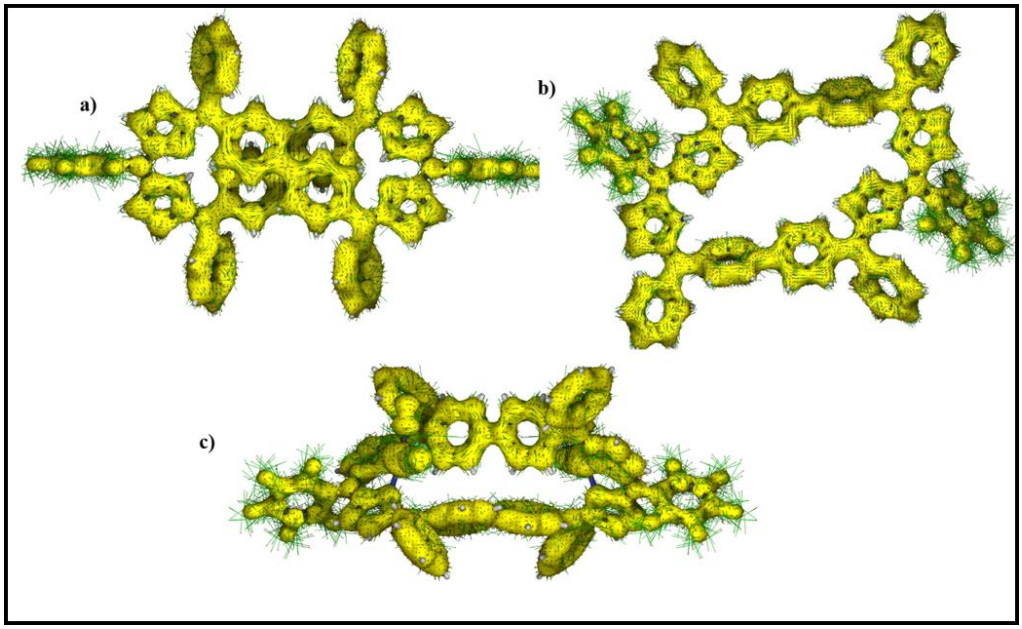

Figure 4.24: ACID plots of **25** (a), **25.2H**$^{+}$ (b) and **26** (c).

4.4 Conclusion

In conclusion, the synthesis of bis-4,4′-biphenyl moieties incorporated octaphyrin along with its protonated and bis-Rh(I) metal complex have been reported.

The interesting structural changes were observed by external stimuli such as; (i) protonation triggered figure-eight conformation into open conformation with pyrrole ring inversion and also, (ii) conversion into single twisted conformation upon bis-Rh(I) ion insertion. The spectral, theoretical studies and crystal analyses revealed that the allowed π-conjugation in the biphenyl unit was restricted by retaining its individual aromatic characteristics, thus adopts nonaromaticity and maintained its characteristics upon protonation as well as metal ion insertion.

4.5 Experimental Section

4.5.1 Genral Information

Solvent and material for the synthess were appliedfrom Sigma Aldrch cheical supplirs. Solvent was purification and dry by standad method. NMR solvnts was applied and the spectrum were resolved in Bruker 300 and 400 MegaHz spectrometers. The ESI mass spectra recorded in Bruker, miro-TOF-QII mas spectrometr. The UV spectra in Jasco V-730 UV-Visible spectrophotometer.. Single-crystal XRD data of **25**, **25.2H**$^{+}$ in a Bruker KAPPA APEX-II and **26** was collected in Rigaku Oxford diffractometer. The crystals were deposited in the Cambridge Crystalographic Data Centre with reference no. CCDC 1936876 (**25**), CCDC 1936880 (**25.2H**$^{+}$) and CCDC 1936890 (**26**).

4.6 Synthetic procedure and spectral characterization

4.6.1 Synthesis of 22: The compound **22** was synthesized as per the literature procedure.[34]

^{1}H (300 MeHz, chloroform, 298K): delta = 10.09 (s, 2H), 8.01 (dd, *J* = 4.2 Hz, 2H), 7.99 (dm, *J* = 3.4 Hz, 2H), 7.81 (s, *J* = 9.3 Hz, 2H), 7.79 (ss, *J* = 2.5 Hz, 2H).

^{13}C NMR (100 MHz, $CDCl_3$, 298K): δ = 191.72, 145.57, 136.00, 130.38, 128.05.

HR-MS (ESI-MS): *m/z* calculated for $C_{14}H_{10}O_2$ = 210.0681; found = 211.0742 (M+1).

4.6.2 Synthesis of 23: THF soluton of **22** (1 g, 4.75 mmol) was added dropwise to freshly prepared phenylmagnesium bromide (5.6 g, 35.75 mmol) solution in THF (20 ml) atmosphere . The mixture to stir at room temp. for 4 h. After 4 h, the react was quenchd with 1N HCl and extractd with EtOAc, dried over Na_2SO_4 and concentrated by rotary evaporator. Compound was silica gel (100 – 200 mesh) column in 20% EtOAc/*n*-hexane mixture to obtain **23** in 88% yield.

^{13}C NMR (100 MHz, $CDCl_3$-CD_3OD, 298K): δ = 144.04, 143.18, 139.75, 128.41, 128.33, 127.32, 127.28, 126.99, 126.95, 126.92, 126.88, 126.54, 75.56.

HR-MS (ESI-MS): *m/z* calculated for $C_{26}H_{22}O_2$ = 366.1620; found = 389.1592 (M+Na).

4.6.3 Synthesis of 24: 4,4'-Bis(phenylhydroxymethyl)biphenyl (1 g, 27.3 mmol) was in DCE (30 mL) and pyrrole (18.7 ml) was added to it in an inert atmosphere. After 10 min, $BF_3{\cdot}OEt_2$ (0.67 mL) for 4 h. The soluton was then quenchd NaOH soluton. The compound was rotary evaporator. Chromatography in 7% EtOAc/*n*-hexane to afford **24** in 64% yield.

^{1}H NMR (400 MHz, $CDCl_3$, 298K): δ = 7.85 (s, 2H), 7.51 – 7.50 (dd, *J* = 8.1, 4.5 Hz, 4H), 7.33 – 7.27 (m, 5H), 7.26 (m, 3H), 7.23 (d, *J* = 7.0 Hz, 6H), 6.73 (s, 2H), 6.18 (s, 2H), 5.85 (s, 2H), 5.51 (s, 2H).

^{13}C NMR (100 MHz, $CDCl_3$, 298K): δ = 143.11, 142.25, 139.29 133.65, 129.39, 129.01, 128.70, 127.23, 126.89, 117.33, 108.44, 108.11, 50.39.

HR-MS (ESI-MS): *m/z* calculated for $C_{34}H_{28}N_2$ = 464.2252; found = 465.2323 (M+1).

4.6.4 Synthesis of 25: Compound **24** (150 mg, 0.32 mmol) was disolved in CH_2Cl_2 (150 ml). Pentafluorobenzaldehyde (75 mg, 0.38 mmol) was aded under inert atmosphere and stirred for 10 min. *p*-Toluenesulfonic acid (27 mg, 0.15mmol) was aded and alowed to stir under same conditions for 2 h. Then DCM (0.217miligm) reaction

mixture stir for 1 h. Crude product was passed through basic alumina column. The green colour fraction with 20% CH_2Cl_2/*n*-hexane in neutral alumina and identified as **25** in 9% yield.

^{1}H NMR (400 MHz, CD_2Cl_2, 298K): δ = 13.80 (s, 2H), 7.93 (d, *J* = 8.4 Hz, 8H), 7.39 (m, 12H), 7.35 (d, *J* = 8.5 Hz, 8H), 7.27 (m, 8H), 6.56 (d, *J* = 5.1 Hz, 4H), 6.12 (d, *J* = 5.1 Hz, 4H).

^{13}C NMR (100 MHz, CD_2Cl_2, 298K): δ = 161.13, 149.63, 141.07, 138.08, 138.05, 135.23, 134.44, 131.67, 131.21, 128.22, 127.89, 126.29, 125.97.

HR-MS (ESI-MS): *m/z* calculated for $C_{82}H_{46}F_{10}N_4$ =1276.3563; found = 1277.3657 (M+1).

UV-Vis (CH_2Cl_2): λ_{max}(nm) [$\varepsilon(M^{-1}cm^{-1})$] = 326 ($0.75 \times 10^5$), 431 ($1.82 \times 10^5$), 642 ($0.32 \times 10^5$).

4.6.5 Spetral analysis of 25.2H$^+$: ^{1}H NMR (400 MHz, CD_2Cl_2, 298K): δ = 8.95 (s, 4H), 7.60 – 7.53 (m, 4H), 7.51 (t, *J* = 1.6 Hz, 8H), 8.46 – 9.40 (ss, 16H), 9.36 (mm, *J* = 7.5 Hz, 8H), 5.32 (dd).

4.6.6 Synthesis of 26: Compound **25** (0.02 g, 0.6millimol) was disolved in 20 milLit dichloromethane and 5 mL CH3OH. $[Rh(CO)_2Cl]_2$ (0.030 g, 1.077 millimol) and stirred. The crude was passed through neutral alumina column. The blue color comp. was collected with 15% DCM/*n*-hexane as **26** in 7% yield.

^{13}C NMR (75 MHz, CD_2Cl_2, 253K): δ = 161.95, 161.21, 156.08, 143.54, 141.56, 140.84, 139.25, 139.02, 138.94, 138.74, 138.46, 134.97, 133.65, 131.48, 129.90, 129.31, 128.54, 128.06, 126.28.

HR-MS (ESI-MS): *m/z* calculated for $C_{86}H_{44}F_{10}N_4O_4Rh_2$=1592.1326; found= 1592.1300 (M).

4.7 References

1. S. Saito, A. Osuka, *Angew. Chem. Int. Ed.* **2011**, *50*, 4342-4373.
2. J. L. Sessler, D. Seidel, *Angew. Chem. Int. Ed.* **2003**, *42*, 5134-5175.
3. M. Stępień, N. Sprutta, L. Latos-Grażyński, *Angew. Chem. Int. Ed.* **2011**, *50*, 4288-4340.
4. B. Szyszko, M. J. Białek, E. P. Dudziak, L. Latos- Grażyński, *Chem. Rev*. **2017**, *117*, 2839-2909.
5. T. Tanaka, A. Osuka, *Chem. Rev*. **2017**, *117*, 2584-2640.
6. A. Ghosh, S. Dash, A. Srinivasan, C. H. Suresh, T. K. Chandrashekar, *Chem. Sci.* **2019**, *10*, 5911-5919.
7. T. Sarma, G. Kim, S. Sen, W.-Y. Cha, Z. Duan, M. D. Moore, V. M. Lynch, Z. Zhang, D. Kim, J. L. Sessler, *J. Am. Chem. Soc.* **2018**, *140*, 12111-12119.
8. S. Gokulnath, T. K. Chandrashekar, *Org. Lett*. **2008**, *10*, 637-640.
9. V. G. Anand, S. Venkatraman, H. Rath, T. K. Chandrashekar, W. Teng, K. R. Senge, *Chem. Eur. J.* **2003**, *9*, 2282-2290.
10. G. Karthik, M. Sneha, V. Prabhuraja, J. M. Lim, D. Kim, A. Srinivasan, T. K. Chandrashekar, *Chem. Eur. J*. **2013**, *19*, 1886-1890.
11. T. K. Chandrashekar, S. Venkatraman, *Acc. Chem. Res.* **2003**, *36*, 676-691.
12. G. R. Geier III, S. C. Grindrod, *J. Org. Chem*. **2004**, *69*, 6404-6412.
13. V. G. Anand, S. Saito, S. Shimizu, A. Osuka, *Angew. Chem. Int. Ed*. **2005**, *44*, 7244-7248.
14. J. M. Lim, J.- Y. Shin, Y. Tanaka, S. Saito, A. Osuka, D. Kim, *J. Am. Chem. Soc.* **2010**, *132*, 3105-3114.
15. G. Karthik, W.-Y. Cha, A. Ghosh, T. Kim, A. Srinivasan, D. Kim, T. K. Chandrashekar, *Chem. Asian J*. **2016**, *11*, 1447-1453.
16. H. Mori, N. Aratani, A. Osuka, *Chem. Asian J*. **2012**, *7*, 1340-1346.
17. H. Hata, Y. Kamimura, H. Shinokubo, A. Osuka, *Org. Lett*. **2006**, *8*, 1169-1172.

18. S. Shimizu, Y. Tanaka, K. Youfu, A. Osuka, *Angew. Chem. Int. Ed.* **2005**, *44*, 3726-3729.

19. Y. Tanaka, H. Mori, T. Koide, H. Yorimitsu, N. Aratani, A. Osuka, *Angew. Chem. Int. Ed.* **2011**, *50*, 11460-11464.

20. W.-Y. Cha, T. Soya, T. Tanaka, H. Mori, Y. Hong, S. Lee, K. H. Park, A. Osuka, D. Kim, *Chem. Commun*. **2016**, *52*, 6076-6078.

21. D. Seidel, V. Lynch, J. L. Sessler, *Angew. Chem. Int. Ed*. **2002**, *41*, 1422-1425.

22. M. Bröring, J. Jendrny, L. Zander, H. Schmickler, J. Lex, Y.-D. Wu, M. Nendel, J. Chen, D. A. Plattner, K. N. Houk, E. Vogel, *Angew. Chem. Int. Ed. Engl*. **1995**, *34*, 2515-2517.

23. H. Rath, J. Sankar, V. P. Raja, T. K. Chandrashekar, B. S. Joshi, R. Roy, *Chem. Commun.* **2005**, 3343-3345.

24. K. Zhang, J. Zhang, X. Li, R. Guo, H. Agren, Z. Ou, M. Ishida, H. Furuta, Y. Xie, *Org. Lett.* **2015**, *17*, 4806-4809.

25. J.-Y. Shin, H. Furuta, K. Yoza, S. Igarashi, A. Osuka, *J. Am. Chem. Soc.* **2001**, *123*, 7190-7191.

26. E. Vogel, M. Bröring, J. Fink, D. Rosen, H. Schmickler, J. Lex, K. W. K. Chan, Y.-D Wu, D. A. Plattner, M. Nendel, K. N. Houk, *Angew. Chem. Int. Ed. Engl.* **1995**, *34*, 2511-2514.

27. K. C. Sahoo, M. A. Majewski, M. Stępień, H. Rath, *J. Org. Chem*. **2017**, *82*, 8317-8322.

28. T. D. Lash, *Chem. Rev.* **2017**, *117*, 2313-2446.

29. B. Adinarayana, M. Das, C. H. Suresh, A. Srinivasan, *Chem. Eur. J*. **2019**, *25*, 4683-4687.

30. J.-i. Setsune, M. Toda, T. Yoshida, K. Imamura, K. Watanabe, *Chem. Eur. J.* **2015**, *21*, 12715-12727.

31. F. F. Awwadi, H. A. Hodali, *J. Mol. Struct*. **2018**, *1154*, 373-381.

32. A. D. Becke, *J. Chem. Phys*. **1993**, *98*, 1372-1377.

33. C. Lee, W. Yang, R. G. Parr, *Phys. Rev. B: Condens. Matter Mater. Phys.* **1988**, *37*, 785-789.

34. B. Saikia, P. R. Boruah, A. A. Ali, D. Sarma, *Tetrahedron Lett*. **2015**, *56*, 633-635.

.

There is no other information and all other information has been provided.

Conclusion chapter

The entire thesis is engrossed on carbaporphyrinoids which are formed by replacing one or more pyrrole units by polycyclic aromatic units such as arene unit. This thesis is comprised of four chapters. Chapter one describes the literature review of carbocylic based contracted and expanded porphyrins and highlights their syntheses, conformation and coordination chemistry. The chemistry of arene ring incorporated contracted and expanded porphyrinoids are well known in the literature, however polycyclic aromatic ring incorporated respective analogues are less known. This chapter mainly describes on the reported synthetic structural and coordination chemistry of contracted and expanded carbaporphyrinoids. The second chapter deals with dicarbacorrole which is a unique ligand that can stabilize metal ions in higher oxidation states. In third chapter, we wish to report the synthesis, structural and photophysical properties of hexaphyrin with *o*-*p*-biphenyl moiety incorporated in the macrocyclic core for the first time. By replacing the *ortho* with *meta* connectivity in the biphenyl unit of hexaphyrin leads to the formation of its structural isomer, octaphyrin. Such isomers with different class of expanded porphyrinoids is reported for the first time. The fourth chapter reports the synthesis, spectral, structural and coordination chemistry of bis-biphenyl moiety (*p*-*p*) based octaphyrin analogue with three distinct conformational structures triggered by protonation and bis Rh metal ion insertion. In conclusion, biphenyl moiety incorporated caraporphyrinoids serve as an astute platform to study their rich coordination chemistry, weak non-covalent interactions, stabilization of higher oxidation state organometallic complexes and aromaticity switching which attracts the porphyrin chemist to explore this field in future.